Recent Advances in Zinc Enzymology

William N. Lipscomb* and Norbert Sträter

Department of Chemistry and Chemical Biology, Harvard University, 12 Oxford Street, Cambridge, Massachusetts 02138

Received May 2, 1996 (Revised Manuscript Received July 25, 1996)

Contents

S0009-2665(95)00042-2 CCC: $25.00

I. Introduction

Posters and lectures presented at the Seventh International Conference on Bioinorganic Chemistry (ICBIC) in Lübeck, Germany, last year was divided into 16 sections, including element-related sections for iron (three sections!), vanadium, manganese, nickel, copper, and molybdenum.[1] For zinc, which is, following iron, the second-most abundant transition metal in biology, and which is represented in metalloenzymes of all six classes of enzymes, no section was available. Do we already know almost everything about the roles and enzymology of zinc in biological systems? Has the bioinorganic research community abandoned this less appreciated (Figure 1) and boring element,[2] as it was once provocatively designated because of its almost complete lack of spectroscopic properties, and moved to current hotspots such as electron transfer or the activation and metabolism of oxygen, nitrogen, and hydrogen? The answers to these questions clearly are "No", as also demonstrated by more than 40 contributions on ICBIC 7 related to zinc biochemistry, or by the 17 contributions to zinc enzymology out of 49 abstracts in the metalloenzyme abstract section of the XVII Congress of the International Union of Crystallography 1996 in Seattle. Zinc enzymology is, compared to some other current areas of metallobiochemistry, a maturing field, but in addition to further

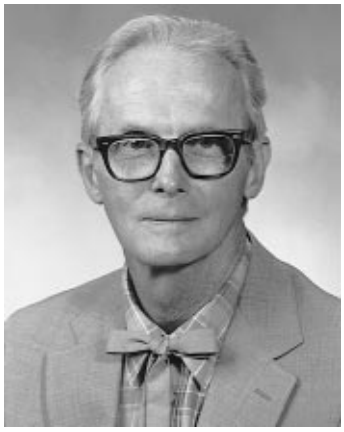

Kentucky Colonel William N. Lipscomb was born in Cleveland, OH, in 1919. After obtaining his B.S. in Chemistry at the University of Kentucky, he earned a Ph.D. in Chemistry at the California Institute of Technology for X-ray and electron diffraction studies in the group of Linus Pauling. He then joined the faculty of the University of Minnesota, studying structure and bonding of volatile boron hydrides by low-temperature single-crystal X-ray diffraction and quantum chemical calculations. He pursued this work after 1959, when he became Professor of Chemistry at Harvard, and was awarded the Nobel Prize in Chemistry in 1976 for these research studies. Crystallographic studies on enzyme structure and function, focusing on metalloenzymes and allosteric enzymes, started in 1962. His research on metalloenzymes included carboxypeptidase A, carbonic anhydrase, leucine aminopeptidase, and fructose-1,6-bisphosphatase.

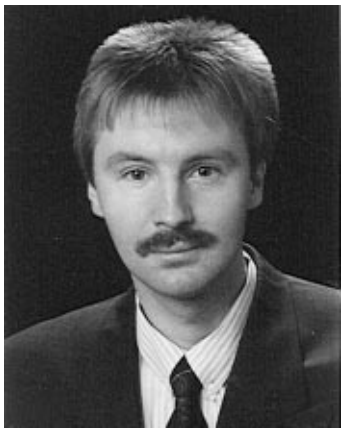

Norbert Sträter was born in Soest, Germany, in 1965. He studied Chemistry at the University of Münster and obtained his Ph.D. in 1994. In the group of Bernt Krebs he worked on the X-ray structure of purple acid phosphatase. As a postdoc in the laboratory of William N. Lipscomb at Harvard he currently studies the two-metal ion mechanisms of leucine aminopeptidase and aminopeptidase A.

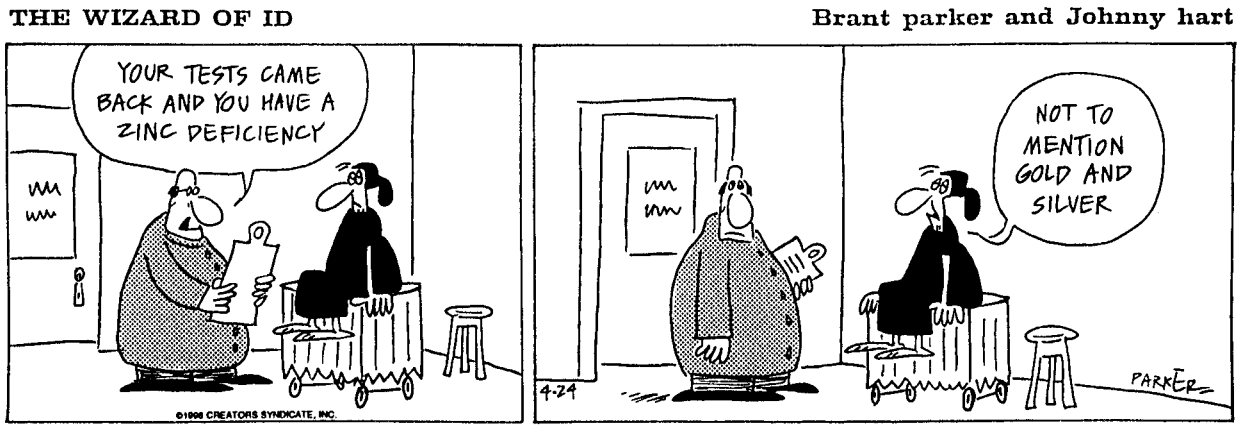

Figure 1. Appreciation of the value of zinc in the public. Reprinted with permission of Johnny Hart and Creators Syndicate, Inc. Copyright 1996.

developments of structure−function relationships it has also provided a number of surprising new results and ideas in the last few years.

In fact, the number of studies makes it impossible to provide a comprehensive review of the recent literature on zinc enzymology here, and we will therefore focus on those zinc enzymes for which structure−function relationships are possible on the basis of structural and biochemical data. This means that, with a few exceptions, only zinc enzymes for which NMR or crystal structures are available are included here. Another seemingly simple, yet experimentally sometimes complex issue concerns the choice of which metalloenzyme is a zinc enzyme. In a strict definition,[3] a metalloenzyme binds its metal ion(s) tightly ($K_d < 10^{-8}$ M), such that the metal remains bound to the protein during the isolation procedure. The type of metal bound *in vivo* can then be assumed to be the same as the metal content determined *in vitro*. A second group of enzymes binds a metal cofactor more loosely ($K_d = 10^{-3}$ to 10^{-8} M) and this cofactor is lost during the isolation procedure. Moreover, usually several divalent metal ions can restore activity, so that it may become quite difficult to determine the type of metal bound *in vivo* (see also section VII). As a result, for many of these enzymes the cofactor used *in vivo* is not known; in some enzymes even more than one of the available divalent metal ions may serve as cofactor. Since there is in principle no difference in chemical catalysis by low-affinity compared to high-affinity metal sites, some of these enzymes are also included in this article, especially if they are or have been discussed as zinc enzymes, or are active with zinc. However, the selection of these enzymes, of which many are considered as magnesium enzymes, might appear somewhat arbitrary. A compilation of "established" zinc enzymes for which spatial structures are available is given in Table 1.

Metallopeptidases. Following structures of the prototypical zinc peptidases carboxypeptidase A (section II.B.1) and thermolysin (section II.C.1), structures of other mononuclear zinc peptidases have become available recently, including those of snake venom proteases (section II.D.3) and matrix metalloproteases (section II.D.5), which are of great interest in relation to several diseases. These structures may thus facilitate structure-based drug design. Whereas many of these zinc peptidases are (although in part very distantly) related to thermolysin, there are also now many mononuclear zinc peptidases known which developed independently including carboxypeptidase A and D-Ala-D-Ala carboxypeptidase. Yet all of these peptidases show a remarkably similar active site arrangement including the coordination of the zinc ion and the activation of the water nucleophile. A surprising finding was the presence of a typical zinc proteolytic site in the crystal structure of Sonic hedgehog protein, which is under intense study for its role in cell signaling and embryonic development (section II.E.1). However, despite these similarities, remarkable new features of zinc-catalyzed peptide bond hydrolysis were also found in these studies, including an association−dissociation switch of a tyrosine zinc ligand in the catalytic cycles of the serralysins (section II.D.4) and possibly the astacins (section II.D.2). Furthermore, a hinge-bending motion probably facilitates catalysis by thermolysin (section II.C.1) and pseudolysin (section II.C.2). A new mechanism of proenzyme activation of some of the metzincins involving dissociation of a zinc-coordinated cysteine residue was found and subsequently characterized by X-ray structures (section II.D.1). This cysteine is replaced by a nucleophilic water molecule to yield an active enzyme. Structures with reaction-coordinate analogues helped to provide detailed structural models for different steps of the catalytic pathway. An example is the very tight binding phosphonate compound complexed to carboxypeptidase A ($K_i = 11$ fM). Structures of five dimetal peptidases (leucine, *Aeromonas proteolytica*, *Streptomyces griseus*, methionine aminopeptidase, and carboxypeptidase G2) are available now (sections II.B.4 and 6−9), of which four are known zinc enzymes, and knowledge of their mechanisms is developing (section II.F). The finding that carboxypeptidase G2 contains a dizinc center similar to those in *Aeromonas* and *Streptomyces* aminopeptidase provides insight into the common evolutionary origin of many mono- and dizinc exopeptidases (section II.B.8).

Metallophosphatases. The zinc phosphatases constitute a structurally and probably also mechanistically much more diverse group than do the peptidases. In particular, the frequent use of two or three metal ions in the cleavage (section III.A−F, IX.A−

Table 1. Established Zinc Enzymes of Known Structure[a]

enzyme	ligands	enzyme	ligands
	Mononuclear Zinc Enzymes		
carboxypeptidase A (cow)	His_{69}, Glu_{72}, His_{196}, W	stromelysin-1 (human)	His_{201}, His_{205}, His_{211}
zinc D-Ala-D-Ala carboxypeptidase (*Streptomyces albus*)	His_{152}, His_{193}, His_{196}	matrilysin (human)	His_{218}, His_{222}, His_{228}
thermolysin (*Bacillus thermoproteolyticus*)	His_{142}, His_{146}, Glu_{166}, W	*Streptomyces* small neutral protease	His_{83}, His_{87}, Asp_{93}, W
pseudolysin (*Pseudomonas aeruginosa*)	His_{140}, His_{144}, Glu_{164}, W	lysozyme of Bacteriophage T7	His_{17}, His_{122}, Cys_{130}, W
bacillolysin (*Bacillus cereus*)	His_{143}, His_{147}, Glu_{167}, W	sonic hedgehog	His_{141}, Asp_{148}, His_{183}, W
astacin (crayfish *Astacus astacus* L.)	His_{92}, His_{96}, His_{102}, Tyr_{149}, W	β-lactamase II (*Bacillus cereus*)	His_{86}, His_{88}, His_{149}, W
adamalysin II (rattlesnake *Crotalus adamanteus*)	His_{142}, His_{146}, His_{152}, W	adenosine deaminase (mouse)	His_{15}, His_{17}, His_{214}, Asp_{295}, W
atrolysin C (rattlesnake *Crotalus atrox*)	His_{142}, His_{146}, His_{152}, W	cytidine deaminase (*E. coli*)	His_{102}, Cys_{129}, Cys_{132}, W
H_2-proteinase (Habu snake)	His_{142}, His_{146}, His_{152}, W	6-pyruvoyl tetrahydropterin synthase (rat)	His_{23}, His_{48}, His_{50}
Pseudomonas alkaline protease	His_{176}, His_{180}, His_{186}, Tyr_{216}, W	carbonic anhydrase, human	His_{94}, His_{96}, His_{119}, W
Serratia alkaline protease	His_{176}, His_{180}, His_{186}, Tyr_{216}, W	carbonic anhydrase, *M. thermophila*	His_{A81}, His_{A122}, His_{B117}
neutrophil collagenase (human)	His_{197}, His_{201}, His_{207}	Ada protein (*E. coli*)	Cys_{38}, Cys_{42}, Cys_{69}, Cys_{72}
fibroblast collagenase (human)	His_{118}, His_{122}, His_{128}	alcohol dehydrogenase (horse liver)	Cys_{46}, His_{67}, Cys_{174}, W
porcine synovial collagenase	His_{218}, His_{222}, His_{228}		
	Polynuclear Zinc Enzymes		
leucine aminopeptidase (cow)	Zn1: Asp_{255}, Asp_{332}, CO_{332}, Glu_{334}, W Zn2: Lys_{250}, Asp_{255}, Asp_{273}, Glu_{334}, W	nuclease P1 (*Penicillium citrinum*)	Zn1: Asp_{45}, His_{60}, His_{116}, Asp_{120}, W Zn2: His_{126}, His_{149}, Asp_{153}, 2W Zn3: $NH2_1$, CO_1, His_6, Asp_{120}, W
Aeromonas proteolytica aminopeptidase	Zn1: Asp_{117}, Glu_{152}, His_{256}, W Zn2: His_{97}, Asp_{117}, Asp_{179}, W	phosphotriesterase (*Pseudomonas diminuta*)	Zn1:[b] His_{55}, His_{57}, Lys-$CO2_{169}$, Asp_{301}, W Zn2:[b] Lys-$CO2_{169}$, His_{201}, His_{230}, 3W
Streptomyces griseus aminopeptidase	Zn1: Asp_{97}, His_{85}, Asp_{160} Zn2: Asp_{97}, Glu_{132}, His_{247}	superoxide dismutase (bovine)	Zn: His_{61}, His_{69}, His_{78}, Asp_{81} Cu: His_{44}, His_{61}, His_{118}, W
carboxypeptidase G2 (*Pseudomonas sp.*)	Zn: Asp_{141}, Glu_{176}, His_{385}, W Zn: His_{112}, Asp_{141}, Glu_{200}, W	purple acid phosphatase (kidney bean)	Zn: Asp_{164}, Asn_{201}, His_{286}, His_{323} Fe: Asp_{135}, Asp_{164}, Tyr_{167}, His_{325}
β-lactamase (*Bacteroides fragilis*)	Zn1: His_{99}, His_{101}, His_{162}, W Zn2: Asp_{103}, Cys_{181}, His_{223}, W	Ser/Thr protein phosphatase 1 (rabbit muscle)	Zn:[b] Asp_{92}, Asn_{124}, His_{173}, His_{248}, W Fe:[b] Asp_{64}, His_{66}, Asp_{92}, 2W
alkaline phosphatase (*E. coli*)	Zn1: Asp_{327}, His_{331}, His_{412} Zn2: Asp_{51}, Asp_{369}, His_{370}	calcineurin (human)	Zn: Asp_{118}, Asn_{150}, His_{199}, His_{281}, W Fe: Asp_{90}, His_{92}, Asp_{118}, 3W
phospholipase C (*Bacillus cereus*)	Zn1: Asp_{55}, His_{69}, His_{118}, Asp_{122}, W Zn2: His_{128}, His_{142}, Glu_{146}, 2W Zn3: NH_{21}, CO_1, His_{14}, Asp_{122}, W		

[a] The apparent absence of water (W) as a zinc ligand may occur because of the limited resolution of some X-ray diffraction studies. For some closely related enzymes only the member for which a structure was first determined is included here. [b] Structure determined for a metal-exchanged enzyme form.

C, E, and possibly F−H) and synthesis (sections IX.D S), of phosphoester or anhydride bonds is noteworthy. Zn−Zn−Mg alkaline phosphatase, unique among the dinuclear metallophosphatases in its two-step mechanism via a phospho-enzyme intermediate, is the best studied member of this group (section III.A). Three zinc ions are found in the active sites of nuclease P1 and phospholipase C (sections III.D and E), which are evolutionarily related to each other. All three zinc ions seem to be involved actively in catalysis. However, despite a close structural resemblance of their active sites, structural data on enzyme−inhibitor complexes imply different substrate binding and mechanisms. The three related enzymes fructose-1,6-bisphosphatase, inositol monophosphatase, and inositol polyphosphatase contain lower affinity metal binding sites and lose, in part, metals during isolation (sections IX.A−C). They also use a two-metal ion mechanism to hydrolyze phosphoesters, possibly by different mechanisms. Another new family of dinuclear metallophosphatases for which structural and biochemical information is rapidly developing is the $\alpha_2\beta_3$ metallophosphatases, which contain a dimetal center at the carboxyl end of three β-strands of a $\beta\alpha\beta\alpha\beta$ motif. This family includes the Ser/Thr protein phosphatases, which contain a mixed zinc-iron site (section III.C). The oxidation state of the iron ion in the active site is not yet clarified. The very distantly related purple acid phosphatases, however, contain a $Fe^{III}-Zn^{II}$ (kidney bean enzyme) or a $Fe^{III}-Fe^{II}$ site (section III.B). These phosphatases are unique in their use of a trivalent ion to facilitate ionization of a water nucleophile to a hydroxide ion at acid pH. Other related enzymes of this family, including 5′-nucleotidase, probably contain a dizinc site. Nature employs two-metal ion catalysis not only to hydrolyze phosphomonoesters and phosphodiesters, but also in the degradation of phosphotriesters, which are not naturally occurring compounds (section III.F). An interesting question is how and from which enzyme the dizinc phosphotriesterase evolved within a relatively short time as a very efficient catalyst, or whether the triesterase activity is adventitious. Other new structures of phosphatases which have multistep mechanisms include *S*-adenosylmethionine synthetase (section IX.R) and glutamine synthetase (section IX.S).

Another very intensely studied field of metalloenzyme catalysis is the synthesis and degradation of the phosphodiester bond of DNA and RNA. Examples are RNA and DNA polymerases (section IX.D), exonuclease sites (section IX.E), ribonuclease H activity (section IX.F), and restriction endonucleases (section IX.G). Here alternative mechanisms, e.g. mono- vs dimetal catalysis, are controversially discussed. At least part of the difficulties encountered in characterizing the reaction mechanisms of these biologically important enzymes arises from low-affinity metal binding sites and the presence of several metal-dependent activities in one protein. Many of these activities utilize magnesium *in vivo*, but zinc is also implicated for some enzymes.

Other Zinc Enzymes. The two zinc deaminases for cytidine and adenosine provide another instructive example of convergent evolution toward similar (but different in detail) active-site structures and mechanisms (sections IV.A and B). Here, once again, structures of the enzymes with reaction coordinate analogues provided structural models for different stages of the reaction pathway. One of the two cysteines coordinated to cytidine deaminase is proposed to change its conformation somewhat during the catalytic cycle, thereby forming a "valence buffer" by changing the zinc−sulfur distance (section IV.B). Interestingly, adenosine deaminase is evolutionarily related to urease, which uses two nickel ions to hydrolyze urea. The zinc metalloenzyme nature of adenosine deaminase was unknown before it was indicated by the crystal structure analysis. Likewise unanticipated catalytic zinc ions were found in Sonic hedgehog (section II.E.1) and 6-pyruvoyltetrahydropterin synthase (section IV.C). For Sonic hedgehog the relevance and activity of the putative zinc active center remains to be demonstrated. Dopachrome tautomerase might be a new, interesting zinc enzyme not least because of its evolutionary relationship and structural similarity to dicopper enzymes such as tyrosinase (section IV.D); however, the nature of its active site metals is still under discussion. Ada of *Escherichia coli* is, so far, a unique zinc enzyme in that it contains a catalytic zinc ion coordinated to four cysteines (section IV.G), a motif which is typical for a purely structural zinc site. Mechanistic insight into the aldol addition of dihydroxyacetone phosphate (DHAP) and an aldehyde substrate, catalyzed by fuculose aldolase, is emerging (section IV.I). Quite remarkably, this mechanism includes a displacement of a bidentate coordinating glutamate ligand to zinc by the α-hydroxy keto group of DHAP upon binding of this reactant.

Why Zinc? The reason why zinc instead of Mg^{2+}, Ca^{2+}, Mn^{2+}, Co^{2+}, Ni^{2+}, and Cu^{2+} as alternatives is used for many hydrolytic, condensation, or other atom and group transfer reactions have been discussed (e.g. refs 4−7). These include its flexible coordination geometry, fast ligand exchange, Lewis acidity, intermediate polarizability (hard−soft character), availability, strong binding to suitable sites, and its lack of redox activity (no generation of reactive radicals). It is the combination of these factors that makes zinc so attractive. In fact, Mg^{2+} and Mn^{2+} are frequently used as alternatives to zinc, especially in low-affinity metal binding sites of many phosphoryl transfer catalyzing enzymes. Zinc can often be replaced by Co^{2+}, Cu^{2+}, Ni^{2+}, Mn^{2+}, or Cd^{2+} to yield active, sometimes even hyperactive, enzymes.[8] Among these Co^{2+} is most likely to replace Zn^{2+} efficiently. The flexibility of zinc in forming complexes with coordination numbers 4, 5, and 6 has been recently analyzed on the basis of crystal structures of small molecules.[9] Whereas for zinc complexes the coordination numbers 4, 5, and 6 were found in 42, 19, and 35% of the structures analyzed, respectively, these percentages are 9, 7, and 79 for magnesium. The preference of Mg^{2+} to form the six-coordinated complex $Mg[H_2O]_6^{2+}$ over $Mg[H_2O]_5^{2+}\cdot[H_2O]$ (five waters in the inner and one water in the outer-shell coordination sphere) and $Mg[H_2O]_4^{2+}\cdot 2[H_2O]$ with energy differences of approximately 4 and 9 kcal/mol could also be demonstrated by *ab initio*

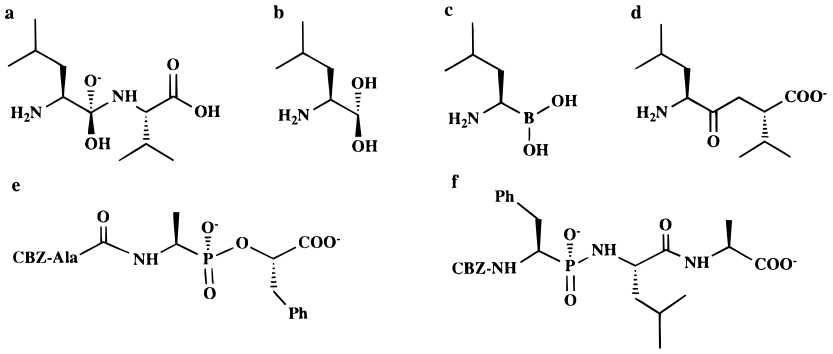

Figure 2. Transition state and analogue inhibitors for peptidases: (a) transition state (or intermediate) of an associative mechanism of peptide hydrolysis; (b) hydrated form of the aminoaldehyde L-leucinal; (c) L-leucineboronic acid; (d) dipeptide inhibitor containing a ketomethylene amide bond replacement; (e) tripeptide inhibitor containing a phosphonate group; (f) tripeptide inhibitor containing a phosphonamidate group. Inhibitors (or transition state) a−d are for an aminopeptidase; e, for a carboxypeptidase; and f, for an endopeptidase. The binding mode of b, e, and f to an enzyme is shown in Figures 6, 3, and 11, respectively.

molecular orbital calculations.[10] In contrast, the corresponding four- to six-coordinated zinc complexes differ by less then 0.4 kcal/mol.[9] For reference, a list of radii of divalent metallic ions (in Å) includes Mg (0.65), Ca (0.99), Ti (0.90), V (0.88), Cr (0.84), Mn (0.80), Fe (0.76), Co (0.74), Ni (0.72), Cu (0.72), Zn (0.74), Cd (0.97), and Hg (1.1).[11]

Although zinc is coordinated to six water molecules in solution, it usually has coordination numbers of 4 or 5 in active sites of enzymes, including bound water molecules, inhibitors, or intermediates. However, both zinc ions of leucine aminopeptidase are five coordinated in the ground state and six coordinated in the presence of bound substrate. In some structural sites (section V) zinc is four coordinated to four Cys residues, as it is in liver alcohol dehydrogenase (section IV.K), apartate transcarbamylase (section V), and cytochrome *c* oxidase,[12] for examples. In other structural or storage sites zinc is actually six coordinated. In the insulin hexamer the ligands are three His residues and three water molecules.[13,14] In apoferritin one octahedral site has three Asp residues and three waters, whereas another octahedral site has three Glu residues and three water molecules as ligands to zinc.[15] A structural zinc ion is also present in many proteins that are not enzymes, such as the zinc fingers and metallothioneins.[16,17]

II. Zinc Peptidases and Amidases

In contrast to many phosphatases, which utilize preferably magnesium or manganese, Nature in metalloenzymes almost exclusively uses zinc for the hydrolysis of peptide bonds. Following the classification by Rawlings and Barrett,[18] these zinc peptidases consist of about 30 families.[19] The families can be divided into five groups ("clans"). In the first group, the thermolysin clan (HEXXH + E), a glutamate residue is present besides the two histidines of the HEXXH motif as metal ligands. The conserved glutamate of the HEXXH motif plays an important catalytic role. A second group, the metzincins (HEXXH + H) has a third histidine coordinated to the catalytic metal ion. In a third group, metal ligands in addition to the HEXXH motif remain to be identified. A fourth group of metallopeptidases has metal ligands, which are not part of an HEXXH motif. Finally, for a fifth group, the metal ligands remain to be established.

The zinc peptidases carboxypeptidase A and thermolysin were among the first proteins to have their structures unraveled by X-ray crystallography, and they have been studied extensively by biochemical and structural means. Thus, these peptidases serve as prototypes for mononuclear zinc proteases. However, many more structures of metallopeptidases, determined in recent years, have yielded great progress in understanding the evolutionary, structural, and mechanistic relationships of these enzymes. In particular, these structures demonstrated that the enzymes of the thermolysin clan and the metzincin clan all contain a topologically similar fold of five β-strands and two α-helices in their catalytic domains. One of these α-helices bears the conserved HEXXH motif. The two clans probably have evolved from a common ancestor.

In the following sections those peptidases that are not related to the thermolysins and metzincins, namely the carboxypeptidases and dizinc peptidases, are discussed first. Recent and more detailed reviews covering the field of metallopeptidases are available.[20,21]

A. Transition-State Analogue Inhibitors

In contrast to the situation of an associative pathway of phosphoester hydrolysis, for which suitable pentavalent transition-state analogues are difficult to obtain, several functional groups resembling the tetrahedral *gem*-diolate group of an associative pathway for peptide hydrolysis are available (Figure 2). These include hydrated aldehydes, boronates, and compounds in which the amide bond is replaced by a hydrated ketomethylene, a phosphonate, or a phosphonamidate group. These compounds have been used in several structural studies in order to gain detailed insight into the interactions, which stabilize the transition state and thereby promote catalysis. Such mechanism-based inhibitors have so far been most extensively used in structural studies of carboxypeptidase A, thermolysin, and leucine aminopeptidase.

Table 2. Metallopeptidases without a HEXXH Metal-Binding Motif[18]

enzyme	EC no.
family M16: pitrilysin	
pitrilysin subfamily	
insulysin	3.4.24.56
metalloendopeptidase (*Bacillus*)	–
pitrilysin	3.4.24.55
sporozoite developmental protein (*Eimeria*)	–
mitochondrial processing peptidase subfamily	3.4.99.41
family M14: carboxypeptidase A	
carboxypeptidase A subfamily	
carboxypeptidase A[a]	3.4.17.1
carboxypeptidase B[a]	3.4.17.2
carboxypeptidase (*Simulium*)	–
carboxypeptidase (*Streptomyces*)	–
carboxypeptidase T (*Thermoactinomyces*)[a]	3.4.17.18
carboxypeptidase II subfamily	
carboxypeptidase II	3.4.17.10
carboxypeptidase M	3.4.17.12
carboxypeptidase (*Drosophila*)	–
lysine carboxypeptidase	3.4.17.3
family M15: zinc D-Ala-D-Ala carboxypeptidase	
muramoyl-pentapeptide carboxypeptidase	3.4.17.8
zinc D-Ala-D-Ala carboxypeptidase[a]	3.4.17.14
family M17: leucine aminopeptidase	
aminopeptidase A (*Escherichia coli*)	–
leucine aminopeptidase[a]	3.4.11.1
family M24: methionine aminopeptidase	
methionine aminopeptidase[a]	3.4.11.18
X-Pro aminopeptidase (*Escherichia coli*)	3.4.11.9
X-Pro dipeptidase	3.4.13.9
family M28: *vibrio* leucine aminopeptidase	
Aeromonas proteolytica aminopeptidase[a]	3.4.11.10
Streptomyces griseus aminopeptidase[a]	
carboxypeptidase G2[a]	3.4.17.11

[a] A three-dimensional structure has been determined.

B. Zinc Peptidases without the HEXXH Motif

This group contains six families of zinc peptidases with metal ligands that are not part of a HEXXH motif (Table 2). The metal ligands are known from crystallographic (carboxypeptidases A, B, G2, and T; DD carboxypeptidase; leucine aminopeptidase; *Aeromonas proteolytica* aminopeptidase; and methionine aminopeptidase) or site-directed mutagenesis studies (pitrilysin). Despite the absence of significant sequence homology a similar folding topology is present, in part, in carboxypeptidase A and leucine aminopeptidase,[22] and in *Aeromonas* aminopeptidase and leucine aminopeptidase.[23] However, the limited structural homology does not extend to the active-site structure or even the active-site location. The structural homology between *Aeromonas* aminopeptidase and carboxypeptidase G2 further indicates that these exopeptidases may have evolved from a common ancestor long ago.[24] If so, a far greater diversity is present between the active-site structures of the enzymes of different families in this group than between the obviously related families of the thermolysin and the metzincin clan.

1. Carboxypeptidase A, a Prototype Zinc Peptidase

Following myoglobin and lysozyme, bovine carboxypeptidase A was the third protein to have its three-dimensional structure solved at high resolution. However, its mechanism has been in controversy for almost 50 years. The active-site zinc ion is bound to His-69, Glu-72, and His-196 (Figure 3) and to a water molecule, which is displaced when a bidentate ligand such as glycyltyrosine binds to Zn^{2+} through its carbonyl oxygen and NH_2 terminus.[25] The zinc-bound water molecule is hydrogen bonded to Glu-270.

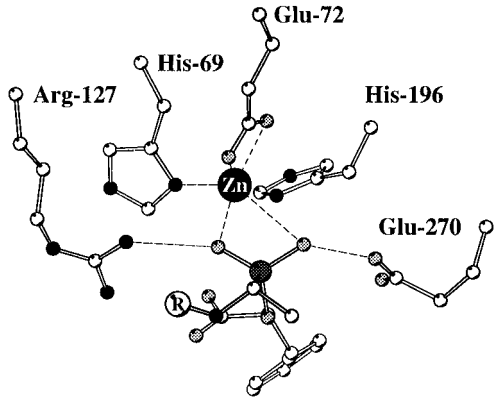

Figure 3. Binding mode of the phosphonate group of the tripeptide inhibitor shown in Figure 2e to carboxypeptidase A. The two N-terminal residues (R) of the inhibitor are omitted for clarity. The phosphonate group coordinates asymmetrically in a bidentate mode: one oxygen, which is also hydrogen bonded to Arg-127, is 2.2 Å away from the zinc. The other zinc-bound oxygen is at a distance of 3.1 Å. Generated from PDB file 6CPA.[45]

Anhydride or Zn−OH⁻ Pathway. Aside from the low-temperature trapping of a possible ES_2 complex for a peptide substrate,[26] most studies have been concentrated on α-(acylamino)cinnamoyl esters of L-β-phenyllactate and related compounds as substrates.[27−30] The evidence for the formation of an anhydride between Glu-270 and the carbonyl of the scissile peptide bond in these experiments, particularly those at low temperature, has been questioned.[31,32] Problems with enzyme precipitation and changes in rate-limiting steps in these viscous solutions at low temperatures are probable. Moreover, the marginal evidence for ^3H labeling needs further study.[33] In general the failure of the enzyme to promote transfer reactions among substrates (e.g. transpeptidation) is further evidence for the "general base" $Zn-OH^-$ pathway (direct attack of a zinc-bound nucleophile on the substrate) for both peptide and ester substrates.

Crystallographic studies of phosphonates or *gem*-diolates of hydrated ketones provide a model for the stabilization of the tetrahedral intermediate by both Zn^{2+} and Arg-127 (Figures 3 and 4).[34] In these complexes the zinc ion is five-coordinated, and Glu-270 is in a position to be hydrogen bonded to one of the two oxygens of this intermediate.

Proton Donor. Candidates for protonation of NH of the scissile peptide bond are Tyr-248, H_2O, or Glu-270 (proton shuttle).[35] Proton donation by Tyr-248, the subject of many early chemical modification studies and originally proposed as a proton donor, has been eliminated by the fully active Tyr-248 to Phe mutant.[36] However, a Glu-270 to Gln mutant of carboxypeptidase A severely compromizes hydrolysis of both peptide and ester substrates; for the ester *O*-(benzoylglycyl)-L-β-phenyllactate k_{cat} decreases 3000-fold and K_m decreases 10-fold.[37] In the E270C or E270D mutants k_{cat} is only reduced about 50-fold. These results are consistent with a mechanism in

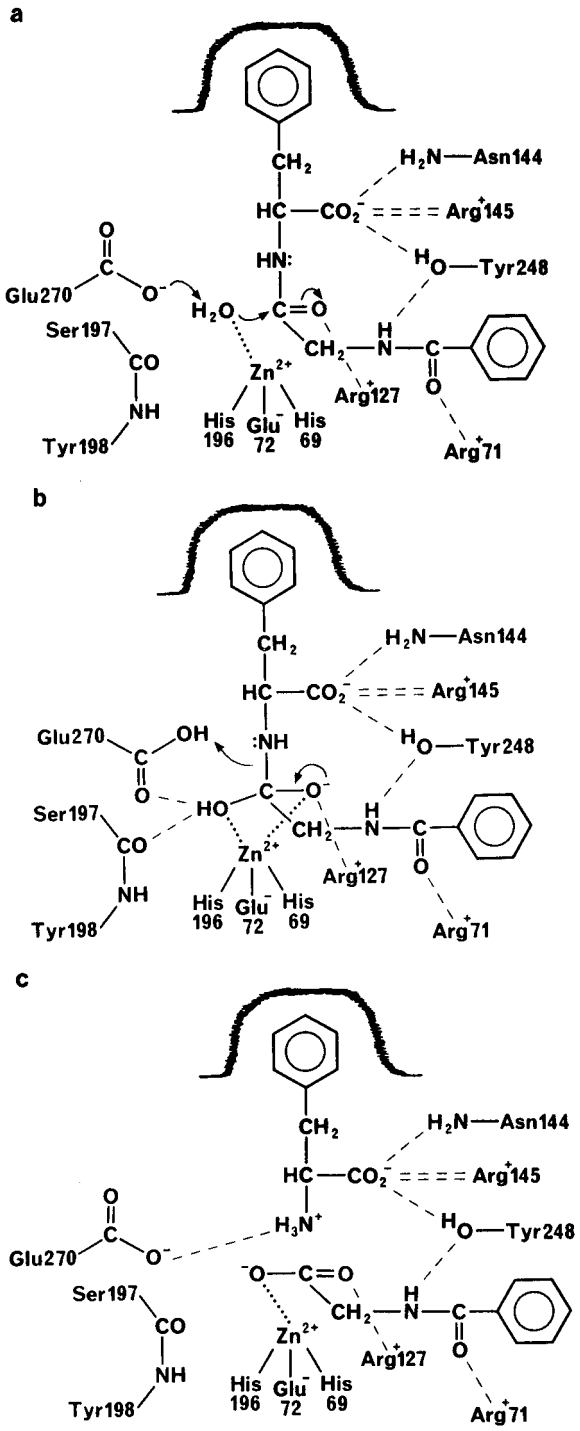

Figure 4. "Zinc−hydroxide" reaction mechanism for the peptide hydrolysis by carboxypeptidase A: (a) the precatalytic Michaelis complex with the substrate's carbonyl oxygen hydrogen bonded to Arg-127 allows for nucleophilic attack by a water molecule promoted by zinc and assisted by Glu-270; (b) the stabilized tetrahedral intermediate collapses with required proton donation by Glu-270; (c) the final product complex. (Reprinted with permission from ref 34. Copyright 1989 American Chemical Society.)

which Glu-270 accepts a proton from a zinc-bound water molecule and transfers the proton to the leaving NH group of the scissile peptide bond (Figure 4).

Reverse Protonation Mechanism. In an alternative proposal for the reaction mechanism a water molecule is activated by the C-terminal carboxylate group of the substrate for nucleophilic attack at the *si* face of the scissile peptide bond.[38,39] (In the mechanism of Figure 4 the nucleophilic attack of OH^- is assumed to occur at the *re* face.) In this mechanism the conserved Glu-270 is assigned a typical pK_a of about 4.0 and given a passive role in the mechanism. The pK_a of 6.3 is assigned to the zinc-bound water ligand, which has to be protonated to be replaced by the substrate (reverse protonation state, see section II.C.1). In contrast, the inactivation of Glu-270 by *N*-ethyl-5-phenylisoxazolium 3′-sulfonate (Woodward's reagent K), or by *N*-(bromoacetyl)-*N*-methyl-L-phenylalanine is governed by a pK_a of about 7, which was attributed to Glu-270.[40−42] It therefore seems reasonable to consider the linkage Glu-COO^-−H_2O−ZnL_3 as a unit in which the proton shifts easily to yield Glu-COOH−HO^-−ZnL_3; protonation of Glu-270 is commonly assumed to be responsible for the acid limb of the bell-shaped pH profiles with pK_a's of ∼6−6.5 and ∼9. A more detailed discussion of the complex problem of assigning these pK_a values to active site residues is given in section II.C.1 (thermolysin).

Concerning the proposed zinc−hydroxide mechanism[34] (Figure 4) the simultaneous activation of a water molecule and polarization of the substrate carbonyl group by the zinc ion has been questioned.[38] However, the additional role of Arg-127 in binding substrate analogues or tetrahedral mimics of the transition state is documented in X-ray diffraction studies, including one of the ketone (−)-3-(*p*-methoxybenzoyl)-2-benzylpropanoic acid where the carbonyl group binds to Arg-127 in preference to Zn.[43]

Tight Binding Inhibitors. Careful design by successive structure determination and modeling steps have yielded binding in the 11 fM range for a phosphonate inhibitor of carboxypeptidase (Figure 2).[44−46] A less extensive modeling technique was introduced to design inhibitors of angiotensin-converting enzyme (ACE), as a new class of orally administered antihypertensive pharmaceuticals;[47] in this procedure carboxypeptidase A (a monoexopeptidase) was used as a surrogate for ACE (an exodipeptidase) because the structure of ACE is not known. More recent studies have employed thermolysin for improvements of these antihypertensive agents.

Procarboxypeptidases. The structures of procarboxypeptidases A[48] and B[49] show that an activation domain of 95 residues makes direct contacts with the active site mostly in subsites S2−S4, similar in part to local interactions in the complex of carboxypeptidase A with a protein inhibitor from the potato.[50,51] The activation process and this inhibition by blocking of the active site are probably similar in the digestive carboxypeptidase A subfamily (carboxypeptidases A1, A2, B, and carboxypeptidase A from mast cell), and the nondigestive subfamily (carboxypeptidases E, N, and M);[50] these two subfamilies probably have structural homology even though the sequence similarity is low (15−20%).

2. Carboxypeptidases B and T Are Homologous to Carboxypeptidase A

X-ray structure analyses of carboxypeptidases B[49,52] and T[53] showed that these enzymes are very similar

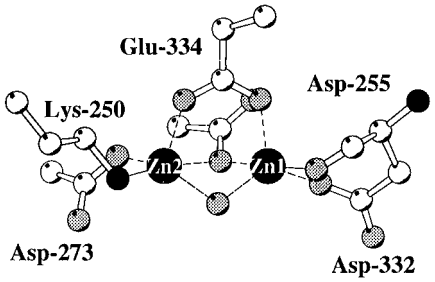

Figure 5. Structure of the dizinc cluster in the active site of leucine aminopeptidase.[60,61] Generated from PDB file 1LAM.[61]

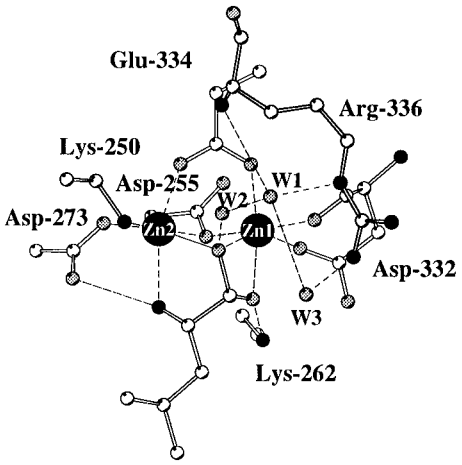

Figure 6. Binding mode of L-leucinal (Figure 2b) to the active site of leucine aminopeptidase.[61] One of the *gem*-diol oxygens displaces the metal-bridging water molecule (Figure 5), whereas the other oxygen is coordinated to the empty ligand position at Zn1. The amino group of the inhibitor coordinates to Zn2. The two water molecules W1 and W2 are only 2.3 Å apart in this structure and are probably a bihydroxide ion ($H_3O_2^-$). Generated from PDB file 1LAN.[61]

to carboxypeptidase A, including the active-site region. All catalytically important residues are conserved. Whereas carboxypeptidase A hydrolyzes preferably substrates with a large hydrophobic residue at the C-terminus, carboxypeptidase B prefers lysine and arginine residues at this position. Interestingly, carboxypeptidase T is able to cleave off both hydrophobic and basic amino acids with comparable efficiency.[54]

3. Zinc D-Ala-D-Ala Carboxypeptidase

In contrast to the serine-type D-Ala-D-Ala carboxypeptidases, the zinc D-alanyl-D-alanine carboxypeptidase does not catalyze transpeptidation reactions and has no structural relationship to the β-lactamases.[55−57] The crystallographic structure of the enzyme from *Streptomyces albus* revealed that His-152, His-193, and His-196 are zinc ligands.[58] Two aspartates (Asp-159 or Asp-192) could function as a general base, and Arg-136 and His-190 are positioned to bind the substrate or stabilize the transition state. The enzyme is homologous to Sonic hedgehog (section II.E.1)

4. Leucine Aminopeptidase, a Dizinc Peptidase

The ubiquitous aminopeptidases play a key role in protein modification and degradation and, in specific, metabolism of biologically active oligopeptides.[59] Altered aminopeptidase activity has been associated with several pathological disorders, e.g. cancer.

Leucine aminopeptidase (LAP) hydrolyzes the N-terminal amino acid from a polypeptide chain. The enzyme is a noncooperative homohexamer of 487 amino acid residues per monomer, including two Zn^{2+} ions, which are 3.0 Å apart, at the active site.[60,61] Each zinc ion is five coordinated in a coordination geometry best described as an octahedron in which one vertex is missing.[61] The two zinc ions are bridged by Glu-334 (bidentately), Asp-255 (monodentately), and a water molecule (Figure 5). Further ligands are Asp-332 (carbonyl and carboxylate groups) to Zn1 and Lys-250 and Asp-273 to Zn2.

The structure of the complex of LAP with L-leucinal shows binding of this potent inhibitor ($K_i = 60$ nM[62]) as the *gem*-diol,[63] thus resembling the *gem*-diolate intermediate in the reaction pathway (Figure 6). On the basis of this and other structures a reaction mechanism has been proposed, in which the substrate binds with its N-terminal amino group at the empty ligand position around Zn2 and the carbonyl group as a sixth ligand to Zn1 (Figure 7). Following this step is a nucleophilic attack of the Zn-bridging water molecule (or hydroxide ion). In contrast to polarization and pK_a reduction of zinc-bound water in the hydrophobic pocket of mononuclear zinc peptidases assisted by a general base, this enzyme apparently requires two Zn^{2+} in order to activate the

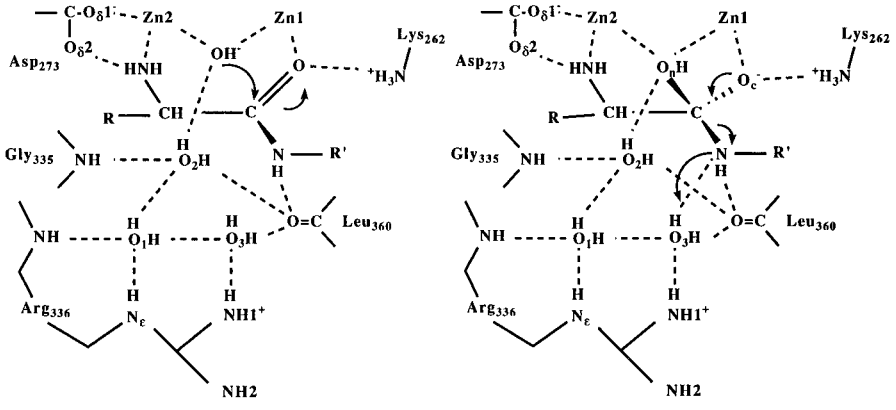

Figure 7. Proposed reaction mechanism for peptide hydrolysis by leucine aminopeptidase.[61] Water ligands 1 and 2 might be a bihydroxide ion which accepts a proton from the attacking nucleophile and shuttles it to the leaving group. (Reprinted with permission from ref 61. Copyright 1995 American Chemical Society.)

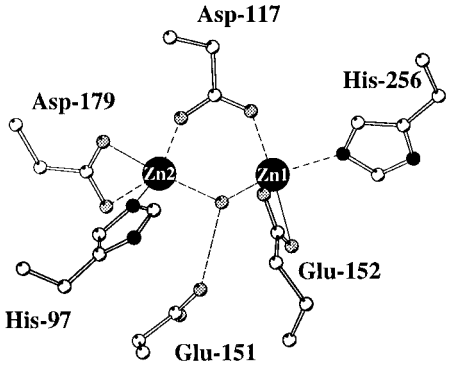

Figure 8. Structure of the dizinc center in the active site of *Aeromonas proteolytica* aminopeptidase.[23] Generated from PDB file 1AMP.[23]

catalytic water molecule. In addition to both zinc ions, Lys-262 and three water molecules, which are hydrogen bonded to Arg-336, stabilize the transition state. The precise role of these water molecules in the catalytic mechanism needs clarification (see also section II.F).

5. Aminopeptidase A has a Recombinase Function in E. coli

Aminopeptidase A from *E. coli* shows 31% sequence identity to bovine lens leucine aminopeptidase.[64] All zinc ligands and the catalytic active side residues are conserved. Interestingly, this enzyme has a role as an accessory protein in Xer site-specific recombination in *E. coli*.[65] The peptidase activity is not required for its recombinase function.

6. Aeromonas proteolytica Aminopeptidase Contains a Symmetrical Dizinc Site

The catalytic center of *A. proteolytica* aminopeptidase (AAP) has two Zn^{2+} ions 3.5 Å apart, bridged by a water molecule and bidentately by the carboxylate group of Asp-117 (Figure 8).[23] Both Zn^{2+} ions are five-coordinated. A striking feature of this metal center is the similarity of the coordination spheres of the two zinc ions. Probably, then, the water molecule is either displaced by substrate, or it might be the attacking nucleophile at the carbonyl carbon of the scissile peptide bond. Glu-151 is hydrogen bonded to the zinc-bridging water molecule.

The structure determination of a complex of AAP with a hydroxamate inhibitor showed that the hydroxamate group binds bidentate to the dizinc center such that the hydroxylamino oxygen bridges the two zinc ions and the keto group is coordinated to Zn1 (Figure 9).[66] The terminal amino group of the inhibitor is hydrogen bonded to Tyr-225. On the basis of this structure and a comparison to monozinc peptidases a role of Glu-151 as a general base was discussed.

The catalytic domain of AAP[23] is topologically similar to that of bovine lens leucine aminopeptidase in the sense that both have an eight-stranded pleated β-sheet and seven similarly placed helices.[64] However, this structural homology does not extend to the precise location or to the structure of the active site. Further studies with mechanism-based inhibitors might reveal if the dissimilarity of the active sites of

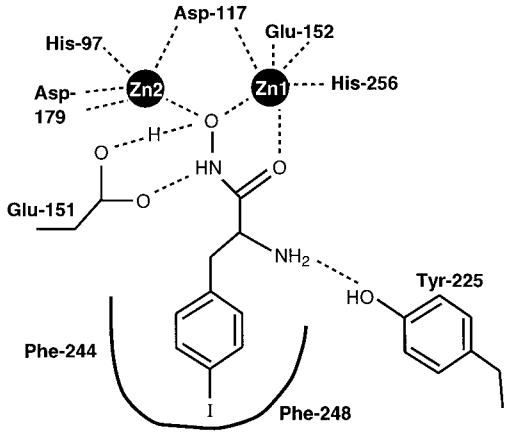

Figure 9. Scheme of the binding mode of *p*-iodo-D-phenylalaninehydroxamate to the active site of *Aeromonas proteolytica* aminopeptidase.[66] It is not clear whether Glu-151 or the hydroxylamine oxygen of the inhibitor is protonated.

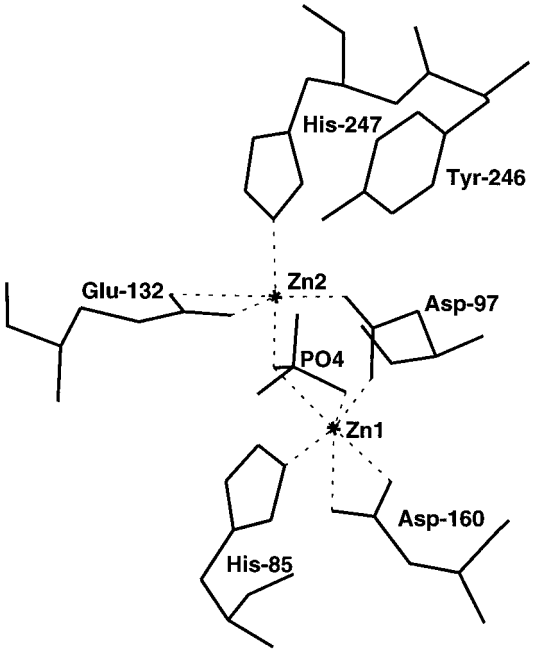

Figure 10. Environment of the dizinc center in *Streptomyces griseus* aminopeptidase.[68] The partially occupied phosphate ion was modeled on the basis of additional electron density in the active site. It was not added to the crystallization buffer. Note that the numbering of the zinc ions is reversed to that of the metal ions in the homologous *Aeromonas* aminopeptidase (Figure 8). (Figure provided by authors.[68])

LAP and AAP also extends to the enzyme mechanisms (see also section II.F).

7. Streptomyces griseus Aminopeptidase Is Homologous to Aeromonas Aminopeptidase

Sharing 24% sequence identity in aligned regions the two aminopeptidases from *S. griseus* (SGAP)[67] and *A. proteolytica* have a similar folding topology (rms deviation 1.1 Å for 161 aligned C_α atoms) and active-site structure.[68] All zinc ligands are conserved between the two enzymes (Figure 10). A remarkable difference in the active site is Tyr-246 in SGAP which replaces Ile-255 in AAP. In the crystal structure a partially occupied unknown molecule, most probably phosphate, is coordinated to the zinc ions. Phosphate binds such that one oxygen bridges the two zinc ions,

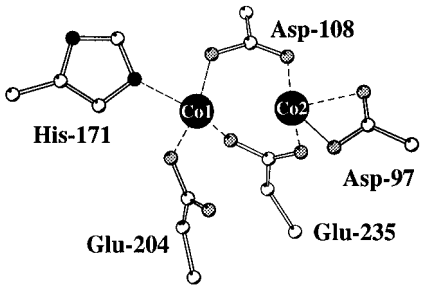

Figure 11. Structure of the dicobalt cluster in the active site of methionine aminopeptidase.[69] The identity of the metal ions bound *in vivo* is not yet clarified. Water ligands could not be unambigously detected at the resolution of this structure analysis. Generated from PDB file 1MAT.[69]

whereas another oxygen is coordinated only to Zn1 (Figure 10). Within hydrogen bonding distance to the remaining two phosphate oxygens are Glu-131, Arg-202, and Tyr-246.

8. Carboxypeptidase G2 Contains a Dizinc Center Similar to That in Aeromonas Aminopeptidase

Enzymes of the carboxypeptidase G class (also named glutamate carboxypeptidase, EC 3.4.17.11) hydrolyze the C-terminal glutamate moiety from peptides and from folic acid. In contrast to many structurally characterized carboxypeptidases and endopeptidases with a monozinc site the dimeric carboxypeptidase G2 from *Pseudomonas* sp. strain RS-16 contains a dizinc center similar to that in *Aeromonas* aminopeptidase in each subunit.[24] Residues Asp-141 (metal-bridging), Glu-176, His-385, Glu-200, and His-112 coordinate the two zinc ions. All ligands are conserved except for Glu-200 which is an Asp in the aminopeptidase. Also, a metal-bridging water ligand and the nearby glutamate side chain (151 in AAP, 175 in carboxypeptidase G2) are found in this structure. The sequence identity between the carboxypeptidase and the aminopeptidase is 14% in a structure-based alignment.

This novel carboxypeptidase structure will provide new insight into the catalysis of peptide hydrolysis, especially in relation to the dizinc aminopeptidases. It may also be a link in the distant evolutionary relationship between many exopeptidases, as outlined in the introduction of section II.B.

9. Methionine Aminopeptidase, a Dicobalt Enzyme?

Methionine aminopeptidase from *E. coli* cleaves the N-terminal amino acid, preferably adjacent to a small residue, from peptides and proteins. A structure has been established for the dicobalt enzyme, which has maximum activity.[69] However, the identity of the metal ions *in vivo* is not known. The two Co^{2+} ions are 2.9 Å apart and are ligated to the side chains of Asp-97, Asp-18, Glu-204, Glu-235, and His-171 (Figure 11). Remarkably, the coordination around both metal ions is approximately octahedral provided that one of the ligand positions is considered to be occupied sterically by the adjacent metal ion and that a water molecule is present as the sixth ligand to each Co^{2+}. These two solvent molecules could form hydrogen bonds to His-178 and Thr-99, respectively. However, it also seems reasonable that a single water molecule bridging the two metal ions may be present instead of these two added water molecules. Except for Glu-235, which is Gln in the enzyme from *Bacillus subtilis*, these metal-binding residues are conserved among homologous enzymes.[70]

Table 3. Metallopeptidases with HEXXH + E Zinc-Binding Motif[18]

enzyme	EC no.
family M4: thermolysin	
bacillolysin (*Bacillus cereus* neutral protease)[a]	3.4.24.28
coccolysin	3.4.24.30
extracellular endopeptidase (*Staphylococcus*)	–
extracellular endopeptidase (*Erwinia*)	–
extracellular endopeptidase (*Serratia*)	–
metalloendopeptidase (*Legionella*)	–
metalloendopeptidase (*Listeria*)	–
pseudolysin[a]	3.4.24.26
thermolysin[a]	3.4.24.27
vibriolysin	–
family M5: mycolysin	3.4.24.31
family M13: neprilysin	
endothelin-converting enzyme	–
kell blood group protein	–
neprilysin	3.4.24.11
peptidase O (*Lactococcus*)	–
family M1: membrane alanyl aminopeptidase	
alanyl/arginyl aminopeptidase (*Saccharomyces*)	–
aminopeptidase yseII (*Saccharomyces*)	–
glutamyl aminopeptidase	–
leukotriene A_4 hydrolase	3.3.2.6
lysyl aminopeptidase (*Lactococcus*)	3.4.11.15
membrane alanyl aminopeptidase	3.4.11.2
family M2: peptidyl-dipeptidase A	3.4.15.1

[a] A three-dimensional structure has been determined.

The structure of methionine aminopeptidase is entirely different from the other three dizinc aminopeptidase structures, both in the folding topology and in the active-site structure. The presence of two homologous domains in methionine aminopeptidase implicates a gene-doubling event.

10. The "Inverzincins" Contain a HXXEH Motif

A group of zinc metalloproteases, including bacterial protease III (pitrilysin) and insulin-degrading enzymes, contains an inverted motif HXXEH. Site-directed mutagenesis showed that the two histidines are involved in zinc binding and that the glutamate has a catalytic role.[71] Another Glu residue is present as a third zinc ligand.[72]

C. The Thermolysins

The thermolysin clan containing the "HEXXH + E" zinc-binding motif consists of five families (Table 3). For its best-studied member, thermolysin, an X-ray structure was solved in 1972 by Matthews and colleagues.[73] Since then also the structures of pseudolysin[74] and bacillolysin[75] have been determined.

1. Thermolysin Has an Active Site Arrangement Similar to That of Carboxypeptidase A Resulting from Convergent Evolution

Bacillus thermoproteolyticus thermolysin is a thermostable zinc endopeptidase with a molecular mass of 34.6 kDa.[76] In addition to the zinc ion thermolysin binds four calcium ions, which are necessary for its thermal stability.[73,76,77] In the unligated enzyme the zinc ion is coordinated by His-142, His-146, Glu-166, and one water molecule (Figure 12).[73,78] The zinc

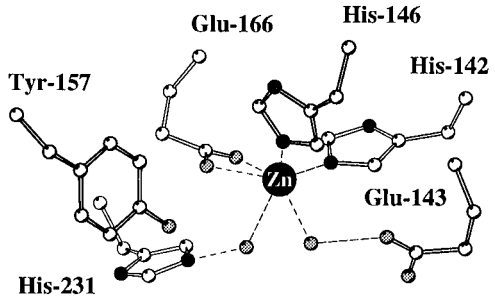

Figure 12. Structure of the active site of thermolysin.[78] Two alternatively occupied water positions were found in this structure analysis at 1.7 Å resolution. Generated from PDB file 1LNF.[78]

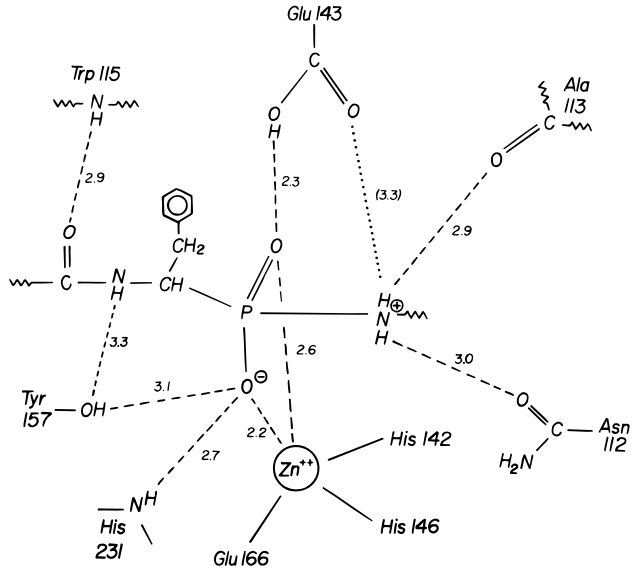

Figure 13. Schematic representation of the binding mode of a tripeptide phosphonamidate inhibitor (Figure 2f) to thermolysin.[81] This inhibitor is supposed to model the *gem*-diolate transition state of peptide hydrolysis. (Reprinted with permission from ref 81. Copyright 1987 American Chemical Society.)

coordination sphere was originally found to be approximately tetrahedral, with a single water position and a monodentate Glu-166.[73] However, in a more recent structure determination of thermolysin Glu-166 binds bidentately, and the coordinated water molecule has two alternatively occupied positions, which are 2 Å apart (Figure 12).[78] In one position the water molecule is hydrogen bonded to Glu-143, and in the other position to His-231. These differences are probably due to a slightly different pH of the buffer solution, from which the crystals were grown.

A number of structures with bound transition-state analogue inhibitors sheds light on the hydrolytic pathway.[79] Among these are complexes with phosphonamidate peptide inhibitors (Figure 2).[80] CBZ-L-Phe^{P}-L-Leu-L-Ala inhibits thermolysin with a K_i of 0.068 nM. Whereas one phosphonamide oxygen is strongly bound to the zinc ion, the other oxygen is more weakly coordinated at a distance of 2.6 Å (Figure 13).[81] However, the latter oxygen is in short hydrogen-bonding distance to the presumably protonated side chain of Glu-143. In addition, the side chains of His-231 and Tyr-157 are hydrogen bonded to the strongly zinc-bound oxygen. These phosphorus-containing inhibitors have also been used to study their binding energies and interactions by biochemical,[80,82] crystallographic,[79,83] and computational means.[84]

In the favored mechanism, which is supported by many crystallographic and biochemical studies and also by studies on homologous or functionally analogous enzymes (e.g. carboxypeptidase A) the zinc ion has two roles: it polarizes the carbonyl group and facilitates deprotonation of the water nucleophile (Figure 14).[79,80] Glu-143 accepts a proton from the zinc-bound water nucleophile and transfers it to the leaving group. Further stabilization of the transition state is provided by the side chains of Tyr-157 and His-231. As seen in several inhibitor complexes, the zinc ion is five-coordinated in the transition state. Thermolysin has a bell-shaped pH profile with pK_a values of about 5.3 and 8.0.[85] The pK_a value of 5.3 was attributed to a protonation of Glu-143 (pK_{a1} in Figure 15), or more specificically to the Glu-COO$^-$−H_2O−Zn linkage, whereas the pK_a of 8.0 is assumed to be due to a deprotonation of His-231.

Reverse Protonation Mechanism. An analysis of the kinetic parameters of the slowly hydrolyzed arazoformyl dipeptide substrates by thermolysin suggests that the bell-shaped pH profile with an acid limb around pH 5 and an alkaline limb at pH 8 results from two protonation equilibria: protonation of a residue affecting k_{cat} with a pK_a of 8.26 causes the acidic limb of the pH profile (around pH 5), whereas deprotonation of a residue with pK_a = 5.16 results in the alkaline limb (around pH 8) by affecting K_m (Figure 16).[86] This situation results in the same bell-shaped profile of k_{cat}/K_m as does a normal pro-

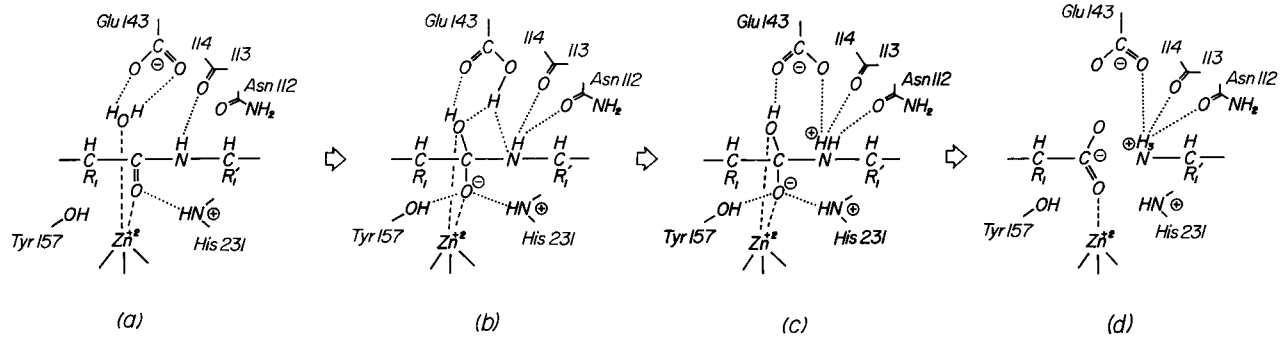

Figure 14. Proposed reaction mechanism for thermolysin in which the zinc-bound water ligand is the nucleophile.[79] Glu-143 serves as a general base and shuttles the proton to the leaving group. (Reprinted with permission from ref 81. Copyright 1987 American Chemical Society.)

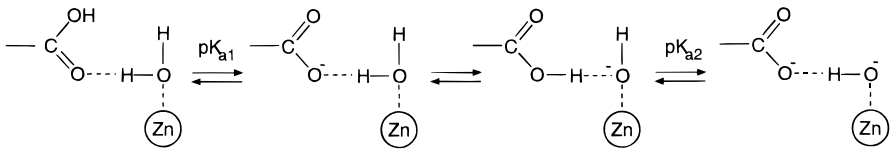

Figure 15. Protonation equilibria of the Glu−COO$^-$−OH$_2$−Zn linkage in many mononuclear zinc hydrolases. Most commonly the monoprotonated state is assumed to be the active configuration, in which the deprotonated catalytic base accepts a proton from a zinc-bound water molecule. As an alternative, the active state might require further deprotonation (pK_{a2}).

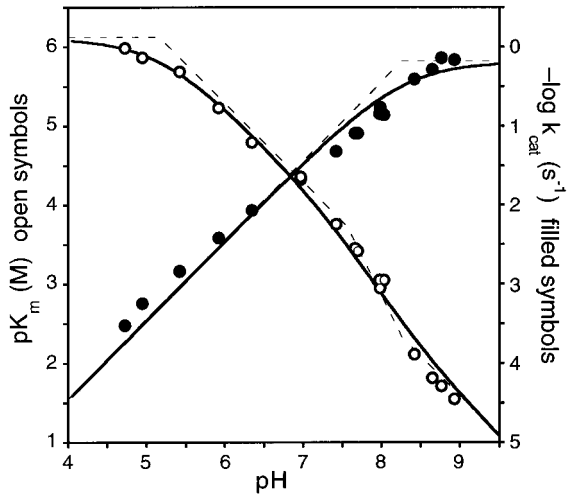

Figure 16. Dixon plot for the hydrolysis of *N*-[[(4-methoxyphenyl)azo]formyl]-L-leucyl-L-leucine catalyzed by thermolysin: −log K_m (open symbols) and log k_{cat} (filled symbols) versus pH.[86] These data support a reverse protonation situation, in which the bell-shaped pH profile of k_{cat}/K_m (not shown) is caused by a *high* pK_a of 8.26 on the acidic limb affecting k_{cat} (filled symbols) and by a *low* pK_a of 5.16 on the alkaline limb affecting K_m. (Reprinted with permission from ref 86. Copyright 1996 American Chemical Society.)

tonation-state mechanism in which the acid limb is caused by protonation of a residue with a pK_a around of 5.3 and the alkaline limb by deprotonation of a residue with a pK_a around 8.[87] The reverse protonation situation implies that the active form of the enzyme is only a small constituent of the distribution of enzymic protonation states, because it requires that a more acidic residue (here pK_a = 5.16) is protonated while the less acidic residue (here pK_a = 8.26) is deprotonated at a pH maximum around 6−7.

On the basis of these kinetic data and other results an alternative mechanism was proposed, in which the pK_a of 5.16 is attributed to the deprotonation of a zinc-bound water molecule causing the alkaline limb (Figure 17).[86] This zinc-coordinated water is replaced by the substrate carbonyl group, upon binding. The Zn−OH$^-$ form is supposed to be inactive because the hydroxide ion is too tightly bound to be replaced by the substrate. Here, the sole role of zinc is to polarize the carbonyl group, but not to facilitate deprotonation the nucleophile. The water nucleophile is activated by His-231 as a general base. This mechanism has no convincing role for the catalytic Glu side chain, which is conserved in almost all zinc peptidases and amidases (an exception is T7 lysozyme—see section II.E.2) and when mutated causes a most dramatic loss in activity. Furthermore, a pK_a of 5.16 appears somewhat low for the zinc-bound water molecule, which is hydrogen bonded to a negatively charged Glu side chain. Site-directed mutagenesis of His-231 demonstrated that loss of the His-231 side chain reduced k_{cat}/K_m by a factor of around 500, mainly due to changes in k_{cat}.[88] The enzymatic activities of these His-231 mutants showed little pH dependence at alkaline pH (no alkaline limb), which indicates that this residue has a pK_a of 5.16 and not 8.36 if one assumes a reverse protonation state. Also, the histidine residue is not conserved in some of the metzincins (section II.D). A similar reverse protonation mechanism has also been proposed for carboxypeptidase A catalysis (section II.B.1).

The reverse protonation situation as supported by the data shown in Figure 16 for slowly hydrolyzed substrates is also compatible with a slightly modified mechanism of Figure 14. Here, the pK_a of 8.26 might be due to the deprotonation of the zinc-bound water molecule (pK_{a2} in Figure 15). This implies that in the active conformation both the catalytic Glu and the water nucleophile are deprotonated. A pK_a around pH 8−9 for the zinc-bound water is supported

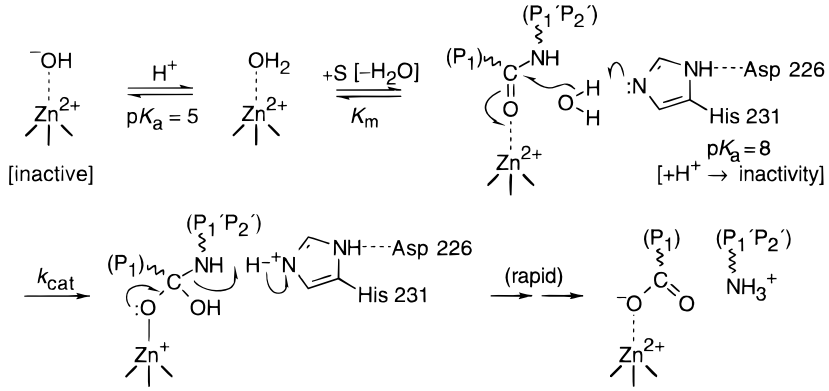

Figure 17. Alternative reaction mechanism for thermolysin catalysis based on the reverse protonation situation (Figure 13a).[86] In this mechanism His-231 acts as a general base. (Reprinted with permission from ref 86. Copyright 1996 American Chemical Society.)

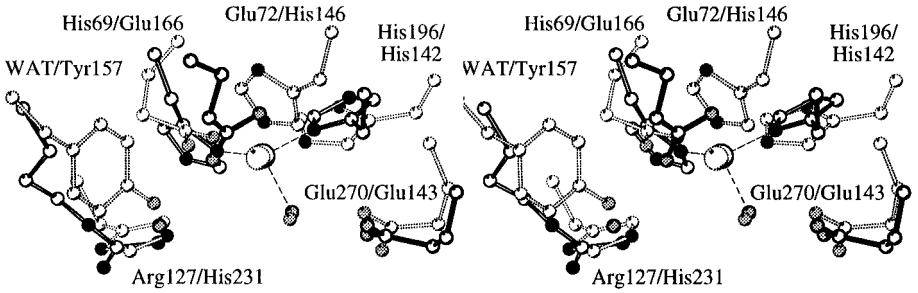

Figure 18. "Functional" superposition of the active sites of thermolysin and carboxypeptidase A, which are not evolutionary related. Residues of thermolysin are shown in broken lines. The labels refer to carboxypeptidase A/thermolysin. Generated from PDB files 5CPA[25] and 1LNF.[78]

by many model compounds[89] and by crystallographic studies on carboxypeptidase A.[90] It is also consistent with the influence of metal substitutions on the pK_a and ionization enthalpy ΔH_i (having values compatible with the (de)protonation of zinc-bound water but not of a Glu side chain) of the acidic limb, and no influence on the alkaline limb.[91] The pK_a of 5.16 can be assigned to His-231 in this mechanism, supported by the absence of the alkaline limb in the kinetics of His-231 mutants.[88]

The zinc ion can be exchanged against Co^{2+}, Mn^{2+}, and Fe^{2+} to yield enzymes with 200%, 10%, and 60% activity, respectively, of thermolysin.[92] X-ray structures of these metal-exchanged enzyme forms showed that the Co^{2+}- and Fe^{2+}-substituted thermolysins display some conformational changes in the active site that might cause the reduced activity.[78] Interestingly, the hyperactivated Co^{2+}-thermolysin has two water molecules bound to a five-coordinated cobalt ion. This finding might explain the hyperactivity of Co^{2+}-thermolysin, in that cobalt more readily adopts the presumed five-coordinate ligand sphere in the transition-state complex. Also, the assumption that both the substrate carbonyl group and the water nucleophile coordinate simultaneously to the metal ion (by increasing the coordination number of zinc in Zn-thermolysin and substituting one coordinated water in Co-thermolysin) is supported by this structure.

The active sites of thermolysin and carboxypeptidase can be functionally superimposed on the basis of the zinc ligands, the zinc-bound water molecule, and the catalytic glutamate side chains (Figure 18).[93] Interestingly, also Arg-127 in carboxypeptidase A and His-231 in thermolysin have similar positions, supporting an equivalent role of these residues in the proposed mechanisms. Thus, thermolysin and carboxypeptidase A, which have different folding topologies, are a classical example of the convergent evolution of active-site structures.

2. Pseudolysin (Elastase) Undergoes Hinge-Bending Motions in Catalysis

Pseudolysin, which was previously called elastase, is a zinc-containing endopeptidase that has 28% overall sequence homology to thermolysin.[94] These two enzymes also share a similar substrate specificity, although some differences exist in their detailed reactivities. Pseudolysin of *Pseudomonas aeruginosa* is one of the virulence factors of infections by this pathogen, as implicated by the enzyme's capability to degrade several molecules of biological significance to the host, including elastin and collagen.

The overall tertiary structure of pseudolysin is similar to that of thermolysin; differences are seen in the active-site cleft, which is more open in pseudolysin than in thermolysin.[74] In particular, all residues that are thought to be important in the mechanism of thermolysin, the zinc ligands and the active site histidine (His-223 in pseudolysin), glutamate (Glu-141), and tyrosine (Tyr-155), are conserved between the two enzymes. These residues were also found in a very similar configuration to that in thermolysin. The crystal structure, which was solved at a resolution of 1.5 Å, showed that Glu-164 (monodentate), His-140, His-144, and one water molecule (at 2.4 Å distance) form a slightly distorted tetrahedral coordination geometry around zinc.

Mutations of His-223 and Glu-141 strongly diminished activity of pseudolysin, consistent with the presumed catalytic roles of these residues.[95] All biochemical and structural results are consistent with a very similar mechanism of peptide hydrolysis by thermolysin and pseudolysin.

The finding that the active-site cleft in thermolysin is more closed than in pseudolysin and bacillolysin led to the hypothesis, that these neutral proteases, including thermolysin, undergo a hinge-bending motion during catalysis, by which the two domains move relative to another by up to 16°.[96] Indeed, the active-site cleft of pseudolysin is more closed in the presence of inhibitors.[74] The fact that such movements are not observed in inhibitor structures of thermolysin compared to the presumed structure of native thermolysin was explained by the observation of residual density in the active-site cleft, which was attributed to a bound dipeptide. This bound dipeptide may keep thermolysin in the closed conformation.

3. Bacillolysin (Bacillus cereus Neutral Protease)

Bacillolysin from *B. cereus* is an extracellular endopeptidase that shares 73% sequence identity to thermolysin.[97] All zinc ligands (His-143, His-147, Glu-167) and also the catalytic Glu (144 in bacillolysin), His (232), and Tyr (158) side chains are conserved and have similar conformations to those in thermolysin.[75] Thus, the two enzymes are assumed to employ the same catalytic mechanism. A water molecule is 2.0 Å away from zinc. The zinc ion may be described as four- or five-coordinated, since the glutamate side chain coordinates such that its two carboxylate oxygens are at distances of 2.1

Table 4. Metallopeptidases with HEXXH + H Zinc-Binding Motif[18]

enzyme	EC no.
family M12: astacin	
astacin subfamily	
astacin[a]	3.4.24.21
blastula protease-10 (*Paracentrotus*)	
bone morphogenetic protein 1	
choriolytic enzyme (*Oryzias*)	
meprin	3.4.24.18
metalloendopeptidase (*Caenorhabditis*)	
PABA-peptide hydrolase	3.4.24.18
SpAN protein (*Strongylocentrotus*)	
tolloid gene product (*Drosophila*)	
UVS.2 protein (*Xenopus*)	
reprolysin subfamily	
adamalysin[a]	3.4.24.46
atrolysin A	3.4.24.1
atrolysin C[a]	3.4.24.42
atrolysin D	3.4.24.42
atrolysin E	3.4.24.44
endopeptidase (green habu snake)	
α-fibrinogenase	
fibrolase (southern copperhead snake)	
haemorrhagic factor LHFII (bushmaster snake)	
HR1B-endopeptidase (habu snake)	
HR2a-endopeptidase (habu snake)	
jararhagin	
myelin-associated metalloproteinase (cattle)	
ORF9 Metalloendopeptidase (human)	
PH-30 α subunit	
ruberlysin	3.4.24.48
russellysin	3.4.24.58
trimerelysin II	3.4.24.53
family M10: interstitial collagenase	
serralysin subfamily	3.4.24.40
metalloprotease from *Serratia marcescens*[a]	
alkaline protease from *Pseudomonas aeruginosa*[a]	
matrixin subfamily	
envelysin	3.4.24.12
gelatinase A	3.4.24.24
gelatinase B	3.4.24.35
interstitial collagenase[a]	3.4.24.7
macrophage elastase	
matrilysin[a]	3.4.24.23
metalloproteinase (soybean)	
neutrophil collagenase[a]	3.4.24.34
stromelysin 1[a]	3.4.24.17
stromelysin 2	3.4.24.22
membrane-bound metalloendopeptidase	
family M11: autolysin	3.4.24.38
family M7: streptomyces small neutral protease[a]	

[a] A three-dimensional structure has been determined.

and 2.5 Å. Like thermolysin, bacillolysin also contains four calcium ions, which may account for a moderate thermostability.[75,98] A difference between the structures of thermolysin and bacillolysin is that the active-site cleft is more open in bacillolysin, similar to the situation in pseudolysin.

Site-directed mutagenesis of Glu-144 and His-232 showed that both residues are critical for catalysis.[99] The mutant enzymes were secreted only at low levels, suggesting autoproteolytic cleavage of the enzyme precursor prior to secretion.

D. The Metzincins

This clan, which contains only endopeptidases, consists of four families (Table 4). In contrast to the peptidases of the HEXXH + E clan a histidine replaces the glutamate as the third protein ligand to zinc. More specifically, the zinc-binding motif is **HE**XX**H**XX**G**XX**H** in these peptidases. Also, a methionine residue is conserved in all enzymes of this clan; this Met is not present in thermolysin and closely related enzymes and led to the name "metzincins".[100] This methionine is part of a turn filling a hydrophobic pocket near the active site and is presumably important for the correct conformation and stabilization of the active site. The metzincins display some structural similarity to the thermolysin clan in four β-strands and two long α-helices of the catalytic domains, indicating that the two clans are distantly related.

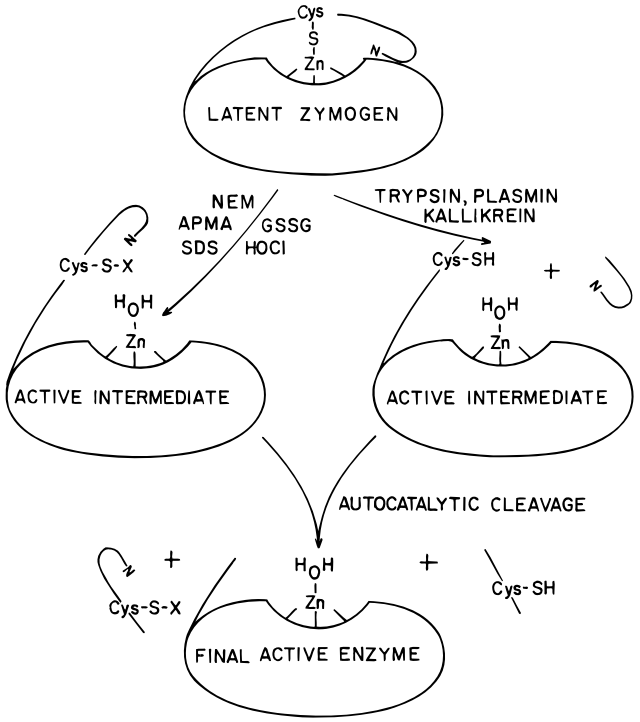

Figure 19. Cysteine switch mechanism for the activation of some metalloproteases.[101] (Reprinted with permission from ref 131. Copyright 1991 FASEB.)

1. A Cysteine-Switch Mechanism of Proenzyme Activation

Many, but not all, metzincins are activated by a cysteine-switch mechanism from an inactive latent form to the active enzyme, prior to autolytic cleavage.[101] As shown in Figure 19 the latent form has a cysteine residue bound to a four-coordinated, inactive zinc ion. This inactive enzyme can be activated by different means, which modify the cysteine group or prevent binding by proteolysis or conformational changes induced by surfactants or chaotropic ions. *In vivo* proteolytic cleavage of the propeptide leads to activation. The X-ray structure of the proenzyme of stromelysin-1 supports this activation mechanism in that it shows that the zinc ion is coordinated to the sulfur of Cys-75 of the propeptide.[102]

2. Astacins Contain Tyrosine as a Fifth Zinc Ligand

Physiological activities of the astacin family, which was recognized in 1990,[103] include digestion (astacin), regulation of embryonic development, and peptide processing (meprin).[104] The zinc content of these enzymes was established for astacin, meprin A, and choriolysin H and L.[105,106] Astacin, a digestive endopeptidase from the crayfish *Astacus astacus* L., was

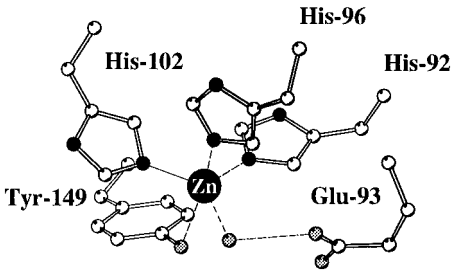

Figure 20. Structure of the zinc center of astacin. Generated from PDB file 1AST.[107]

the first peptidase of the metzincin clan to have its three-dimensional structure determined.[107] This structure also inferred structural features of other members of the astacin family, including meprin A.[108,109] In particular, the amino termini of all astacins can be modeled in a position near the active site, implicating an activation mechanism by proteolytic cleavage of the N-terminus of proforms of the enzyme. The astacins are not activated by a cysteine-switch mechanism.

In contrast to the enzymes of the thermolysin clan, the zinc ion in astacin is coordinated by five ligands in a trigonal-bipyramidal way: Tyr-149 and His-96 occupy the axial positions, whereas His-92, His-102, and a water molecule are in the equatorial plane (Figures 20−22).[107,110] A carboxylate side chain (Glu-93) is hydrogen bonded to the zinc-bound water nucleophile, similar to the situation in carboxypeptidase A and thermolysin (and homologues). Despite the very low sequence homology (only five out of 200 sequence positions are identical) astacin and thermolysin can be superimposed on the basis of the active-site helix bearing the HEXXH motif (Figure 21).[107,110] The zinc−water−glutamate linkage and the two imidazole zinc ligands superimpose fairly well. Also His-102 has a similar position to that of Glu-166 in thermolysin. The additional zinc ligand, Tyr-149, is near His-231 in thermolysin. Thus, both enzymes probably employ similar reaction mechanisms in which the zinc-bound water molecule is the nucleophile. Tyr-149 might have a similar role to that of His-231 of thermolysin in the polarization of the substrate carbonyl group (see also the section on serralysins).[107,108]

The zinc ion of astacin can be removed by chelation with 10 mM *o*-phenanthroline, yielding the inactive apoenzyme.[105] Besides Zn^{2+} (100% activity) Co^{2+} and Cu^{2+} restore 140% and 37% of the activity, respectively, whereas Ni^{2+}- and Hg^{2+}-astacin display almost no activity. The activities of the various metal-exchanged enzymes could be related to the structure of the metal coordination sphere: Co^{2+} and Cu^{2+} are five-coordinated like Zn^{2+}; Ni^{2+} coordinates an additional water ligand, yielding 6-fold coordination, whereas Hg^{2+} has no observable ordered water solvent structure in its coordination sphere (Figure 22).[111]

3. The Snake Venom Metalloproteinases (Reprolysins): Adamalysin, Atrolysin C, and H_2-Proteinase

Reprolysins[112] are among the most poisonous agents of snake venoms. Like the functionally similar matrix metalloproteinases they seem to be primarily involved in the hydrolysis of the extracellular matrix. All reprolysins characterized so far are inhibited by metal chelators and contain zinc. The hemorrhagic and proteolytic activity of atrolysin is dependent on the presence of zinc.[113] X-ray structures of adamalysin[114] and atrolysin[115] revealed the presence of one calcium ion, which probably serves a structural role.

Adamalysin II, previously known as proteinase II, was the first reprolysin for which a crystal structure

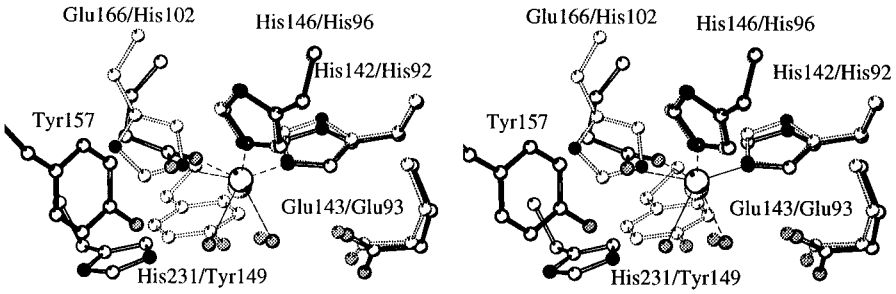

Figure 21. Superposition of the active sites of astacin and thermolysin. Residues for astacin are shown in broken lines. The labels refer to thermolysin/astacin. Generated from coordinate files 1LNF[78] and 1AST.[107]

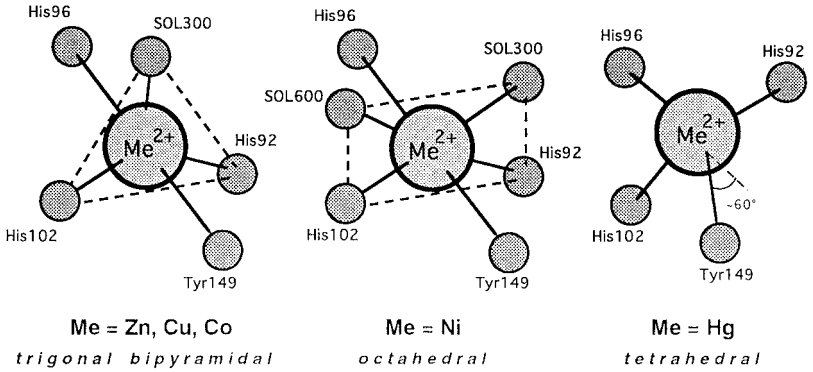

Figure 22. Metal coordination in Zn(II)-, Cu(II)-, Co(II)-, Hg(II)-, and Ni(II)-astacin structures.[111] (Reprinted with permission from ref 111. Copyright 1994 The American Society for Biochemistry and Molecular Biology.)

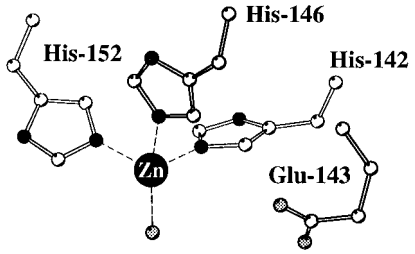

Figure 23. Active site structure of adamalysin II.[114] The distance between the zinc-bound water molecule and Glu-143 is 4.1 Å. Generated from PDB file 1IAG.[114]

became available (2.0 Å resolution).[114] The 24 kDa zinc endopeptidase was isolated from the venom of the eastern diamondback rattlesnake *Crotalus adamanteus*.[116] Its structure of the active site revealed very close similarity to that of astacin. However, the tyrosine ligand to zinc in astacin is missing in adamalysin II (the equivalent sequence position is a proline in adamalysin). Thus, the zinc ion is tetrahedrally coordinated by three histidines (142, 146, and 152) and a water ligand (Figure 23). Interestingly, the nearest carboxylate oxygen atom of Glu-143, the presumed general base, is relatively far away (4.1 Å) from the zinc-bound water molecule. Another remarkable result from this structure is the absence of residues equivalent to His-231 or Tyr-157 in thermolysin (superposition not shown). Thus, adamalysin achieves an efficient catalysis with an apparently simpler active-site arrangement.

A conserved PKM**C**GVT sequences is located in several reprolysin precursors. The cysteine has been proposed to bind to the zinc ion in an inactive form of the enzyme, prior to activation by a cysteine-switch mechanism as previously proposed for the matrix metalloproteinases.[117] Strong experimental support for this hypothesis could be obtained from the inhibition kinetics of several synthesized cysteine-containing peptides,[118] one of which, PKMCGV-NH_2 corresponding to the conserved sequence, was the strongest inhibitor (K_i = 3.4 μM) of adamalysin II.

Atrolysins are homologous zinc proteases from the western diamondback rattlesnake *Crotalus atrox*.[119] The zinc ion is critical for proteolytic and hemorrhagic activities, but it can be replaced with Co^{2+} without significant loss of activity.[120] This cobalt-exchanged enzyme displays an electronic spectrum in the visible region typical for a distorted tetrahedrally coordinated Co^{2+} ion.

The 2.2 Å structure of native atrolysin C showed a zinc ion tetrahedrally coordinated by three histidines (142, 146, and 152) and a water molecule.[115] As in adamalysin II this water molecule is relatively far away (4.1 Å) from Glu-143. Besides the structure of the native enzyme two cocrystal structures with dipeptide analogue inhibitors were determined. Figure 24 shows the binding mode of a dipeptide inhibitor (SCH 47890, K_i = 0.52 μM) to atrolysin C. The dipeptide coordinates to the zinc ion with both carboxylate oxygens of the C-terminal side chain. One of these oxygens is also hydrogen bonded to Glu-143 (3.3 Å). The other zinc-bound oxygen is not at a hydrogen-bonding distance to any other protein residue. This structure might model a product binding mode. In contrast to the proposed hinge-bending

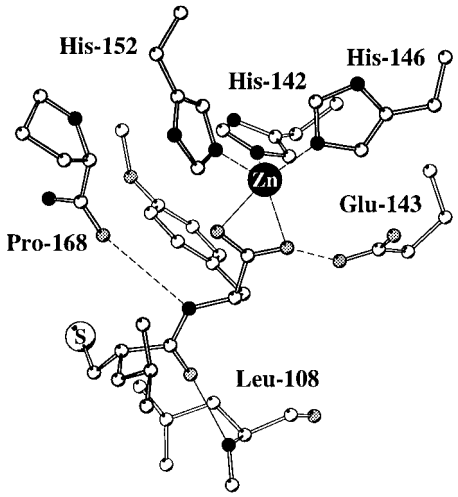

Figure 24. Binding mode of a dipeptide inhibitor (SCH 47890) to atrolysin C.[115] The terminal carboxyl group coordinates bidentately to the zinc ion. Generated from PDB file 1ATL.[115]

motions for catalysis by enzymes of the thermolysin clan, the structures of adamalysin and atrolysin indicate no significant conformational changes upon substrate or inhibitor binding.

In the X-ray structure of *H_2-proteinase* (which is distinct from proteinase II) from the venom of *Trimeresurus flavoviridis* (Habu snake), the catalytic water molecule is closer to the catalytic base Glu-143 (3.4 Å).[121] This structure was determined at pH 8.0, near the pH optimum of the activity. The longer distance of 4.1 Å between the zinc-bound water and the catalytic base observed in adamalysin II may be due to the lower pH value of 5.0 in that structure determination, causing a protonation of the glutamate. The crystals of atrolysin C were grown at pH 6.8.

4. Serralysins and a "Tyrosine-Switch" Catalytic Mechanism

The serralysins produced by *Pseudomonas aeruginosa* and *Serratia marcescens* show sequence identities of 55%.[122] The proteases secreted by these pathogenic bacteria contain one zinc ion per molecule.[123] Their specific targets *in vivo* are not known with certainty. Alkaline protease of *P. aeruginosa* was the first X-ray structure of a serralysin, determined at 1.64 Å resolution.[124] A mixture of different peptides (four residues) was found in the active site, probably products of enzymatic cleavage. The zinc ion is coordinated by the three histidines (176, 180, and 186), and the two carboxylate oxygens of the C-terminus of the tetrapeptide (Figure 25). Glu-177 and Tyr-216 are hydrogen bonded to these carboxylate oxygens. However, in the structure of the unliganded enzyme Tyr-216 has a different side chain conformation and is liganded to the zinc ion (Figure 25).[125] Thus, in native *P. aeruginosa* alkaline protease the zinc ion has a trigonal-bipyramidal ligand sphere similar to that previously found in astacin. It appears possible that during a catalytic cycle of *P. aeruginosa* alkaline protease (and possibly of astacin) Tyr-216 changes its conformation between zinc-ligation and transition-state stabilization, serving a similar role as that of His-231 in thermolysin.

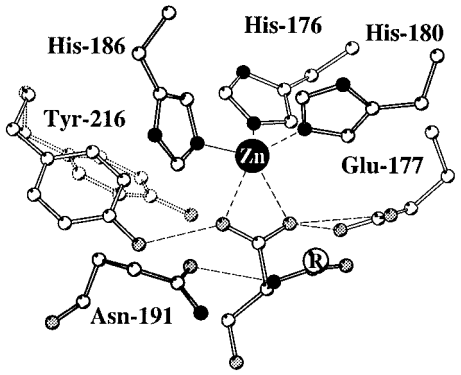

Figure 25. Structure of the active site of *P. aerigunosa* alkaline protease with a bound heterogenous tetrapeptide, of which only the C-terminal serine residue is shown.[124] Superimposed onto this structure is the conformation of the Tyr-216 side chain in the unliganded enzyme, where it is coordinated to the zinc ion.[125] Generated from PDB files 1KAP[124] and 1AKL.[125]

Crystal structures of the protease of *S. marcescens* in the presence and absence of a protein inhibitor (10 kDa) also showed that Tyr-216 is coordinated to the zinc ion in the unliganded enzyme, whereas in the cocrystal structure it is hydrogen bonded to the carbonyl group of the N-terminal residue of the protein inhibitor.[126] Thus, the N-terminus of the inhibitor protrudes into the active site. The carbonyl group of Ser-1 of the inhibitor is bound to the four-coordinated zinc ion. It is difficult at this stage to determine to what extent the binding mode of the inhibitor's N-terminal residues, which occupy the S′ sites of the protease, model the substrate binding mode. However, Tyr-216 has the same conformation in this structure as it has in the structure of the alkaline protease with a bound peptide. In the native enzyme the zinc ion is five-coordinated by the three histidines (same residue numbers in both enzymes), the tyrosine, and a water molecule in a very similar way as is the zinc ion in the alkaline protease structure (Figure 25).[126]

In both structures of the unliganded proteases the loop of residues 190 to about 200 at the entrance of the active site is disordered.[125,126] This loop becomes ordered in the presence of substrate and closes the active site. Asn-191 forms hydrogen bonds to amide bonds of the bound peptide (Figure 25).[124,126] This interaction seems to be a unique feature of the serralysins compared to other metzincins.

5. Matrix Metalloproteases (Matrixins): Cleavage of a Triple Helix

The interstitial collagenases are endopeptidases that cleave the undenatured, triple-helical portions of collagen.[127] Whereas the bacterial collagenases digest collagen into a mixture of small peptides, the vertebrate collagenases, including neutrophil and fibroblast collagenases,[127,128] gelatinases,[129] and stromelysin,[130] hydrolyze the peptide bonds of all three α peptide chains at one specific site. Acting on the extracellular matrix the matrixins are involved in tissue remodeling, e.g. in growth, development, and wound healing, but also in pathological processes, such as tumor invasion and arthritis.[131]

Most matrixins consist of three domains (from N- to C-terminus): the propeptide domain, which is

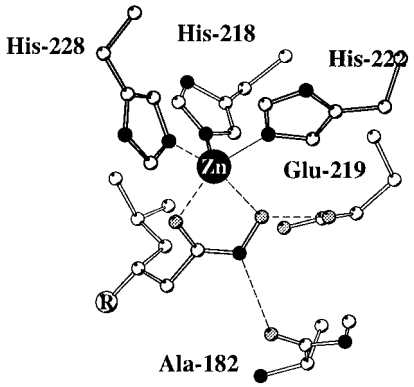

Figure 26. Binding mode of a peptide hydroxamate inhibitor to the zinc center in fibroblast collagenase.[142] The hydroxamate group coordinates bidentate to zinc such that the carbonyl group and the hydroxyl group are in *cis* conformation. Generated from PDB file 1HFC.[142]

cleaved off during activation of the proenzyme by the cysteine-switch mechanism, the catalytic domain, and a hemopexin-like domain. The catalytic domain alone is able to hydrolyze peptide substrates. However, the cleavage of the triple-helix of collagen requires the presence of the C-terminal hemopexin-like domain. This domain has significant sequence homology to hemopexin, a glycoprotein involved in heme transport.[132] Human neutrophil collagenase is highly glycosylated; one-third of its molecular weight consists of carbohydrates.[133]

Spatial structures are available for human neutrophil collagenase,[134−138] human fibroblast collagenase,[139−142] porcine synovial collagenase,[143] stromelysin-1,[102,144] and matrilysin.[145] The catalytic domains of these enzymes are similar to the catalytic domains of the astacins, reprolysins, and serralysins. Besides the catalytic zinc ion, which is bound to the protein by the three conserved histidines, another tetrahedrally coordinated structural zinc ion is present in the catalytic domain. Determination of the zinc content indicated that only one zinc ion is present in the full-length enzyme (including the C-terminal domain).[146] However, the X-ray structure of full-length porcine synovial collagenase showed the presence of two zinc ions in the catalytic domain.[143] In addition, one to three calcium ions were found in the catalytic domains in these matrixins. In contrast to the astacins and serralysins no zinc-coordinated tyrosine ligand is present in the matrixin structures.

Most of the crystallographic studies are cocrystal structures with a bound inhibitor which was added in order to prevent autolysis and to study the binding mode of these inhibitors, which could serve as drugs.[21] Peptide hydroxamates coordinate to the zinc ion such that the hydroxamate group adopts a *cis* conformation, and its carbonyl and hydroxyl group coordinate to the zinc ion which is then five coordinated (Figure 26).[134−136,138,141−143,145] The hydroxyl group is also hydrogen bonded to the catalytic glutamate side chain. Other inhibitor complexes include peptide analogues which have a carboxylate,[139,140,144,145,102] sulfodiimine,[145] or a thiol group[135] coordinated to zinc. The carboxylate groups bind bidentate to the zinc ion, whereas the sulfodiimine and thiol groups bind monodentately. In two crystal forms of human fibroblast collagenase the molecules

are packed such that the amino terminus binds to the active site of a another molecule of the crystal structure.[140] The amino-terminal peptide strand protrudes toward the zinc ion and coordinates to the metal via the backbone amino and carbonyl groups of the NH_2-terminal residue. Interestingly, the propeptide chain in the structure of prostromelysin-1 binds in an opposite amino-to-carboxyl direction from that of the peptide inhibitor complexes of collagenases.[102]

When compared, for example, to the phosphoamidates, these inhibitors are less perfect transition-state analogues, and they also do not resemble a substrate very closely. Nevertheless, these structures can be used to model the substrate binding mode by replacing the inhibiting functional group with a amide bond, followed by remodeling or energy minimization.[135,145,140,142] Such studies indicate that the reaction mechanism is very similar to the one proposed for thermolysin (Figure 14). The binding modes for the substrate's carbonyl group and the water nucleophile to the zinc ion as well as the role of the catalytic glutamate as a general base are proposed to be similar. Also, the NH group of the cleavable substrate's amide bond is hydrogen bonded to a backbone carbonyl group of the protein as in thermolysin. Notable differences are the absence of residues equivalent to Tyr-157 and His-231 in thermolysin, which could assist in the stabilization of the negatively charged transition state.

Most of the X-ray structures of the matrixins were of a fragment in which the C-terminal hemopexin-like domain is missing. The structure of this hemopexin-like domain, which is necessary for cleavage of the collagen triple helix was determined by the structure analysis of full-length porcine synovial collagenase[143] and as the isolated C-terminal domain of human gelatinase.[147] This domain consists of a four-bladed β-propeller that is connected to the N-terminal domain via an exposed linker of 17 residues, which is probably flexible. Matrilysin, which cleaves gelatins but not the triple-helix collagens, does not contain a hemopexin-like C-terminal domain.[148] Modeling studies further indicate that the whole triple helix of collagen would not fit into the active site. Therefore, the helix must partially unfold around the cleavage site in order to allow one peptide strand to bind to the active site.

The matrixins are selectively inhibited by certain protein inhibitors of 20−30 kDa molecular mass.[149] These tissue inhibitors of matrix metalloproteinases (TIMPs) share around 40% sequence identity with one another. TIMPs inhibit active matrixins by forming tight-binding, noncovalent 1:1 complexes. These inhibitors are found in body fluids and tissue extracts, and regulate the diverse processes in which the matrixins are involved. A structural analysis of a TIMP−matrixin complex is not yet available; however, the structure of TIMP-2 was obtained by NMR.[150]

6. Leishmanolysin Contains an Insert into the $HEX_2HX_2GX_2H$ Motif

Leishmanolysin has an active site structure that is similar to that of collagenase and other metzincins.[151] The zinc is coordinated by three histidines. However, a large insert is present between the second and the third histidine of the longer consensus sequence **HE**XX**H**XX**G**XX**H**.

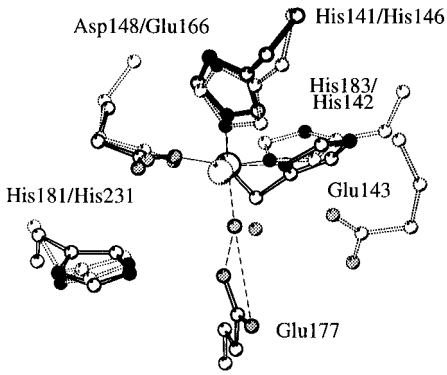

Figure 27. Superpostion of the zinc site in sonic hedgehog onto the active site in thermolysin (broken lines).[154] Labels refer to sonic hedgehog/thermolysin. Generated from PDB files 1VHH[154] and 1LNF.[78]

7. Streptomyces caespitosus Small Neutral Protease, a Metzincin Homologue That Has One of the His Ligands Mutated to Asp

The recently determined amino acid sequence and 1.6 Å X-ray structure of a zinc metalloendoprotease from *Streptomyces caespitosus* showed that the zinc ion is coordinated by two histidines (83 and 87) and one aspartate (93) of the motif **HE**XX**H**XX**G**XX**D**.[152] Thus, the histidine of the enzymes of the HEXXH + H clan is replaced by an aspartate (HEXXH + D). Despite the lack of further sequence homology, the *S. caespitosus* protease is topologically similar to the thermolysins and metzincins, including a Met-turn equivalent to the metzincins. A water molecule, which is hydrogen bonded to Glu-84, completes the tetrahedral zinc ligand sphere.

E. Other Peptidases or Amidases

1. Sonic Hedgehog and an Unanticipated Zinc Hydrolase Active Site

The secreted proteins of the hedgehog family play an important role in cell-to-cell signaling during embryonic development of several organisms, from *Drosophila* to mouse.[153] A surprising result of the 1.7 Å X-ray structure of the amino-terminal domain of murine Sonic hedgehog was the presence of a zinc ion, tetrahedrally coordinated by His-141, His-183, Asp-148, and a water molecule.[154] Furthermore, the side chain of Glu-177 is hydrogen bonded to the zinc-bound water, yielding an active-site arrangement similar to that in thermolysin and other zinc peptidases (Figure 27). However, Sonic hedgehog has obviously no evolutionary relationship to thermolysin, as revealed by its dissimilar folding topology. The similarity of the active site arrangement led to the hypothesis that sonic hedgehog might catalyze a proteolytic reaction, possibly by a similar mechanism as assumed for the other mononuclear zinc peptidases.[154] His-135 appears to be appropriately positioned to polarize the peptide carbonyl group. Sonic hedgehog shows structural homology to the zinc DD-carboxypeptidase from *Streptomyces albus* G (section

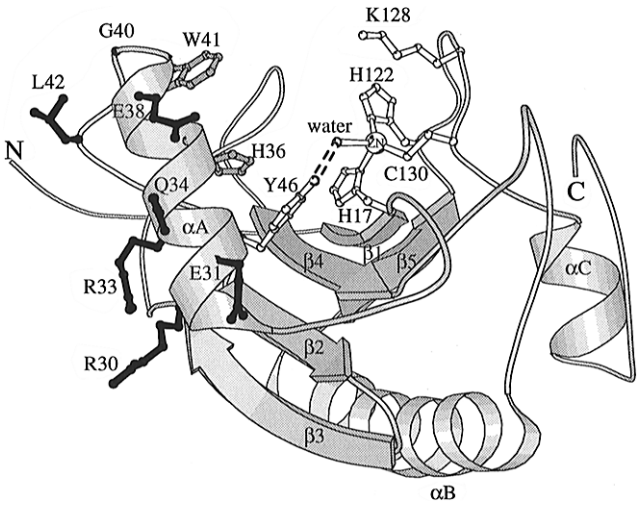

Figure 28. Structure of T7 lysozyme including the active center. Note that this amidase contains no Asp/Glu side chain but a Tyr side chain hydrogen bonded to the zinc-bound water ligand.[158] (Reprinted with permission from ref 158. Copyright 1994 National Acadamy of Sciences USA.)

II.B.3).[155] All residues of the zinc-binding sites are conserved (see ref 155 for a superposition).

A proteolytic function of the zinc center of sonic hedgehog is also supported by the finding that the carboxy-terminal peptide strand is bound to the active site of an adjacent protein molecule in the crystal structure, revealing potential substrate binding pockets. Possible functions of a proteolytic activity include autoproteolytic action in order to release the cell-tethered protein from the membrane, or proteolytic processing of a receptor for activation. However, the ability of sonic hedgehog to hydrolyze peptide bonds, and its natural target, remains to be determined.

2. T7 Lysozyme, a Monozinc Hydrolase without a Catalytic Glu/Asp Residue

The small 150 amino acid lysozyme of bacteriophage T7 cleaves the amide bond between *N*-acetyl muramic acid and L-alanine in the peptidoglycan layer of bacterial cell walls.[156] In addition, T7 lysozyme binds specifically to T7 RNA polymerase and thereby inhibits its transcription activity.[157,158]

The catalytic divalent metal ion is Zn^{2+}, although Co^{2+} and to a lesser extent Mn^{2+} show activity. This zinc ion is coordinated by His-17, His-122, Cys-130, and a water ligand which is hydrogen bonded to Tyr-46 (Figure 28).[158] These features superimpose on His-69, Glu-72, His-196, H_2O and Glu-270 of carboxypeptidase A, respectively, and on Glu-166, His-146, His-142, H_2O, and Glu-143 in thermolysin, respectively, although the structures of these enzymes are entirely different. In addition, Lys-128 of T7 lysozyme is in the position of Arg-127 of carboxypeptidase A or His-231 of thermolysin; these residues aid in polarization of the carbonyl group of the scissile peptide bond. A remarkable feature of this structure is the absence of a carboxylate side chain hydrogen bonded to the zinc-bound water molecule. Instead, Tyr-46 of T7 lysozyme is in a position to be involved in the proton transfer from the zinc-bound water to the NH of the scissile amide bond, a function attributed to Glu-270 in carboxypeptidase A[34] and Glu-143 in thermolysin.[79] Thus, further mechanistic and structural studies on this enzyme promise fundamental insight into zinc hydrolase mechanisms. Mutational analysis of Lys-128 and Tyr-46 support important roles of these two residues (kinetic parameters have not been determined).[158]

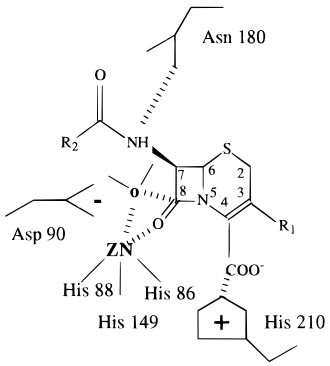

Figure 29. Schematic diagram of the proposed substrate binding mode of a cephalosporin molecule to β-lactamase II.[55] (Reprinted with permission from ref 55. Copyright 1995 Oxford University Press.)

3. Peptide Deformylase

This enzyme removes the formyl group from the N-terminus of polypeptides. A three-dimensional structure is not known yet, but a study of mutants indicate that Cys-90, in addition to His-132 and His-136 of an HEXXH motif, also binds to the catalytic zinc ion.[159] These mutant studies indicate that peptide deformylase may belong to a new class of zinc enzymes bearing the HEXXH motif, and also indicate that zinc is involved in the catalytic mechanism.

4. β-Lactamase Confers Resistance to Antibiotics

The use of Zn^{2+} as a cofactor is somewhat unusual among β-lactamases (penicillinases), which open the four-membered β-lactam ring by a hydrolytic reaction (Figure 29). More prevalent are metal-independent β-lactamases which have a serine nucleophile. *Bacillus cereus* β-lactamase II catalyzes the hydrolysis of essentially all β-lactams. The Zn^{2+} ion is coordinated to His-86, His-88, and His-149 and probably to a water molecule.[55] This zinc ion can be replaced by Mn^{2+}, Co^{2+}, Cd^{2+}, or Hg^{2+} yielding active enzymes; of these, the zinc enzyme is the most active.[162,163] Modeling of a cephalosporin molecule in the active site places the substrate's carboxylate group near His-210, a carbonyl group of the substrate on Zn^{2+}, and the zinc-bound H_2O (or OH^-) near the carbon of the carbonyl group of the β-lactam ring (Figure 29). Proton transfers in the hydrolysis step may be mediated by Asp-90, and possibly by Cys-168 which is 2.9 Å from the oxygen of the zinc-bound water ligand. This mechanism is further supported by a comparison of the active sites of this β-lactamase and carboxypeptidase A, although there is no structural homology in the remainder of these two enzymes. In addition, mutants of Asp-90, Cys-168, and His-210 imply a catalytic role for these residues.[160,161]

B. cereus β-lactamase is homologous to the metallo β-lactamase from *Bacteroides fragilis*, which contains two active-site zinc ions (see next section). Indeed, two binding sites for zinc were also identified by

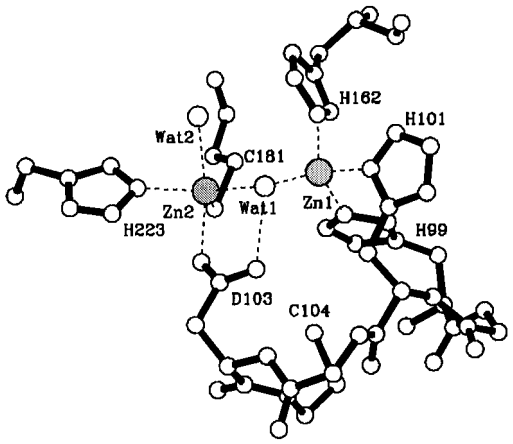

Figure 30. Structure of the dizinc center in β-lactamase of *Bacteroides fragilis*.[164] Figure provided by authors.[164]

equilibrium dialysis and ^{1}H NMR data, a high-affinity ($K_d = 2.4\ \mu$M) and a low-affinity binding site (K_d = 24 mM), determined at pH 5.3 and 5.7, respectively.

5. The Dizinc β-Lactamase from Bacteroides fragilis

The metallo β-lactamase from *Bacteroides fragilis* hydrolyzes a wide range of β-lactam antibiotics and is not susceptible to any known β-lactamase inhibitor. The recently determined 1.85 Å crystal structure shows that the enzyme contains two zinc ions, which are 3.5 Å apart (Figure 30).[164] Zn1 is tetrahedrally coordinated by three histidines (99, 101, 162) and a water ligand, which bridges the two Zn^{2+}. Zn2 has a trigonal-bipyramidal coordination sphere, formed by Cys-181, Asp-103, His-223, and two water residues. Outstanding features of this dizinc center are the absence of metal-bridging protein ligands, the high effective charge on Zn1 (no negatively charged protein ligands), and the presence of a cysteinate ligand to Zn2. On the basis of modeled substrate binding modes a role of the zinc-bridging water ligand as the nucleophile appears likely.[164] Because of the dimetal coordination and the dipositive effective charge on Zn1 the bridging water residue is probably deprotonated.

The two β-lactamases from *B. cereus* and *B. fragilis* share 34% sequence homology and the zinc ligands and other active site residues are conserved.[164] A mutation of Cys-104 in the dizinc β-lactamase to an Arg in the *B. cereus* enzyme might be responsible for the low affinity of the nearby second metal binding site in the latter enzyme as a result of a change in the electrostatic potential. However, further studies may clarify whether the two enzymes indeed utilize significantly different mechanisms, as is currently implicated by modeled substrate binding modes based on the native enzymes.

F. Comparison of the Mono- and Dizinc Peptidases

A comparison of the structurally characterized zinc peptidases shows that two main functional groups are absolutely "conserved" (in a functional sense) besides the zinc ion: the zinc-bound water molecule and a carboxylate group (usually of a glutamate) hydrogen bonded to this water. This structurally similar arrangement is not only strictly conserved in the evolutionarily related enzymes of the thermolysin and metzincin clans and in the small neutral protease of *S. caespitosus*, but is also found in carboxypeptidases A, B, and T, in zinc D-Ala-D-Ala carboxypeptidase, and in sonic hedgehog, obviously as a result of convergent evolution. However, the function of the glutamate side chain is probably fulfilled by a tyrosine in the possibly mechanistically related zinc amidase T7 lysozyme. In the most probable catalytic mechanism for this arrangement, supported by many structural and biochemical studies, the substrate's carbonyl group coordinates to the zinc ion in addition to the zinc-bound water, which attacks the polarized carbonyl group. The carboxylate group of the glutamate side chain accepts a proton from the water nucleophile and shuttles it to the amide nitrogen, thereby facilitating the breakdown of the tetrahedral intermediate. This negatively charged intermediate is stabilized by the zinc ion.

Mutation of the catalytic glutamate usually results in completely or by several orders of magnitude diminished activity. The importance of this carboxylate side chain might not only be that of a general base and a proton shuttle (to the leaving group), but also in transition-state stabilization. In cytidine deaminase (section IV.B) and mandelate racemase (section IX.K) protonated carboxymethyl groups provide major stabilization of the negatively charged intermediates.

Additional stabilization of the intermediate is provided by a presumably positively charged histidine side chain and a tyrosine in the thermolysins. In the astacins and serralysins the active-site tyrosine (a zinc ligand in the free enzyme) might serve a similar role. However, in the other metzincins no positively charged or electrophilic protein side chain is positioned to form a hydrogen bond to the negatively charged *gem*-diolate group. In addition to stabilization by zinc, active-site water molecules might provide some additional transition-state stabilization in these enzymes. It has been noted that the zinc ion might compensate for the loss of the positively charged histidine in transition-state stabilization, because of its more positive effective charge as a result of the replacement of glutamate by histidine in the zinc ligand sphere among thermolysin and metzincin clans.[139,140] This assumption also holds true for the active sites of carboxypeptidases A, B, and T, and sonic hedgehog. In these enzymes a positively charged residue positioned to interact with the intermediate correlates with the presence of an aspartate or glutamate side chain as a zinc ligand.

An interesting feature of the presumed mechanisms of the serralysins and possibly of the astacins is the conformational change of the active-site tyrosine side chain between zinc ligation in the free enzyme and interaction with the substrate carbonyl group or one of the *gem*-diolate oxygens in the transition state. Such a conformational change is strongly implicated by structures of the free enzyme compared to the inhibitor-bound state. Although such a dissociation of a ligand from the metal ion in order to actively participate in catalytic steps has been proposed for other metalloenzymes occasionally,

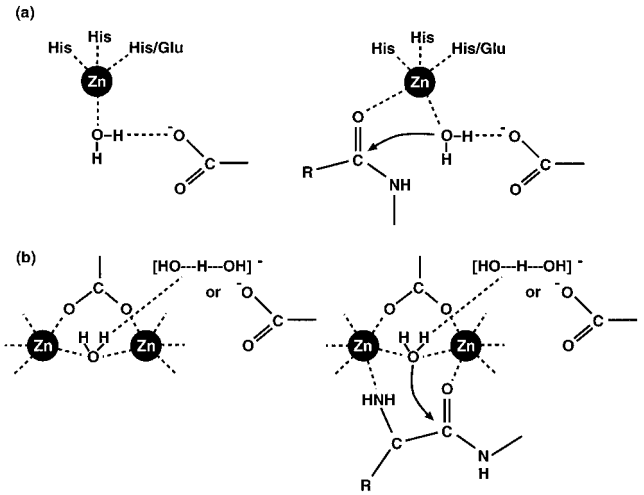

Figure 31. Simplified scheme of the activation of a water nucleophile and the substrate-binding mode to mononuclear zinc peptidases (a) and to dizinc aminopeptidases (b). A bihydroxide ion ($H_3O_2^-$) might be stabilized next to Arg-336 in leucine aminopeptidase and may have a role in the deprotonation of the water nucleophile similar to the catalytic glutamate side chains in the monozinc peptidases. Other dizinc amino- and carboxypeptidases also contain a catalytic carboxylate side chain.

such a conformational change has rarely been demonstrated experimentally. A related example is the dissociation of a zinc-bound glutamate ligand in fuculose aldolase to allow substrate binding (see section IV.I).

Dizinc Peptidases. In contrast to the mononuclear zinc peptidases, structural and mechanistic information about dinuclear zinc peptidases is more limited. The active sites of leucine aminopeptidase (LAP, Figure 5) and the aminopeptidases from *Aeromonas proteolytica* (AAP, Figure 8) or *Streptomyces griseus* (SGAP, Figure 10) are significantly different from each other. However, they share some common features in addition to the dizinc sites: the presence of exactly one zinc-coordinated water molecule, which is bridging the two metal ions, and the presence of one empty coordination site at each of the two zinc ions. The active sites may be superimposed on the basis of the two zinc ions and the bridging water molecule such that the more buried Zn2 of LAP, which coordinates the terminal amino group of the substrate, is superimposed onto the more buried Zn2 of AAP. Interestingly, this superposition also maps the hydrophobic binding pocket of LAP for the N-terminal side chain of the substrate onto the presumed specificity site for this residue of AAP. Furthermore, the carboxylate side chain of Glu-151 of AAP superimposes onto the position of the three water ligands (or one water plus a bihydroxide ion $H_3O_2^-$) in LAP. In the absence of further structural data supporting a mechanistic proposal for AAP both enzymes might employ a similar mechanism in which Glu-151 in AAP and the water/hydroxide molecules in LAP have a role as a general base and proton shuttle to the leaving group, somewhat similar to the catalytic Glu residue of the mononuclear zinc peptidases (Figure 31). However, Lys-262 of LAP, which stabilizes the tetrahedral *gem*-diolate group of the transition state, has no counterpart in AAP in the superposition. The absence of a positively charged

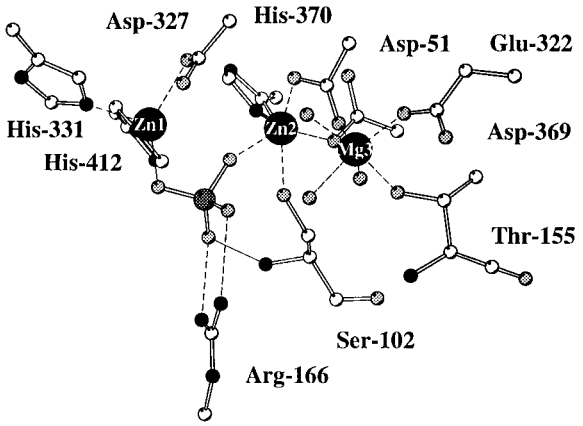

Figure 32. Phosphate bound to the active site of alkaline phosphatase.[168] This binding mode of the phosphate anion probably also resembles the binding mode of the substrate's phosphate group. The Ser-102 side chain is positioned for attack at the phosphorus. Generated from PDB file 1ALK.[168]

side chain positioned to further stabilize the intermediate in AAP is accompanied by a higher positive net charge of the dizinc center in AAP (+1) compared to LAP (0); a similar situation as found in some of the metzincins compared to carboxypeptidase A and thermolysin (as noted above in this section).

A phosphate ion might be regarded as a "simple" transition-state analogue of the *gem*-diolate group of a tetrahedral intermediate of peptide hydrolyses. The binding mode of phosphate to SGAP resembles that of the transition-state analogue leucinal to LAP in that one oxygen bridges the two zinc ions, whereas another oxygen binds to one zinc ion. However, these zinc ions are different ones in the above-mentioned superposition of AAP/SGAP and LAP.[68]

A comparison of the proposed mechanisms of LAP with that of the monozinc peptidases suggests that in LAP both zinc ions have catalytic roles in the activation of substrate and nucleophile (Figure 31). In addition, one of the zinc ions also participates in substrate recognition and binding by coordinating to the unprotonated terminal amino group of the substrate. Further studies are needed to show if the active-site glutamate residue in AAP and SGAP and the presumed bihydroxide ion in LAP, all hydrogen bonded to the zinc-bridging water nucleophile, indeed serve a similar role as the catalytic carboxylate residues in monozinc peptidases, as implicated in Figure 31.

III. Zinc Enzymes and Phosphoryl Transfer

A. Alkaline Phosphatase: A Zn–Zn–Mg Site and a Phosphoserine Intermediate

Both prokaryotes and eukaryotes produce alkaline phosphatase (EC 3.1.3.1), which cleaves phosphate from phosphomonoesters nonspecifically, or transfers the phosphoryl group to other alcohols. *E. coli* alkaline phosphatase is dimeric, and each monomer has two Zn^{2+} and one Mg^{2+} in its active site. Recent reviews have appeared.[165−167]

In the crystal structure of the enzyme from *E. coli*, the two zinc ions, essential for full activity, are about 4.0 Å apart.[168] Although the Mg^{2+} is close to Zn2 (Figure 32), it does not directly participate in the

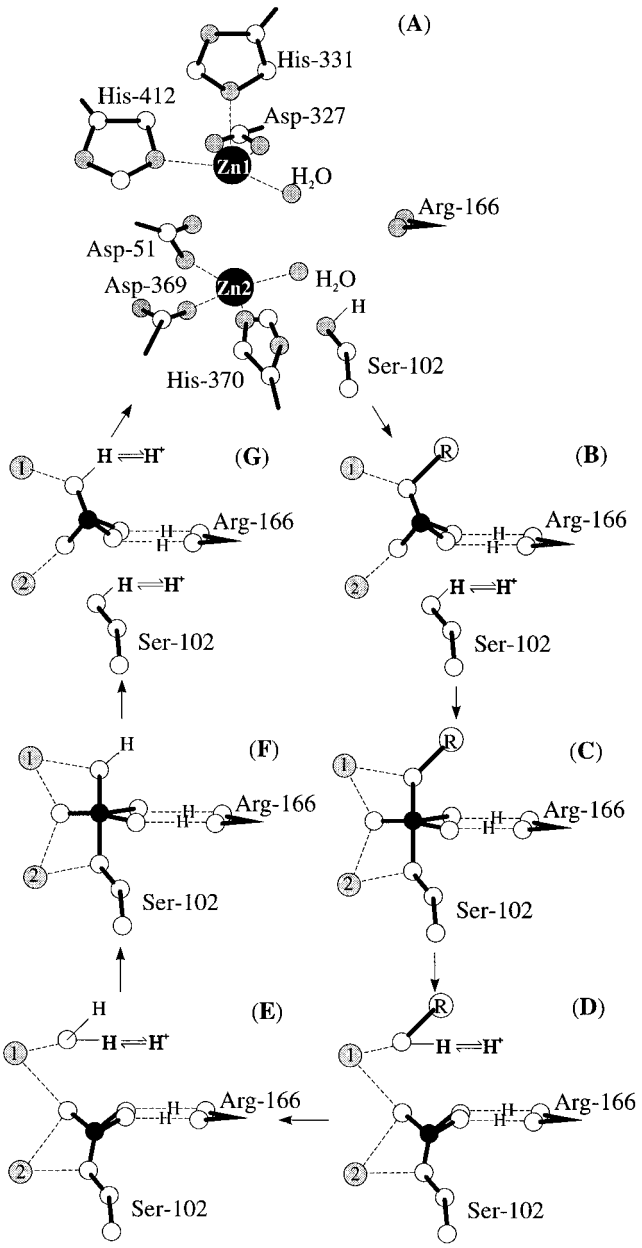

Figure 33. The two-step mechanism of alkaline phosphatase.[168] The two zinc ions and Arg-166 stabilize the transition state of both phosphoryl transfer steps.

catalytic steps. When phosphate, Zn^{2+} and Mg^{2+} are present, the coordination is as follows: for Zn1, His-412, His-331, Asp-327, and one oxygen of phosphate; for Zn-2, His-370, Asp-51, Asp-369, and one oxygen of the phosphate; and for Mg, Thr-155, Asp-51, Glu-322, and three water molecules.

In contrast to most other metallophosphatases the reaction mechanism (Figure 33) involves a covalent intermediate: phosphorylated Ser-102.[169] Dissociation of the product phosphate limits enzyme turnover at high pH, whereas dephosphorylation of the phosphoenzyme intermediate is rate limiting at lower pH.[170,171] The overall reaction proceeds with retention of configuration at phosphorus as a result of inversion in the two in-line steps.[172]

The structure is consistent with this mechanism, and accomodates both phosphoryl transfer reactions.[168] Both zinc ions play an active role in the activation of the nucleophile and the leaving group

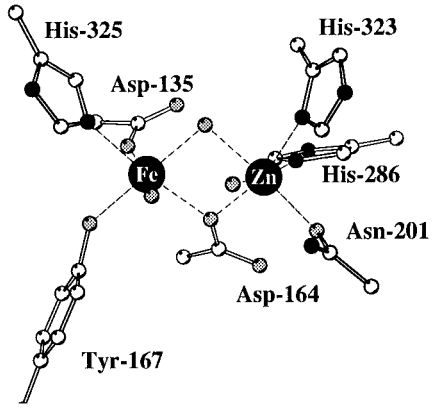

Figure 34. Structure of the Fe^{III}-Zn^{II} cluster in purple acid phosphatase from kidney beans.[174] The three water ligands, which could not be found in the electron density maps, are modeled based on biochemical results and the observed coordination geometry of the metal ions. Generated from PDB file 1KBP.[174]

and, along with Arg-166, in the stabilization of the transition state. It is especially interesting that the roles of the two Zn^{2+} ions are reversed in the phosphorylation and dephosphorylation stages of the overall reaction of phosphate ester hydrolysis. The role of the magnesium ion in alkaline phosphatase has been studied by mutagenesis (see section VI).

B. Purple Acid Phosphatase, a Fe^{III}–Zn^{II} Hydrolase

Purple acid phosphatases are characterized by an intense purple color, which results from a tyrosine→ Fe^{III} charge transfer (λ_{max} around 550 nm). Some of the mammalian enzymes are probably involved in degradative biological processes, such as phagocytosis and active bone resorption.[173] The X-ray structure at 2.65 Å resolution of the enzyme from kidney bean establishes the Fe^{III}–Zn^{II} coordination site (Figure 34),[174] where the two metals are 3.1−3.3 Å apart. The structure also provides a basis for relating this plant enzyme to the Fe^{III}–Fe^{II} mammalian enzymes, including uteroferrin, even though the sequence identity is only about 20%.[175] All metal ligands seem to be conserved between the plant and the mammalian enzymes. A diiron center also occurs in hemerythrin,[176] ribonucleotide reductase,[177] methane monooxygenase,[178] and rubrerythrin;[179] however, these enzymes differ significantly from purple acid phosphatase in their folding topology and active-site structures. The structure and properties of the dimetal centers in the purple phosphatases have been studied intensively by spectroscopic means; a more detailed recent review can be found in a related review (see ref 180) in this issue of *Chemical Reviews* and in ref 181.

Because of the moderate resolution of the crystallographic data, the presence of OH^- or H_2O as metal ligands was ambiguous. However, satisfactory coordination is consistent with OH^- on Fe(III), H_2O on Zn(II), and a bridging OH^- linked to both iron and zinc (Figure 34). Both metal ions than have an octahedral coordination sphere. In the proposed reaction mechanism the phosphate group of the substrate binds monodentately to zinc by displacing the presumed water ligand (Figure 35).[182,183,184,174]

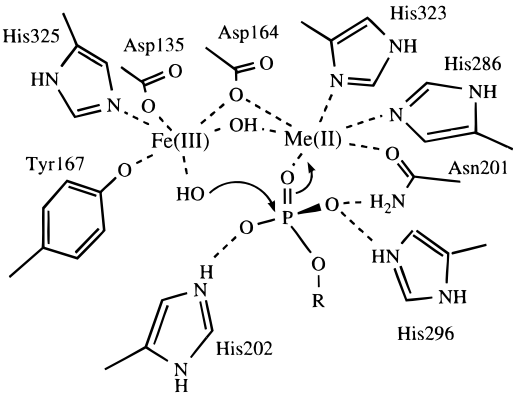

Figure 35. Substrate binding mode and attack of the Fe(III)-bound hydroxide ion in the proposed mechanism of phosphate ester hydrolysis by purple acid phosphatase.[174] In the kidney bean enzyme Me(II) is zinc.

Consistent with the inversion at phosphorus,[183] the terminal Fe(III)-bound OH^- attacks to form a five-coordinated intermediate, and the P−O bond opposite from the OH^- attack breaks to form the leaving group and phosphate. His-202 and His-296 may stabilize the transition state or protonate the leaving group. A phosphate anion bidentately bridges the two metal ions by displacing the two terminal water ligands presumed to be present at Fe and Zn.[174] This structure represents the product binding mode and is not assumed to model the substrate binding mode, in contrast to some mechanistic proposals for the similar two-metal ion mechanisms of the Ser/Thr protein phosphatases, which together with the purple phosphatase belong to a family $\alpha_2\beta_3$ metallophosphoesterases (see next section).

The function of Fe(III) is probably to maintain the attacking Fe(III)-bound nucleophile as OH^- at low pH (maximum activity around pH 5). A structural analysis of a mammalian purple acid phosphatase may show whether its diiron center is identical to that in the plant enzyme and how the different specificity for metal binding (zinc vs iron) in the divalent site is achieved.

C. Ser/Thr Protein Phosphatases (PP1 and Calcineurin) Contain Dinuclear Metal Sites

Phosphorylation by kinases and dephosphorylation by phosphatases provide a critical role in signal transduction by a reversible process. Therefore, the various kinases and phosphatases are subject to complex regulation. Unlike alkaline phosphatase (phosphoserine intermediate) and certain acid phosphatases (phosphohistidine intermediate), the Ser/Thr PPs including PP1, PP2A, and PP2B (calcineurin), catalyze without the formation of a phosphoenzyme intermediate.[185] These enzymes show about 40% sequence identity with one another, but no structural resemblance to the other phosphatases or to the Mg^{2+}-dependent PP2C.

Two metal ions are bound by a "metallophosphoesterase signature motif" ($DXHX_nGDXXDX_nGNHD/E$)[186,187,188] containing four metal ligands and a catalytic Asp-His pair. The three conserved parts of this motif are part of a $\beta\alpha\beta\alpha\beta$ structural core, which was first found in the more distantly related purple acid phosphatase from the kidney bean (previous section).[174] This core structure and the metallophosphoesterase motif appear to have an ancient common origin.[186] There is conflicting evidence concerning the nature of the two metal ions in the PPs. Calcineurin[189] and probably also PP1[190] are Fe-Zn metalloproteins. However, it remains to be shown whether the iron ion is divalent or trivalent in the active form.[191]

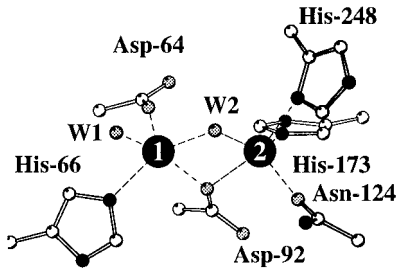

Figure 36. Structure of the dimetal center in rabbit muscle Ser/Thr phosphatase-1.[186] In the structure determination both metal sites were probably occupied by manganese. *In vivo* site 1 is probably occupied by iron and site 2 by zinc.

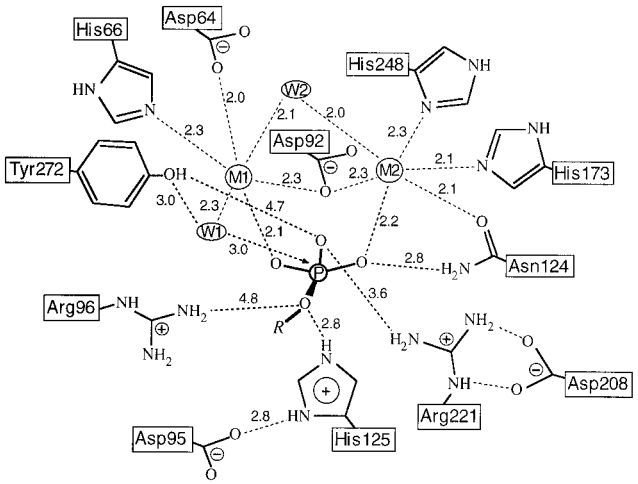

Figure 37. Active-site structure and possible substrate binding mode in the catalytic mechanism of Ser/Thr protein phosphatase 1.[186] Figure provided by authors.[186]

Rabbit Muscle PP1. The crystal structure of rabbit muscle PP1 to 2.1 Å resolution shows two metal sites with a strong anomalous diffraction signal from Cu K_α radiation, indicating Mn, Fe, or Co but not Mg, Ni, Cu, or Zn.[186] Restoration of activity by Mn^{2+} is consistent with Mn^{2+} as a choice for both metal sites,[192] and in this crystallographic study Mn^{2+} was present in the crystallization buffer.[186] The distance between the two Mn^{2+} ions is 3.3 Å, and these two ions are bridged monodentately by Asp-92 and by a hydroxide ion (or water) (Figure 36). Another water ligand (W1) is bound terminal to M1. In one possible mechanism the phosphate group of the substrate binds bidentately to the empty sixth ligand positions of M1 and M2 (Figure 37), followed by nucleophilic attack of W1 on the phosphorus atom. The departure of the leaving Ser or Thr groups of the substrate could be assisted by His-125, which might protonate the leaving group.

Human PP1. The structure of human PP1 to 2.5 Å resolution shows a two-metal site in which Fe and Mn ions were identified by proton induced X-ray emission spectroscopy.[193] Interestingly, despite the

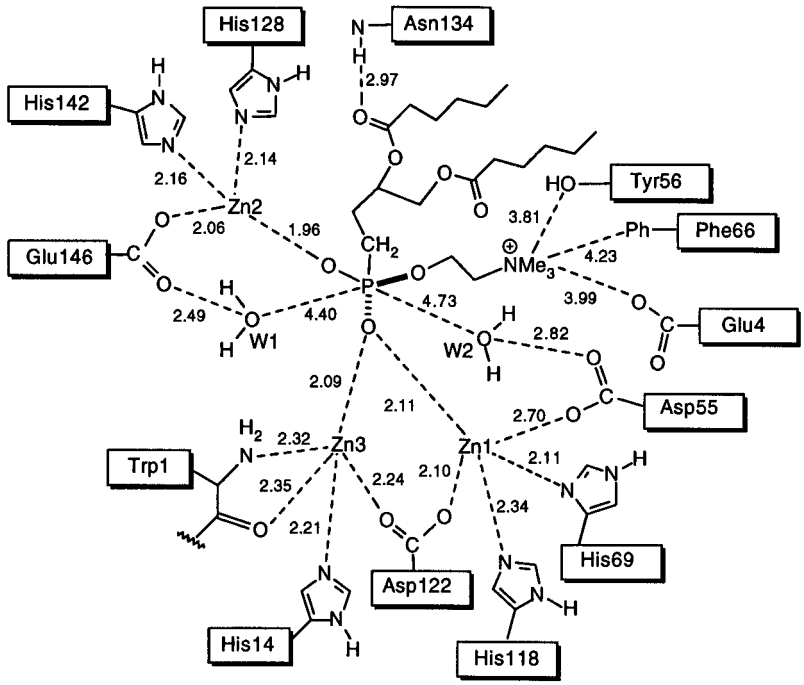

Figure 38. Structure of the active site of phospholipase C with a bound substrate analogue inhibitor.[204,205] Two water molecules are shown (W1 and W2) which are discussed as potential nucleophiles. In an alternative mechanism a water ligand bridging Zn1 and Zn3 is the favored nucleophile, assuming that this structure does not model the productive substrate binding mode.[206] Figure provided by authors.[205]

very similar structure to that of rabbit PP1, the metal−metal distance was refined to 4.0 Å under somewhat different experimental conditions of 30% glycerol in the crystallization buffer. A third water ligand (W3) was located bound terminally to the iron ion in site M1 as a sixth ligand (Figure 36). Assignment of Fe at M1 and Mn at M2 in PP1 is consistent with the homologous sites of Fe and Zn in purple acid phosphatase.[174] In addition, a cocrystal structure of human PP1 with tungstate was determined.[193] The tetrahedral tungstate ion, an analogue of phosphate as the reaction product, bidentately bridges the two metal ions, displacing W3. In an alternative mechanism for the PPs, the bridging water ligand W2 is the nucleophile.[193]

Calcineurin. The activation of T cells is suppressed when the phosphatase activity of calcineurin A is inhibited by binding of the two immunophilin-immunosupressant pairs: FKBP12-FK506 and cyclophilin A-cyclosporin A.[194−196] Crystal structures are available for human[197] and bovine[198] calcineurin. The active site, which is very similar to that in PP1, contains Zn and Fe separated by 3.0−3.1 Å. A phosphate ion binds bidentately to the two metal ions.[198] A third alternative for the mechanism of the PPs is that water W3 is the nucleophile which attacks the phosphorus center. This last mechanism is similar to that proposed for the purple acid phosphatases.[197]

D. Phospholipase C Contains a Trinuclear Zinc Center

Phospholipase C from *Bacillus cereus* hydrolyzes phosphatidylinositol and phosphatidylcholine, and is similar to the mammalian enzymes which are involved in generating second messengers (e.g. inositol triphosphate).[199,200] The presence of two tightly bound zinc ions in this enzyme is implicated by biochemical data.[201,202] However, the 1.5 Å resolution structure reveals three Zn^{2+}, which have interatomic distances of 3.3 Å (Zn1−Zn3), 6.0 Å (Zn1−Zn2), and 4.7 Å (Zn2−Zn3) (Figure 38).[203]

Binding of a substrate analogue, 3(*S*),4-bis[(hexanoyloxy)butyl]-1-phosphonylcholine to phospholipase C at 1.9 Å resolution shows interactions of the phosphono group oxygens with all three zinc ions, displacing the two water molecules which were bound to Zn2 in the unligated enzyme (Figure 38).[204,205] Thus, the water which attacks the phosphorus may not be zinc bound, but may be the water molecule which is hydrogen bonded to Glu-146.[204] However, a molecular modeling study (see also section VIII) indicates that this binding mode of the inhibitor might not model the productive substrate-binding mode.[206] Instead, this study suggests that the Zn1−Zn3 bridging water molecule might be the nucleophile, similar to the proposed mechanism of nuclease P1. The leaving group could be stabilized by Zn2. Further studies of other complexes, as well as a verification of the implied inversion of configuration at phosphorus, are needed. A 1.9 Å data set on a complex of the enzyme with inorganic phosphate also shows that the phosphate anion binds to all three zinc ions.[203]

E. Nuclease P1 is Homologous to Phospholipase C

Nuclease P1 cleaves preferably single-stranded RNA and DNA to 5′-mononucleotides[207] and also acts as a phosphomonoesterase at the 3′ terminal phosphate of a polynucleotide, thus yielding 5′-mononucleotides as the final cleavage products.[208] The structure to 2.8 Å resolution of the enzyme from *Penicillium citrinum* shows three zinc ions and two *N*-actetylglucosamines per 270 amino acids in the polypeptide chain.[209] The fold is very similar to that

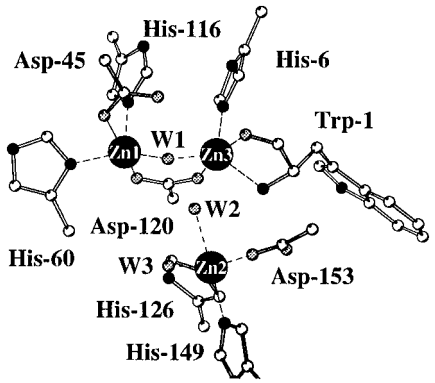

Figure 39. Structure of the trizinc center in the active site of nuclease P1.[209]

of phospholipase C, and the trizinc clusters are also similar.

In this trizinc cluster, distances are about 3.2 Å for Zn1−Zn3, 5.8 Å for Zn2−Zn1, and 4.7 Å for Zn2−Zn3. The three metal ions are liganded to His-60, His-116, Asp-45, Asp-120, His-6, His-126, His-149, Asp-153, and to the amino terminus and carbonyl oxygen of Trp-1 (Figure 39). A further study to 2.2 Å resolution shows evidence of two water molecules (W2 and W3) on Zn2, and of a bridging water (W1) between Zn1 and Zn3.[209] All three Zn ions have approximately a trigonal-bipyramidal coordination of two nitrogen and three oxygen atoms.

When a thiophosphodinucleotide (dA-P(S)-dA), a supposedly uncleavable substrate analogue, is soaked into crystals of the enzyme, two sites about 20 Å apart are occupied, but only one base was found at each of these sites. A model of 5′-AMP, which fits better than 3′-AMP, also reveals the binding mode of the phosphate group.[209] In contrast to phospholipase C, in which all three zinc ions bind the phosphate group, this group is interacting with Arg-48 and with Zn2 but not with Zn1 or Zn3. Thus, despite the similar active-site structures, nuclease P1 and phospholipase C may differ significantly in their substrate binding modes. However, as mentioned in section VIII, a modeling study indicates an alternative substrate binding mode for phospholipase C, which might resemble that of nuclease P1. The other mononucleotide binding site is not near the zinc cluster.

An in-line displacement mechanism is indicated by inversion of the configuration at phosphorus.[210] The attacking water nucleophile might be the bridging water W1 or one of the Zn2-bound waters.[209] Furthermore, W1 is hydrogen bonded to W2, and the Zn1−W1−Zn3 system plus Zn2 may activate W2 as a nucleophile.

F. Phosphotriesterase Cleaves Nonnatural Organophosphorus Compounds

This bacterial enzyme, also called organophosphorus hydrolase, catalyzes the hydrolysis of paraoxon, parathion, sarin, soman, and other related inhibitors of acetylcholinesterase[211] and is useful for detoxification of this class of nerve toxins and of agricultural pesticides. The native enzyme from *Pseudomonas diminuta* contains two zinc ions, although comparable activity is seen when these zinc ions are replaced by Co^{2+}, Ni^{2+}, Cd^{2+}, or Mn^{2+}. The insecticide

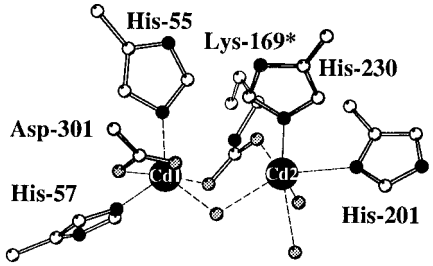

Figure 40. Coordination sphere of the dimetal site in phosphotriesterase, a dizinc enzyme.[213] This structure was determined from the Cd−Cd form of the enzyme. Generated from PDB file 1PSC.[213]

paraoxon is hydrolyzed by phosphotriesterase at the diffusion limit. It remains a puzzling question how and from which origin this enzyme emerged within about 40 years to be such an efficient catalyst toward organophosphates and phosphonates, which are not naturally occurring compounds.[212]

A structure of the dicadmium enzyme form[213] shows that the Cd−Cd distance is 3.8 Å. The two Cd's are bridged by a carbamylated lysine[213,214] and by a water molecule (Figure 40). Additional ligands are His-55, His-57, Asp-301 to M1, and His 201, His 230 and another water molecule to M2.[213] Comparison of the metal-containing enzyme with the apoenzyme[215] shows that significant structural rearrangements take place upon metal binding.[213]

In the proposed mechanism,[216] which inverts the configuration at phosphorus,[217] one metal ion polarizes a PO bond by binding to its oxygen, which probably displaces a water molecule, and OH^- is delivered to form a trigonal-bipyramidal intermediate. However, further details must await structural studies of complexes between the enzyme and suitable inhibitors.

IV. Other Zinc Enzymes

A. Adenosine Deaminase, and the Contribution of a Single Hydroxyl Group to the Inhibitor Binding Affinity

Adenosine deaminase (ADA) catalyzes the hydrolysis of adenosine to inosine and ammonia (Figure 41).[218] The deamination reaction catalyzed by ADA is encounter limited with a rate enhancement factor[219] of about 10^{12}. Lack of this enzyme, which is present in virtually all mammalian cells, results in a severe combined immunodeficiency disease (SCID). Notably, the first clinical trial of gene therapy was carried out on a patient with a defect of the ADA gene.

Nebularine (Figure 41) is a very strong inhibitor of ADA ($K_i = 3 \times 10^{-13}$ M).[220] However, the tight binding is a result of the formation of the 1,6-hydrate of this compound, probably catalyzed by ADA in a way similar to the deamination reaction.[220] Nebularine 1,6-hydrate (Figure 41) is thus an almost perfect transition-state analogue. The crystal structure analysis established its binding mode to murine ADA (Figure 42)[221,222] and also revealed the unexpected presence of a zinc ion, which coordinates to the 6-hydroxyl group of the inhibitor. Further ligands to zinc are histidines 15, 17, and 214 and Asp-295.

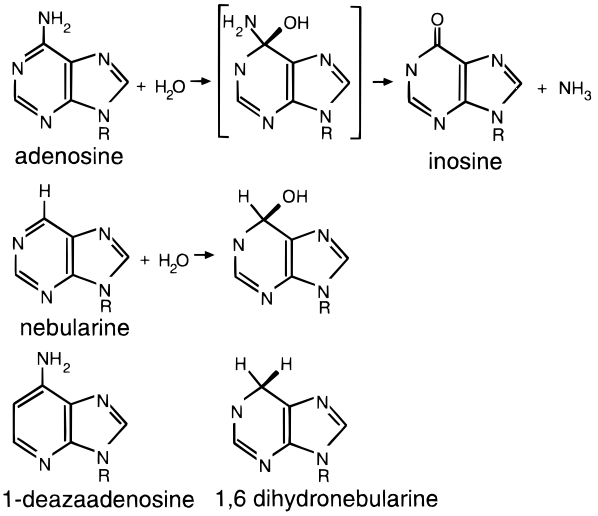

Figure 41. Catalyzed reaction (top) and reaction coordinate analogue inhibitors for adenosine deaminase. The inhibition constants are 3×10^{-10} M for nebularine 1,6-hydrate, 0.18 mM for 1-deazaadenosine, and 5.4 μM for 1,6 dihydronebularine.

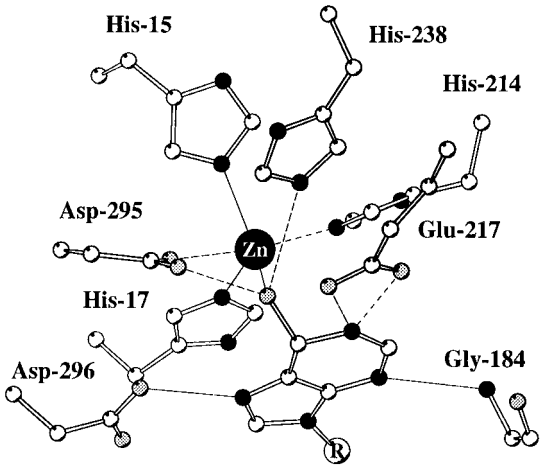

Figure 42. Nebularine 1,6-hydrate bound to the active site of adenosine deaminase.[221,222] Generated from PDB file 2ADA.[221]

Inosine, the reaction product, was found to bind as a *gem*-diol at C6, similar to the transition-state analogue, on the basis of X-ray diffraction data at 2.3 Å resolution.[223] This result has been questioned on the basis of NMR data and theoretical calculations, suggesting that this water adduct resembling the transition state should not accumulate in the active site, because the enzyme-bound transition state-like species is too unstable compared to the enzyme-bound ground state-like species.[324]

1-Deazaadenosine, which inhibits ADA with a K_i of 0.18 μM, serves as a substrate analogue (Figure 41).[224] Its binding to the active site is similar to that of nebularine (Figure 42). A water molecule is the fifth ligand to zinc in this structure.[225] This water (or hydroxide ion) is probably the nucleophile attacking the 6-carbon atom of the substrate (Figure 43). The N1 is proposed to become protonated by Glu-217 in order to enhance the electrophilicity of C6. His-238 may act as a general base to accept a proton from the zinc-bound water. In the next step this proton is transferred to the leaving group. In agreement with this mechanism mutational analysis showed that replacements of His-238, Glu-217, and Asp-295 resulted in dramatic losses of activity, a result of a diminished k_{cat}, whereas mutation of Asp-296 affects K_m.[226]

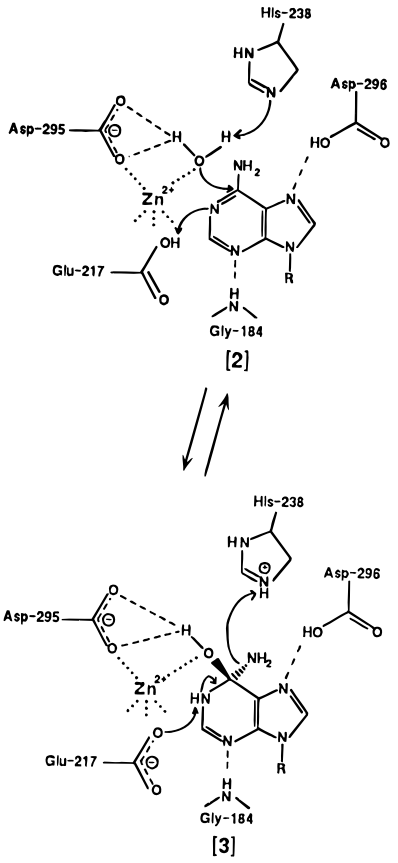

Figure 43. Substrate binding mode and formation of the transition state in the proposed reaction mechanism for adenosine deaminase.[225] (Reprinted with permission from ref 225. Copyright 1993 American Chemical Society.)

1,6-Dihydronebularine lacks the 6-hydroxyl of nebularine (Figure 41). This compound inhibits ADA with an inhibition constant of "only" 1.0×10^{-5} M.[227] Thus, the 6-hydroxyl group contributes −9.8 kcal/mol to the free energy of binding of the transition-state analogue, a large contribution for a single hydroxyl group that reflects its multiple binding interactions with the zinc ion, Asp-295, and His-238. However, other groups of the inhibitor provide comparably strong contributions to the binding affinity, indicating a synergistic effect of many substrate groups for strong binding.[228] Nebularine 1,6-dihydrate is a very rare species in solution. However, the strong binding energy of ADA toward the hydrated transition-state analogue compensates efficiently for the loss of entropy, which accompanies formation of the adduct of the two molecules ("entropy trap" mechanism).[227,229]

Adenosine 5′-monophosphate (AMP) deaminase from yeast, which is allosterically regulated by ATP, is homologous to ADA and contains one zinc per subunit.[230] The zinc ligands and other residues involved in substrate binding are conserved, indicating a similar reaction mechanism to that of ADA.

B. Cytidine Deaminase, and a "Valence Buffer" in Zinc Catalysis

Cytidine deaminase (CDA) is a mononuclear zinc enzyme that catalyzes the hydrolytic deamination of

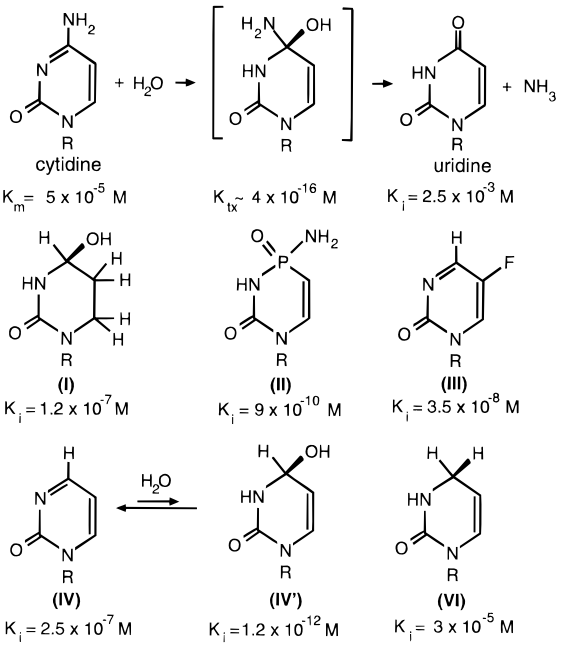

Figure 44. Catalyzed reaction (top) and reaction coordinate analogue inhibitors for cytidine deaminase.[232] Inhibitors shown are 3,4,5,6-tetrahydrouridine (I), a phosphapyrimidine ribonucleoside (II), 5-fluoropyrimidin-2-one ribonucleoside (III), zebularine (IV), zebularine 3,4-dihydrate (IV′), 3,4-dihydrozebularine (VI). (Adapted from ref 232.)

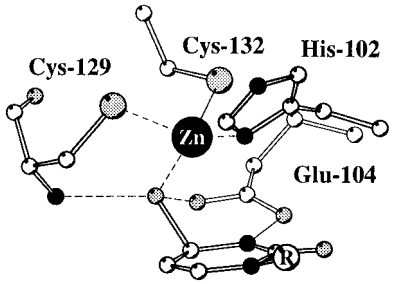

Figure 45. Binding mode of zebularine as zebularine 3,4-dihydrate (Figure 40-IV′) to the active site of cytidine deaminase.[235] Generated from PDB file 1CTU.[235]

cytidine to uridine, in a reaction similar to that catalyzed by ADA (Figure 44). However, although ADA and CDA share some similarities in their presumed reaction mechanisms and active-site structures, the two enzymes have different folding topologies and no sequence homology. Thus, these similarities are obviously a result of convergent evolution.[231]

Transition-state analogue compounds which contain a tetrahedral carbon or phosphorus atom at C4 are potent inhibitors of CDA (Figure 44).[232,233] Zebularine (pyrimidin-2-one ribonucleoside) binds in a hydrated form (zebularine 3,4-dihydrate) to the enzyme active site (Figure 45).[232] This hydration may be catalyzed by CDA, probably by a mechanism similar to the formation of the transition state of the cytidine deamination reaction. X-ray structures of CDA from *E. coli* with bound 5-fluoropyrimidin-2-one riboside (Figure 44, III) and of CDA with zebularine revealed the interactions causing the tight binding of these inhibitors, and shed light on the characterization of the reaction pathway.[234,235] The 4-hydroxyl group of the inhibitor is coordinated to the zinc ion and hydrogen bonded to Glu-104 and the backbone NH of Cys-129. Glu-104 also receives a hydrogen

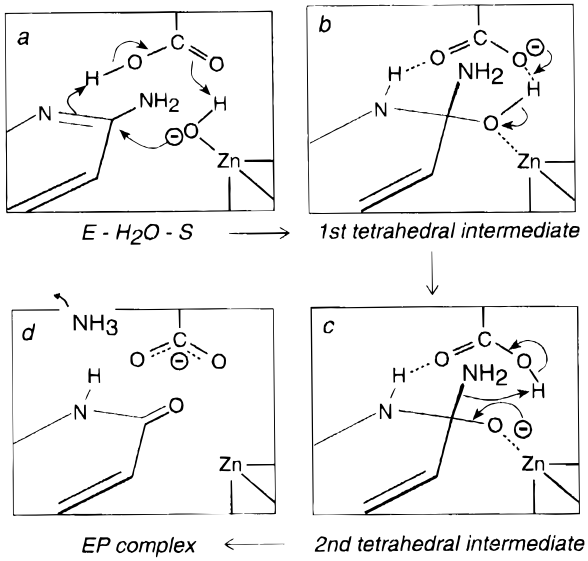

Figure 46. Proposed reaction mechanism for the deamination of cytidine by cytidine deaminase.[234] (Reprinted with permission from ref 234. Copyright 1994 Academic Press Ltd.)

bond to its other carboxylate oxygen from the 3-NH group of the inhibitor. Further ligands to zinc are His-102, Cys-129, and Cys-132.

Besides the differences in the zinc ligand spheres of CDA and ADA, CDA also has a somewhat simpler or "economic" active-site arrangement. Glu-104 serves in multiple roles: in the deprotonation of the zinc-bound water nucleophile, in the protonation of the substrate 3-nitrogen and the leaving amino group, and in transition-state stabilization (Figure 46).[234] Thus, Glu-104 fulfills the roles of Asp-295, His-238, and Asp-296 in the proposed mechanism for ADA. The importance of this glutamate residue in catalysis is also demonstrated by a mutation to alanine, which resulted in a 10^8-fold reduction of k_{cat}.[236] Interestingly, this mutation *increased* the affinity toward substrate cytidine and product uridine. Thus, it appears as though Glu-104 promotes catalysis not only by lowering the transition state energy by protonation of the 3-nitrogen but also by destabilizing the ground-state energies of enzyme−substrate and enzyme−product complexes.[236] In corroboration of these results, it was recently shown that 5-fluorozebularine (Figure 44) binds to the E104A mutant enzyme as a ground-state analogue, i.e. without formation of a 3,4-hydrate as seen in the wild-type enzyme.[237]

Carter and colleagues also determined the binding mode of 3,4-dihydrozebularine, in which the 4-OH group is replaced by a proton (Figure 44), to the active site of CDA.[235] This structure revealed that the zinc-bound water molecule is present in this complex and that it is at a short distance (2.5 Å) from the 4-carbon atom. This unfavorably close contact on one hand, and the strong polar contacts of the 4-OH group in zebularine 3,4-hydrate on the other hand, obviously account for the drastically different binding constants of these two compounds to CDA.

A crystal structure analysis of 3-deazacytidine (Figure 44) bound to CDA provided a model for the substrate binding mode.[238] Thus, with the help of ground-state and transition-state analogues struc-

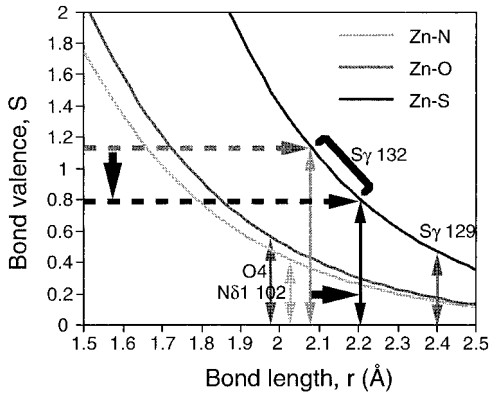

Figure 47. Variation of bond strength vs bond length (empirical expression for the bond valence, $S = \exp[(r_0 - r)/B]$, where r_0 and r are constants).[238] In the reaction mechanism of cytidine deaminase the Zn−S_γ(Cys-132) distance is proposed to increase in order to compensate for the developing negative charge on the zinc-coordinated hydroxyl group of the substrate. (Reprinted with permission from ref 238. Copyright 1996 American Chemical Society.)

tural models for various stages of CDA catalysis were obtained. Interestingly, a change in the zinc−sulfur bond distance of Cys-132 ranging from 1.9 to 2.2 Å was detected by comparison of the various electron density maps, all at resolutions around 2.3−2.1 Å. The lengthening of this coordination bond, if significant with respect to the intermediate resolution of crystallographic data, can be correlated to the development of negative charge on the zinc-coordinated hydroxyl group of the substrate.[238] This effect can be explained quantitatively with the "bond valence model", which quantifies the strength of a metal−ligand bond as a function of the metal−ligand distance (Figure 47).[239] A very useful application of this model is that the oxidation state of the metal ion can be predicted from the metal−ligand distances, because the sum of the bond valences (as a measure of the strength of each coordinating bond) is close to the formal oxidation state of the metal. Since zinc has a strong tendency to preserve the oxidation state 2+, changes in one metal−ligand interaction will cause changes in the distances of the other metal−ligand bonds. These differences are usually too small to be detected by X-ray crystallography at the resolutions commonly obtained from protein crystals. However, in CDA only one ligand, Cys-132, is proposed to serve as a valence buffer by changing its conformation and metal−ligand distance to compensate for the changing interactions of the catalytic zinc ion with the substrate (Figure 48).[238] Thus, the change in the bonding distance is just beyond the estimated standard deviations of the X-ray analysis. X-ray absorption spectroscopy by which very accurate metal−ligand distances can be obtained, is in general a suitable method to reliably detect or verify such changes.

Several cytidine and deoxycytidylate deaminases from different organisms are homologous to CDA, including the zinc ligands.[240] However, in some cytidine deaminases the zinc-coordinated histidine is replaced by an another cysteine. Interestingly, CDA displays also homology to mRNA editing proteins from rat and rabbit, which posses RNA sequence-specific cytidine deaminase activity that converts a CAA codon to UAA.[241] The three zinc ligands and the catalytic glutamate residue are conserved.

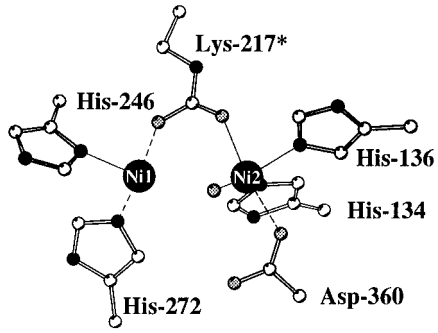

Figure 48. Structure of the dinickel center in urease. Generated from PDB file 1KAU.[246]

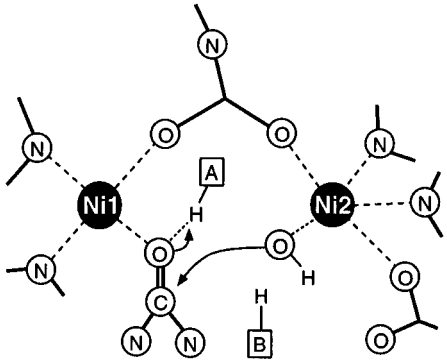

Figure 49. Proposed reaction mechanism for urease.[246,249] AH represents a general acid and BH a general base.

1. Urease, a Hydrolytic Nickel Enzyme, Shares a Common Ancestor with Adenosine Deaminase and Phosphotriesterase

Urease (EC 3.5.1.5) hydrolyzes urea to ammonia and carbon dioxide. Crystals of the pure enzyme, obtained by Sumner in 1926,[242] were of great influence in showing that enzymes are well-defined chemical compounds. Later, urease was established as the first nickel-containing enzyme.[243] A more detailed recent review on this enzyme can be found in this issue of *Chemical Reviews*.[180] An X-ray structure was obtained recently from urease of *Klebsiella aerogenes*.

The assembly of the dinuclear nickel center requires carbon dioxide which carbamylates Lys-217.[244] A similar carbamylation occurs in ribulose-1,5-bisphosphate carboxylase/oxygenase[245] (section IX.N) in order that Mg^{2+} becomes bound, and also in phosphotriesterase (section III.F). The resulting carbamate group is stabilized by the two Ni ions, which are 3.5 Å apart (Figure 48).[246] Also, in addition to the three genes which lead to the three polypeptide chains, assembling to an $(\alpha\beta\gamma)_3$ stoichiometry,[246] there are four accessory genes *ureD*, *ureE*, *ureF*, and *ureG* which are required to assemble the dinickel center *in vivo*.[247,248]

In addition to the carbamylated Lys-217, which bidentately bridges the two metal ions, His-246, His-272, His-134, His-136, Asp-360, and a water molecule are metal ligands (Figure 48). Accordingly it appears reasonable that the carbonyl oxygen of the substrate urea binds to the three-coordinated Ni1 (Figure 49), and that the water bound to Ni2 attacks the carbon

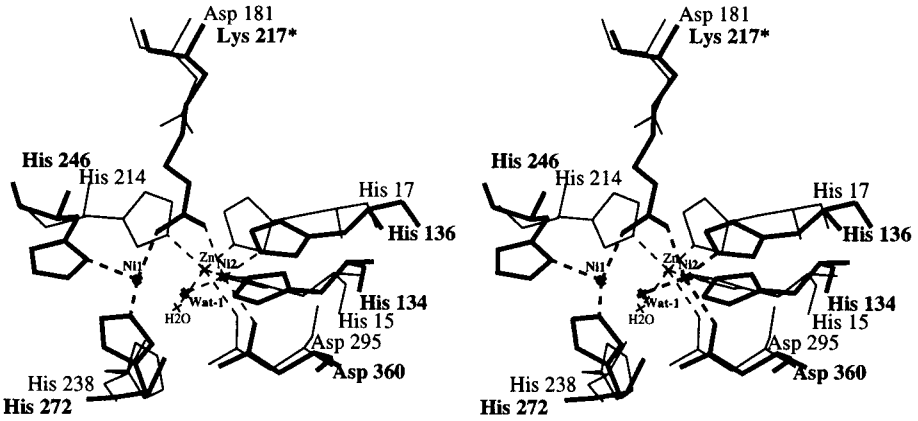

Figure 50. Superposition of the active sites of adenosine deaminase (thin lines) and urease.[246] (Reprinted with permission from ref 246. Copyright 1995 American Association for the Advancement of Science.)

of urea.[246,249] Proton movements aid the formation of the final products CO_2 and $2NH_3$ (Figure 49).

It is now clear that Zn^{2+}, Cu^{2+}, Co^{2+}, and Mn^{2+} bind to urease apoprotein *in vitro*. Of these only Mn^{2+} restores as much as 2% of the activity of the Ni-activated apoenzyme.[250] Thus, two puzzling questions remain: why can only nickel (and in part manganese) activate urease, and why does nature invest so much effort to assemble this dinickel center to catalyze a seemingly "simple" hydrolytic reaction?

Interestingly, the α subunit of urease contains an $(\alpha\beta)_8$ barrel similar to that in adenosine deaminase,[221] which binds one Zn^{2+} in its active site.[246] The structural similarity extends to the active site (Figure 50),[246] where the Ni2 and an associated H_2O of urease coincide with zinc and its coordinated H_2O in adenosine deaminase. It has been suggested[246] that these two enzymes have evolved from a common ancestor, as did other eight-stranded α/β-barrels,[251,252] including phosphotriesterase. Considering the similarity in the hydrolytic reactions catalyzed by urease and adenosine deaminase, the relationship between the two enzymes provides an instructive example of how these enzymes, one containing a dinuclear and the other a mononuclear metal center, have evolved from a common ancestor, possibly containing a single metal site.

C. 6-Pyruvoyl Tetrahydropterin Synthase

Following conversion of GTP to dihydroneopterin-P_3 this enzyme (PTPS) makes 6-pyruvoyl tetrahydropterin (eliminating triphosphate), which is then converted by sepiapterin reductase to tetrahydrobiopterin. Deficiency of PTPS leads to reduced levels of dopamine and serotonin, and leads to associated disorders such as Parkinson's disease, Alzheimer's disease, dystonia, and depression.[253]

The hexameric PTPS from rat is a dimer of trimers in *D*3 symmetry and exhibits a barrel-like structure which encloses a hydrophilic pore about 6−12 Å in diameter.[254] The active site contains a zinc ion[255] coordinated by three histidine residues (23, 48, 50); no zinc-bound water ligands could be located in the 2.3 Å electron density maps of the native enzyme.[254] Three functional groups are proposed to play major catalytic roles: the zinc ion, Glu-A133, and a catalytic triad consisting of Asp-B88, His-B89 (both from the neighboring B chain), and Cys-A42 (Figure 51). The

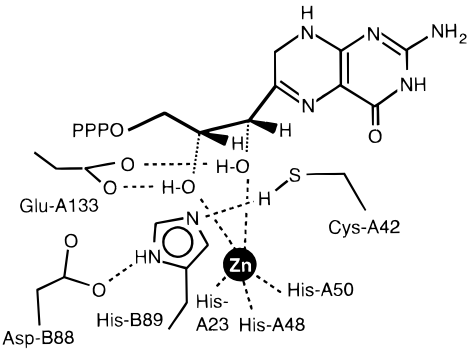

Figure 51. Modeled binding mode of the substrate dihydroneopterin triphosphate to 6-pyruvoyl tetrahydropterin synthase.[255] (Adapted from ref 255.)

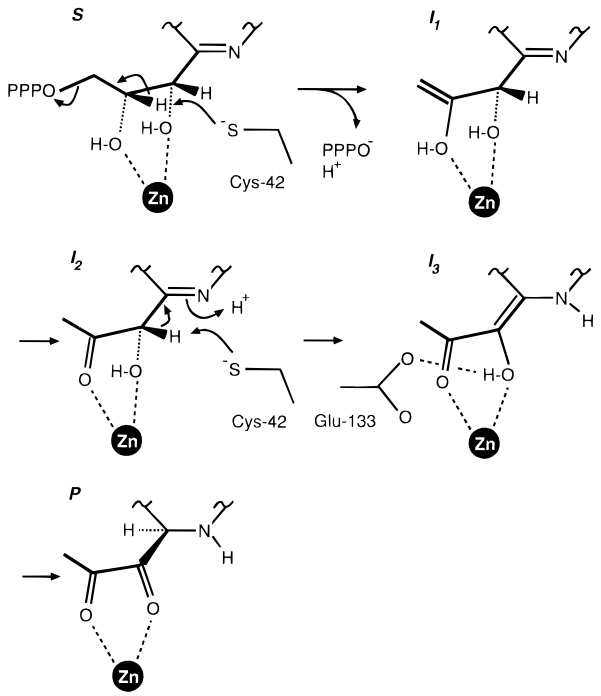

Figure 52. Possible reaction mechanism for 6-pyruvoyltetrahydropterin synthase.[255] (Adapted from ref 255.)

Zn^{2+} probably binds the two substrate hydroxyl groups. Cys-A42 is activated to remove the C-2′ proton so that the triphosphate is eliminated (Figure 52).[255] Following a keto−enol tautomerism to intermediate I_2 (Figure 52) a second proton is abstracted by Cys-A42 to yield I_3, which makes a stereospecific

	1st Metal Binding Site
Tyrosinase:	^{162}**H**YYVSRDTLLGGSEI-WRDIDFA**H**EAPGFLPW**H**^{193}
TRP1:	^{168}**H**YYSVKKTFLGTGQESFGDVDFS**H**EGPAFLTW**H**^{200}
TRP2:	^{167}**H**YYSVKDTLLGPGRP-YKAIDFS**H**QGPAFVYW**H**^{198}
	2nd Metal Binding Site
Tyrosinase:	^{345}**H**NAL**H**IFMNGTMSQVQGSANDPIFLLH**H**^{372}
TRP1:	^{353}**H**NLA**H**LFLNGTGGQTHLSPNDPIFVLL**H**^{380}
TRP2:	^{347}**H**NLA**H**SFLNGTNALPHSAANDPVFVVL**H**^{374}

Figure 53. Sequence alignment of the presumed metal-binding sites of murine dopachrome tautomerase (TRP2) to tyrosinase and a second tyrosinase (TRP1).[258,257] (Adapted from ref 258.)

keto−enol tautomerism to yield the product; Glu-A133 may assist this last step. Thus, Zn^{2+} is an electron pair acceptor in this mechanism, whereas the catalytic triad forms an electron pair donor. Although this is the preferred mechanism, supported by the X-ray structure, model building, and mutagenesis results,[254,255] further studies are needed to establish the sequential order of the two deprotonation steps.

D. Dopachrome Tautomerase Probably Contains a Dinuclear Zinc Center Homologous to the Dicopper Site in Tyrosinase

Dopachrome tautomerase, also named TRP2 (EC 5.3.3.12), belongs to a family of three metalloenzymes that are homologous to tyrosinase. The enzyme converts L-dopachrome to 5,6-dihydroxyindole-2-carboxylic acid. In the melanin synthesis pathway the initial oxidation of L-tyrosine to L-dopaquinone is catalyzed by the dinuclear copper enzyme tyrosinase. Regulation of this pathway involves two tyrosinase-related proteins: a second tyrosinase (TRP1) which oxidizes 5,6-dihydroxyindole-2-carboxylic acid and dopachrome tautomerase. None of these three enzymes has been structurally characterized, but the coordination of each of the two copper ions of tyrosinase to three histidines is well established.[256] Each of the two metal ions in TRP1, and of the two zinc ions of dopachrome tautomerase are also probably bonded to three His residues (Figure 53) in these three highly homologous enzymes.[257] Other deprotonated ligands are likely to be present in order to neutralize the large positive charge.

In dopachrome tautomerase, each Zn^{2+} probably has a water molecule which is presumed to be displaced by the substrate as it binds to both zinc ions, which then promote the tautomerization (Figure 54).[258] The relationship among these three enzymes, the two oxygenases with a dicopper site and the dizinc tautomerase, is likely to provide an instructive example of the evolution of metalloenzyme catalysis.

E. Carbonic Anhydrase, Diffusion-Limited Hydration of Carbon Dioxide

The first enzyme known to require zinc as a cofactor,[259] carbonic anhydrase (CA, EC 4.2.1.1) catalyzes the reversible formation of bicarbonate and a hydrogen ion from water and carbon dioxide. Of the seven isozymes in mammals, most of the chemical and structural studies have been done on cytosolic CAII. The diffusion-controlled reaction has two steps

$$H_2O + E^*Zn{-}OH^- + CO_2 = E^*Zn{-}OH_2 + HCO_3^-$$

$$E^*Zn{-}OH_2 = E^*Zn{-}OH^- + H^+$$

For CAII, the rate approaches that permitted by diffusion control and is limited by the second (proton transfer) step which regenerates the $Zn{-}OH^-$ form.

The $Zn(His)_3$ catalytic unit is buried in a cavity which has a hydrophobic side for CO_2 binding and a hydrophilic side for the activation of the zinc-bound water to a hydroxide ion (pK_a about 7). This deprotonation is aided by the Thr-199−Glu-106 pair (Figure 55),[260] which also helps in selecting protonated ligands, such as HCO_3^- in the reverse reaction.[260,261]

In the first step of the hydration of CO_2 (Figure 55, top) this substrate probably binds at a position which is known as the binding site for the isoelectronic cyanate ion (OCN^-).[260] Cyanate does not directly coordinate to the zinc ion but is 3.2 Å away from the metal ion. This noncoordinating binding of CO_2 to the active site is in agreement with molecular dynamics studies.[262] Attack of the zinc-bound OH^-

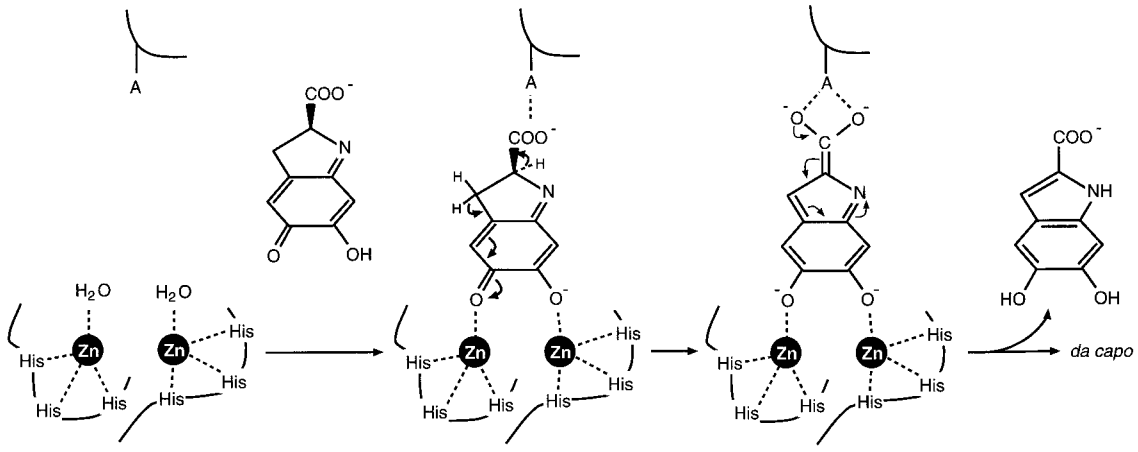

Figure 54. Tentative reaction mechanism for the tautomerization of L-dopachrome to 5,6-dihydroxyindole-2-carboxylic acid at the presumed dizinc center in dopachrome tautomerase. Residues involved in the removal of the two CH-acidic protons remain to be identified. The two zinc ions and a positively charged residue (A) might stabilize the putative intermediate.[258] (Largely modified from ref 258.)

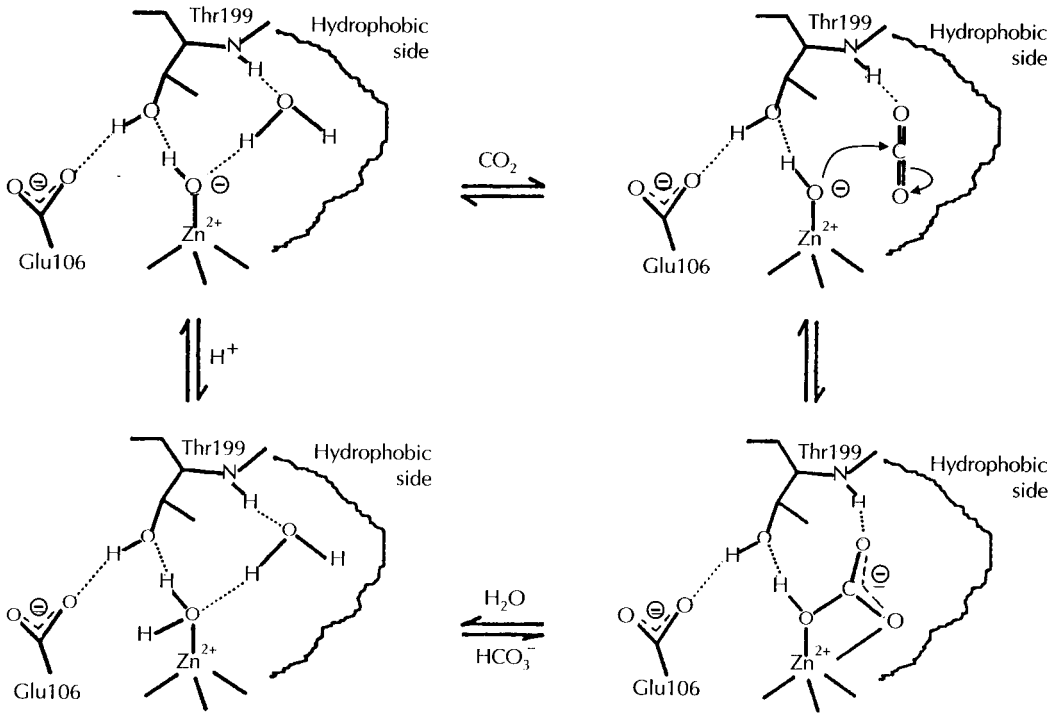

Figure 55. Proposed pathway for the hydration of carbon dioxide by carbonic anhydrase.[260] (Reprinted with permission from ref 260. Copyright 1993 Current Biology Ltd.)

at the carbon of CO_2 yields bicarbonate which binds such that its OH group is coordinated to Zn^{2+} and is stabilized by Thr-199 reinforced by Glu-106. Here, a crystallographic model is available in the structure of bicarbonate bound to the T200H mutant of CAII.[263] In this mutant the carbonate ion bidentately coordinates to zinc such that two oxygens of CO_3^{2-} are at distances of 2.2 and 2.5 Å. Further, some distortions around the cyanate (i.e. CO_2) site in the bicarbonate complex of the Co^{2+}-exchanged enzyme allow an additional H_2O to bind near the metal ion, suggesting that the bicarbonate is exchanged for H_2O through a quasi six-coordinated metal ion (addition−elimination ligand exchange mechanism).[264] A plausible reason that Zn^{2+}, and to a lesser extent Co^{2+}, are most active among divalent cations is that a variety of stable complexes of coordination numbers of 4, 5 and possibly 6 occur in the reaction pathway. Such flexible coordination geometries are more readily obtained with Zn^{2+} and Co^{2+} compared to other divalent cations. Finally, the stabilization of the OH of bicarbonate as a Zn^{2+} ligand does not require plausible mechanisms which transfer a proton among the oxygen atoms of bicarbonate in the reverse reaction. The definite separation of the two steps in the reaction and the $Zn-OH^-$ in preference to a $Zn-OH_2$ mechanism have also been supported by ^{13}C kinetic isotope studies.[265,266]

Following the inital discovery that sulfonamides inhibit carbonic anhydrase,[267] therapeutic applications include reduction of intraocular pressure in glaucoma treatment (isozyme II),[268−270] and possible blocking of the mitochondrial isozyme V to reduce blood glucose levels in type II diabetes.[271,272] In the structures of (acetoxymercuri)benzenesulfonamide (AMSulf) to 2.0 Å and of acetazolamide to 3 Å, the nitrogen is bound to zinc and one of the sulfonamide oxygens binds to Asn-199 and replaces the "deep" water of the enzyme's cavity.[273] Indeed most multiatom inhibitors bind so that two of their atoms are near the cyanate (i.e. CO_2) binding site.[274]

The crystallographic studies toward the mechanism of CA have recently been reviewed.[274] Analysis of structure−function relationships in the zinc-binding site allows an evaluation of the protein−metal affinity, equilibrium kinetics, and reactivity of zinc-bound solvent.[275] Moreover, conditions are being developed for use of CAII as a sensitive metal ion biosensor.[275,276]

Carbonic Anhydrase from the Archaeon Methanosarcina thermophila. CA from this thermophilic organism shows no sequence homology to the other two classes of this enzyme.[277] However, similarities occur in the zinc coordination environment as a result of convergent evolution. The 2.8 Å crystal structure of the homotrimer showed the active-site zinc ions at the interface between two subunits (Figure 56).[278] Each zinc ion is coordinated by three histidines, namely His-81 and His-122 from one subunit and His-117 from another subunit, and probably by a water ligand. This putative water molecule is in hydrogen-bonding distance to Gln-75. The active site of this novel CA can be superimposed onto that of CAII such that the zinc ion and the three histidines have similar positions and conformations.[278] In addition, Glu-62 and Gln-75 of *M. thermophila* may be counterparts of Glu-106 and Thr-199 in CAII, respectively.

F. A Proposed Active-Site Structure for Dihydroorotase, Based on Mutational Analysis and Homology Modeling

A structure is not yet available for dihydroorotase, but a model for the active site structure and mechanism was proposed by modeling studies and site-directed mutagenesis.[279] This trimeric zinc enzyme[280]

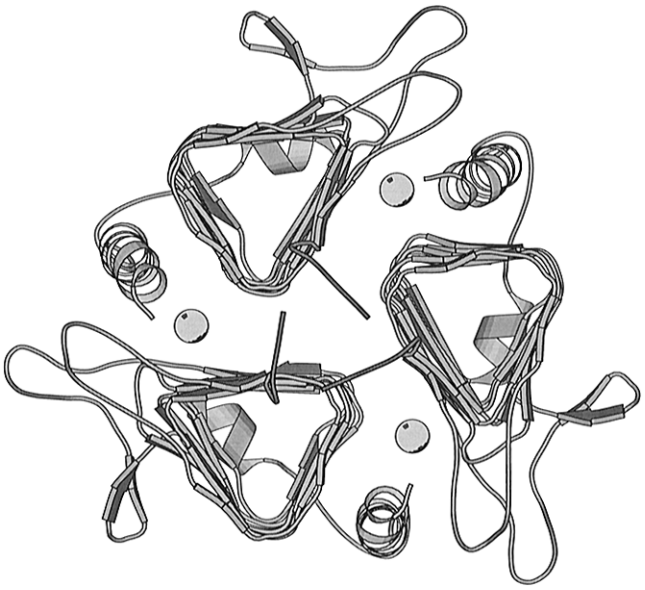

Figure 56. View of the trimeric structure of carbonic anhydrase from the archaeon *Methanosarcina thermophila* along the molecular 3-fold axis.[278] The active site zinc ions are located at subunit interfaces between two left-handed β-helices. Figure provided by authors.[278]

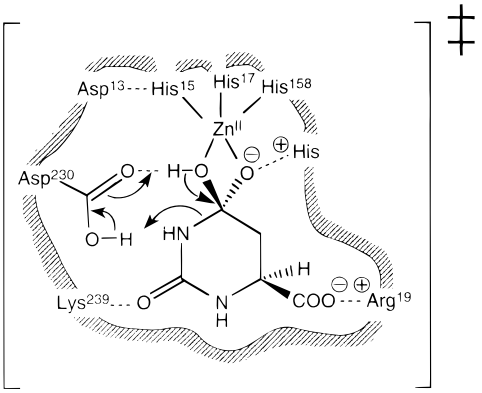

Figure 57. Model for the enzyme−transition state complex for hamster dihydroorotase.[279] (Reprinted with permission from ref 279. Copyright 1995 American Chemical Society.)

cyclizes carbamyl aspartate to form dihydroorate as a member of the CAD trifunctional unit (carbamyl phosphate synthetase, aspartate transcarbamylase and dihydroorotase) in mammals, here the hamster.

Effect of mutations on zinc binding of six of the seven histidines are consistent with histidines 15, 17, and 158 as ligands to Zn^{2+}, and mutation at Asp-13 then led to a proposal[279] of metal binding triad Asp-13−His-15−Zn, similar to the ligand spheres in carbonic anhydrase[281] and adenosine deaminase.[225] Furthermore, a local sequence homology of a nonapeptide involved in zinc binding in all three enzymes was used to obtain a preliminary model for the active-site structure and substrate binding. This apparently conserved nonapeptide zinc-binding motif probably arose by convergent evolution.[279]

The proposed mechanism is most conveniently shown for the reverse reaction (Figure 57).[279] The forward reaction is probably initiated by nucleophilic attack of a zinc-bound OH^- to form a tetrahedral oxyanion transition state, which is stabilized by zinc coordination[279,282] (Figure 57). Following is the cyclization facilitated by Asp-230, as shown in reversed form in Figure 57.

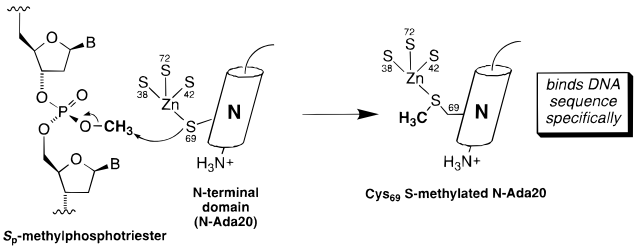

Figure 58. DNA demethylation by the Ada protein of *E. coli*.[286] (Figure provided by authors.[286])

G. DNA Methyl Phosphotriester Repair Domain of Ada (*E. coli*): A Zinc-Activated Cysteine Nucleophile

E.coli Ada protein repairs methyl phosphotriesters in DNA by direct, irreversible transfer of the methyl group to one of its cysteines, Cys-69. The methyl transfer is autocatalyzed by coordination of the acceptor Cys-69 to the Zn^{2+} ion (Figure 58).[253] Following methylation Ada induces the transcription of genes that confer resistance to the toxic effects of methylating agents. This process reduces the effect of threat in which aberrant methylation of DNA occurs. The N-terminal 10 kDa fragment of Ada retains the zinc binding and repair function.

In addition to the nucleophilic Cys-69 the zinc ion is coordinated to three further cysteines (38, 42, and 72) (Figure 58).[283−285] This enzyme is thus far unique in having a functional, catalytic $Zn(Cys)_4$ center, in contrast to many structural zinc centers of this type. The role of the zinc ion might be to facilitate ionization of the cysteine side chain to the more nucleophilic cysteinate, a process of activation which is similar to the activation of a water nucleophile in many zinc hydrolases, or to the activation of the serine nucleophile in alkaline phosphatase. However, the pK_a of a cysteine side chain ($pK_a = 8.4$) is close to physiological pH values, so that deprotonation is relatively easily achieved, and coordination of the deprotonated Cys-69 to a positively charged metal ion will reduce its nucleophilicity. To avoid this, the three cysteinate ligands (if all are assumed to be deprotonated) probably reduce the positive charge of the zinc ion largely by charge transfer considering the negative net charge of the ZnL_n complex and the soft, polarizable character of the sulfur ligands. In contrast, the net charge of other ZnL_n coordination sites involved in the deprotonation of OH groups or in transition-state stabilization is neutral to dipositive and contains a maximum of two cysteine ligands (alcohol dehydrogenase, cytidine deaminase) (Table 1). Cd^{2+} can replace Zn^{2+} in Ada, yielding only a 4-fold reduction of enzyme activity.[286] The ability to activate transcription of a methylation resistance regulon is not affected by this substitution. After methylation the Cys-69 side chain remains coordinated to the zinc ion.[287]

H. Glyoxalase I

The interconversion of glutathione−methylglyoxal thiohemiacetal and *S*-D-lactoylglutathione occurs

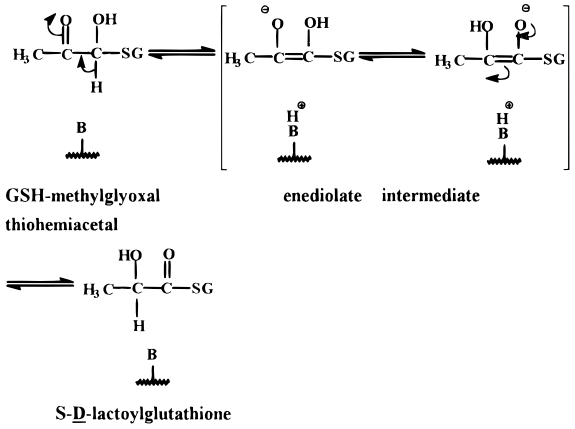

Figure 59. Interconversion of glutathione-methylglyoxal thiohemiacetal and *S*-D-lactoylglutathione through an enediolate intermediate.[288] (Reprinted with permission from ref 288. Copyright 1995 The American Society for Biochemistry and Molecular Biology, Inc.)

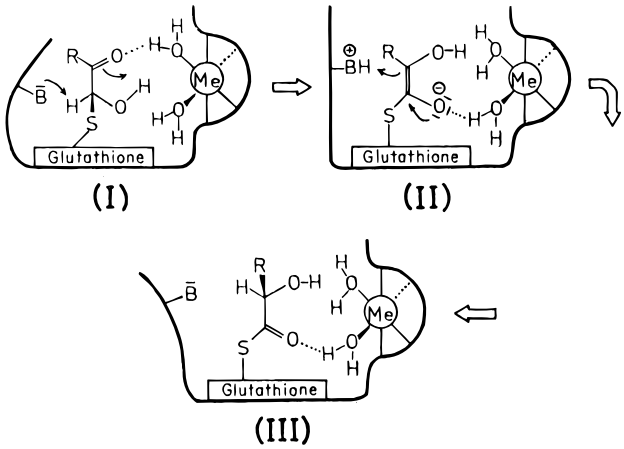

Figure 60. Proposed steps in the catalytic mechanism of glyoxalase I.[289] (Reprinted with permission from ref 289. Copyright 1982 American Chemical Society.)

through an enediolate intermediate (Figure 59). The proteolytic cleavage regions near residues 100−111 in human and 93−105 in *Pseudomonas putida* glyoxylase I show significant homology with the catalytic loop of triose phosphate isomerase (TIM), which has a similar mechanism.[288] In particular the active-site base Glu-165 of TIM correlates with Glu-93 of the *Pseudomonas* glyoxalase I.

The role of the single zinc ion per subunit in this dimeric enzyme is not yet completely clarified. Although a structural role in stabilizing the active conformation is not excluded,[289] a somewhat more direct role in processing the enediol intermediate has also been proposed (Figure 60).[290] In this mechanism the substrate does not directly coordinate to zinc but interacts with the two zinc-coordinated water molecules. On the basis of EXAFS spectra of the zinc enzyme,[291] EPR studies of the Co^{2+} enzyme, the nuclear relaxation enhancement of the Mn^{2+} enzyme,[292] and the full activity of the Mg^{2+} enzyme, a six-coordinated divalent metal ion site is proposed[290] in which there are four enzyme ligands and two water molecules in an octahedral configuration.

A structural analysis of human glyoxalase I with the inhibitor benzylglutathione is under way, which shows the the active site located at the interface of

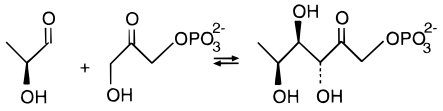

Figure 61. Reaction of L-lactaldehyde with dihydroxyacetone phosphate to give L-fuculose 1-phosphate.

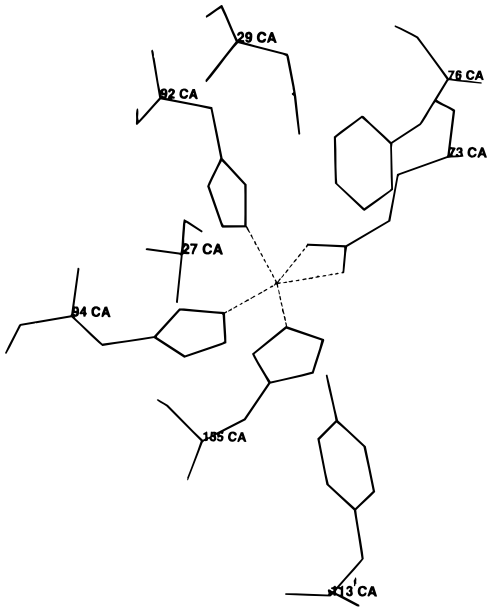

Figure 62. Environment of the zinc ion in the active center of L-fuculose-1-phosphate aldolase.[295] (Reprinted with permission from ref 295. Copyright 1993 Academic Press Limited.)

the dimeric 50 kDa protein.[293] Each subunit provides two of the four protein ligands to zinc (1 His, 2 Glu, 1 Gln). In addition, one water molecule is observed in the zinc ligand sphere.

I. L-Fuculose-1-phosphate Aldolase: Displacement of a Zinc-Bound Glutamate Ligand by the Substrate

The tetrameric fuculose aldolase (C_4 symmetry) from *E. coli* catalyzes the reversible cleavage of L-fuculose-1-phosphate to dihydroxyacetone phosphate (DHAP) and L-lactaldehyde (Figure 61).[294] As a class II aldolase it uses a metal ion to activate a bound sugar molecule in contrast to the class I aldolases which form a Schiff's base intermediate at an active-site lysine residue. Its 2.1 Å resolution X-ray structure shows an active site zinc ion coordinated by His-92, His-94, His-155, and Glu-73 (bidentately) (Figure 62).[295] In the crystal structure of a complex of the enzyme with phosphoglycolohydroxamate, an inhibitor resembling the enediolate transition state, Glu-73 is displaced as a zinc ligand and the hydroxamate group bidentately coordinates the metal ion.[296]

On the basis of these structures a reaction mechanism was proposed in which the DHAP binds first to the active site and displaces Glu-73 as a zinc ligand, which in turn accepts a proton from the 3-carbon of DHAP (Figure 63).[296] The negatively charged enediolate group is stabilized by the metal ion. It is not yet clear whether the carbonyl group of the aldehyde substrate is polarized by zinc coordination for C−C bond formation. However, Tyr-113

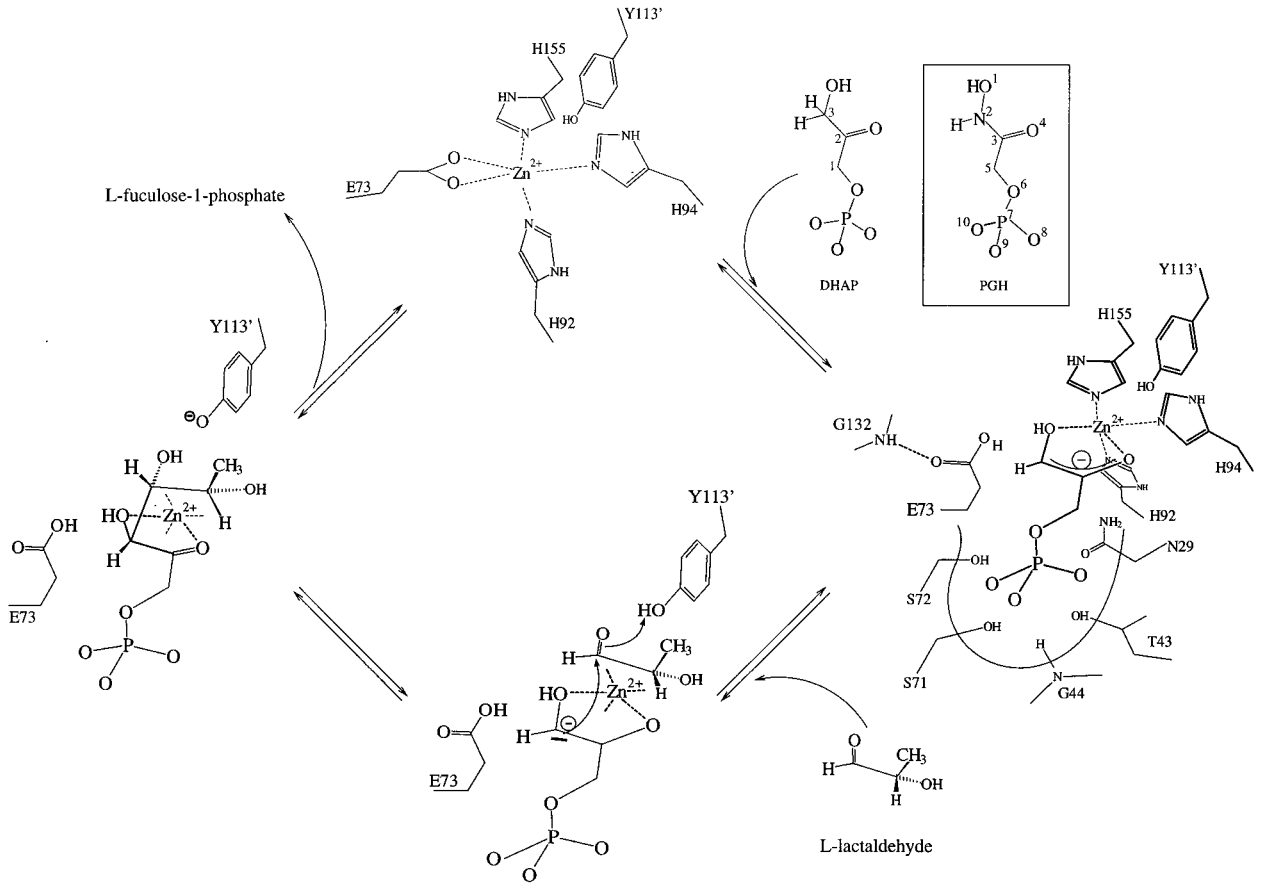

Figure 63. Proposed reaction mechanism for the aldol condensation reaction of dihydroxyacetone phosphate (DHAP) and L-lactaldehyde, yielding L-fuculose-1-phosphate.[296] Also shown is the inhibitor phosphoglycolohydroxamate (PGH). Figure provided by authors.[296]

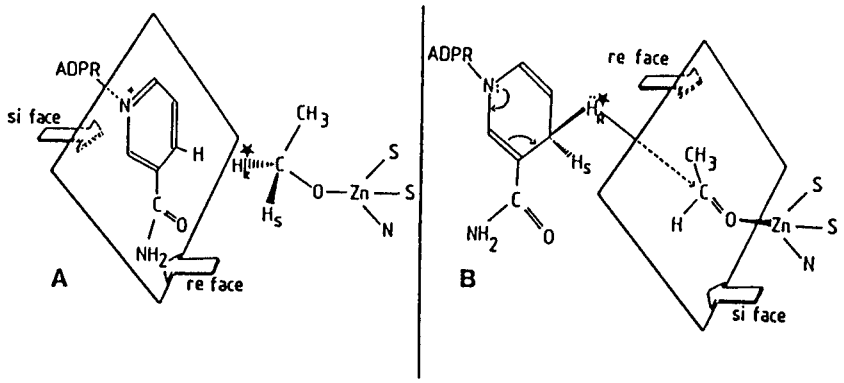

Figure 64. The stereospecificity of ethanol oxidation in alcohol dehydrogenase.[300] (Reprinted with permission from ref 300. Copyright 1986 Birkhäuser Boston, Inc.)

appears appropriately positioned to protonate the aldehyde oxygen.

J. Fructose-1,6-bisphosphatase Aldolase

The class II aldolase of *E. coli* is a zinc-containing glycolytic enzyme. The zinc ion is five-coordinated by His-110, His-226, His-264, Glu-176, and one water ligand.[297]

K. Alcohol Dehydrogenase: Orientation and Polarization of the Substrate for Hydride Transfer

The NAD^+-dependent alcohol dehydrogenase (ADH) catalyzes the oxidation of primary or secondary alcohols to aldehydes or ketones. Each monomer of the dimeric horse liver ADH (EC 1.1.1.1) binds two zinc ions, one structural and one catalytic.[298] The catalytic zinc is bound to Cys-46, His-67, Cys-174, and a water ligand which is displaced by the deprotonated alcoholate group of the substrate. Four cysteines (97, 100, 103, 111) coordinate the structural zinc. Binding of the nicotinamide ring of NAD^+ induces a conformational change of ADH which brings the catalytic zinc of the zinc domain about 1 Å closer to the NAD^+ binding domain. This NAD^+ is then in a position to receive the actual or incipient hydride from the zinc-bound substrate,[299] as the aldehyde or ketone product forms (Figure 64).[300] In the reverse reaction Zn^{2+} polarizes the carbonyl bond

and promotes the transfer of a hydride ion from NADH to the carbonyl group.[301]

Quantum mechanical tunneling has been shown to contribute to H^- transfer in horse liver ADH[302] and yeast ADH[303,304] (and also in bovine serum amine oxidase[303]). These studies were made possible by the fortunate circumstance that this critical catalytic step is rate limiting for secondary alcohols, as compared with reactions of most other enzymes for which product leaving, conformational changes or, less frequently, diffusion of substrates or products limits enzyme turnover.

The proton relay system[298,305] in the apoenzyme (NAD^+ absent) involves a chain of the hydrogen-bonded groups $Zn-OH_2$, Ser-48, H_2O, and His-51. Mutation of His-51 to Gln in the homologous human liver isoenzyme β_1, β_1 ADH reduces k_{cat}/K_m for ethanol by a factor of 6 at pH 7.0 and 12 at pH 6.5. These effects of the mutation can be reversed when buffers are added to the solution.[306]

L. Glucose Dehydrogenase and Some Other Enzymes That Are Homologous to Alcohol Dehydrogenase

Involved in an unusual pathway of sugar metabolism in an archaeon (archaebacteria), the catalytic domain of the tetrameric zinc enzyme glucose dehydrogenase (GDH) from *Thermoplasma acidophilum* (160 kDa) shows significant structural homology with horse liver ADH.[307] Its cofactor can be $NADP^+$ (K_m = 0.11 mM) or the less strongly bound NAD^+ (K_m > 30 mM). The reaction catalyzed is

$$\text{glucose} + \text{NAD(P)} \rightarrow \text{gluconate} + \text{NAD(P)H} + H^+$$

In spite of the low sequence identities of GDH to horse liver ADH (19%) the three-dimensional structures of the two enzymes show significant similarities in both the catalytic domain and in the regulatory domain, including the positions of the structural and catalytic zinc ions. Also, the zinc ligands are conserved (Cys-46, His-67, and Cys-174). Structures modeled for yeast ADH (20% identity to GDH) and sorbitol dehydrogenase (21%) imply that these enzymes also have similar three-dimensional structures. The catalytic mechanism is probably similar to that of the well-studied horse liver ADH.[307] Finally, quinone oxidoreductase also belongs to this family, and the structure of its complex with NADPH has recently been determined.[308]

M. The $Cu^{II/III}$–Zn Center in Superoxide Dismutase

Superoxide dismutase (SOD) catalyzes the dismutation of a superoxide radical (O_2^-) to form O_2 and H_2O_2.[309] The copper ion is the redox center for this reaction and is only 6 Å away from a zinc ion in each monomer of this dimeric enzyme.[310] X-ray structures of SOD from several organisms have been determined for the oxidized form (Cu^{II}).[311,312,313–316] In bovine erythrocyte SOD two metal ions are bridged by the imidazolate side chain of His-61. Further ligands to zinc are His-69, His-78, and Asp-81, whereas Cu^{II} is also coordinated to His-44, His-46, His-118, and one water molecule.[311,312] The zinc coordination sphere is distorted tetrahedral, while that of Cu^{II} is approximately trigonal bipyramidal with His-44, His-46 and H_2O as equatorial ligands.[312] A bridge between His-44 (Cu ligand) and His-69 (Zn ligand) is formed by Asp-122. In the proposed reaction mechanism an electron from the first O_2^- reduces Cu^{II} to Cu^I and yields O_2; the Cu^I then donates an electron to a second O_2^- which picks up two protons to make H_2O_2 and Cu^{II}.

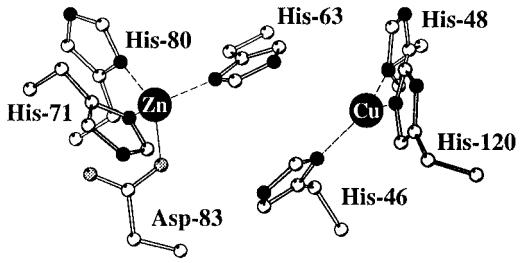

Figure 65. Structure of the reduced Cu^IZn^{II} center in yeast superoxide dismutase.[320] The Cu^I has a trigonal-planar coordination sphere and the bond to the metal-bridging His-63 is broken. Generated from PDB file 1JCV.[320]

Recent structural studies have focused on the characterization of the reduced state of the enzyme. Several spectroscopic studies indicate the breaking of the copper–nitrogen bond to His-63 in the Cu^I enzyme.[317–319] Structural studies yielded conflicting results: whereas a trigonal-planar coordinated Cu^I and a broken bond to the bridging histidine was indeed found in a crystal structure of SOD from yeast (Figure 65),[320] reduced SOD from bovine erythrocytes had largely unchanged metal coordination spheres.[321] In both reduced forms the zinc ligand spheres remained unchanged.

The role of the zinc ion is to promote the organization of the active site, as indicated by an NMR study of exchangeable protons of histidines, together with chemical modification of some of these histidines using diethyl pyrocarbonate.[322] Site-directed mutagenesis may sharpen this general picture, as this method has recently done for the pH dependence of the catalytic rate.[323]

V. Structural Zinc Sites

Reviews on the important structural roles of zinc in proteins, including many DNA-binding proteins, metallothionein, but also enzymes, can be found in refs 5 and 17. These structural zinc sites have in common a tetrahedral zinc binding site formed by side chains of Cys, His, and occasionally Asp or Glu. Following are four examples of structural zinc sites in enzymes, including the prototypical regulatory zinc site in *E. coli* aspartate transcarbamylase.

A Clathrated Zinc Ion in Ribonuclease T1. Ribonuclease T1 does not have a functional or structural zinc ion, although it is inhibited by Zn^{2+}.[325] In the complex with the enzyme at pH 5.2 in 2 mM Zn^{2+}, this metal ion binds not to the active site (probably because two active-site histidines are protonated at pH 5.2) but to a previously observed calcium binding site.[326] It is coordinated to both carboxylate oxygens of Asp-15 and to six water molecules. The coordination geometry is a dodecahedron, approximating a square antiprism, and all zinc–oxygen distances are remarkably long, about 2.5 Å. It is therefore sug-

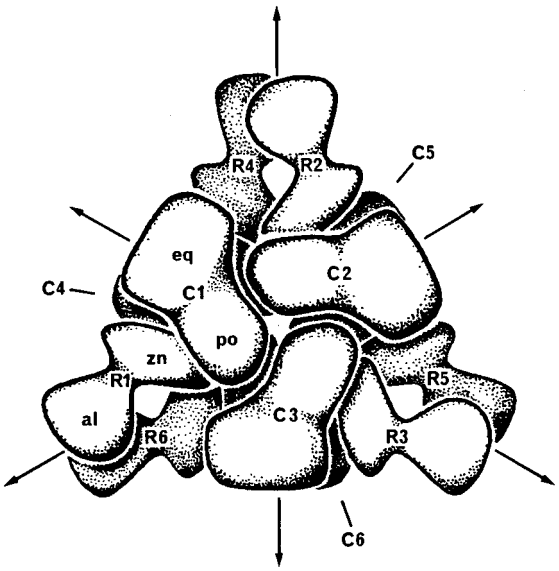

Figure 66. Quaternary structure of aspartate transcarbamylase.[327]

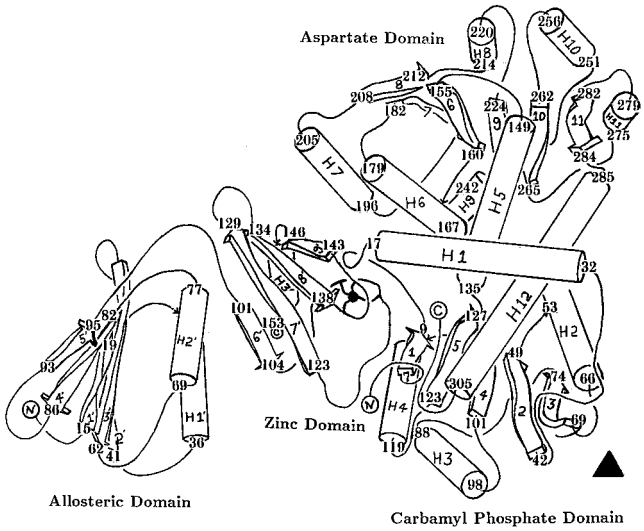

Figure 67. Tertiary structure of a (cr) subunit of aspartate transcarbamylase. The structural zinc site (filled circle) is located at the interface between the catalytic chain and the regulatory chain.

gested that the Zn^{2+} (radius 0.74 Å) is clathrated, rather than coordinated at a more usual distance of 2.0 Å. The clathrate description for Zn^{2+} binding is suported by the temperature (disorder) factor of 22 $Å^2$, as compared with that of 13 $Å^2$ for Ca^{2+}. The water molecules are hydrogen bonded to several other protein atoms, which stabilize this clathrate cavity. Presumably a tighter coordination of fewer water molecules to the zinc ion would result in a less stable arrangement.

Aspartate Transcarbamylase. This dodecameric allosteric enzyme composed of two catalytic trimers (c_3), and three regulatory dimers (r_2) (Figure 66) has one Zn^{2+} in each regulatory chain. This Zn^{2+} is bound to four cysteines (109, 114, 138, and 141) (Figure 67) in a part of the r chain that resembles a zinc finger.[327−329] The zinc ion is required for assembly of the allosteric dodecamer from r_2's and c_3's, and has been substituted by Cu^{2+}, Co^{2+}, Ni^{2+}, Cd^{2+}, and Hg^{2+} to yield active enzymes,[330] and by Mn^{2+} to evaluate distances to the active and regulatory sites.[331] The spectra of the Ni^{2+}-substituted enzyme have been employed to monitor the allosteric transition.[332] Without a divalent metal cation, this enzyme is a nonallosteric catalytic trimer.

Ornithine Transcarbamylase: Zinc-Induced Allosteric Behavior. The trimeric *E. coli* ornithine transcarbamylase is an anabolic enzyme, which catalyzes the reaction of carbamoyl phosphate with L-ornithine to yield L-citrulline and phosphate. In the presence of Zn^{2+}, cooperative behavior is induced: the saturation curve for L-ornithine becomes sigmoidal.[333] The structural basis for this allosteric effect has not yet been established. A three-dimensional structure has recently become available for the closely related catabolic enzyme from *Pseudomonas aeroginosa*, which is a cooperative enzyme consisting of four catalytic trimers in a compact dodecamer of 32 symmetry.[334] Further studies are expected to reveal the basis of allosteric behavior in both of these species variants, as well as that of the cooperativity induced in the isolated catalytic trimers of aspartate transcarbamylase by mutation of Arg-105 to Ala in the *E. coli* enzyme,[335] and of the equivalent Arg-99 to Ala in the *Bacillus subtilis* enzyme.[336]

Human Immunodeficiency Virus Type 1 Integrase. HIV-1 integrase catalyzes 3′-donor processing (cleavage of the 3′ ends of the linear double-stranded viral DNA termini) as well as strand transfer reactions (joining of the recessed viral DNA into the host chromosomal DNA).[337] An NH_2-terminal domain (residues 1−50), containing an HHCC sequence as a zinc finger motif,[338] a central core (60−160), and a carboxy-terminal domain (200−270) constitute the polypeptide chain. An X-ray structure of the central core domain showed a dimeric arrangement of this domain in the crystal and also revealed a structural homology to the core domain of bacteriophage MuA transposase.[339] Both of these enzymes employ Mg^{2+} or Mn^{2+} for activity *in vitro*, although HIV-1 integrase probably requires Mg^{2+} for activity *in vivo*. Whereas neither Ca^{2+} nor Zn^{2+} is active in the absence of Mg^{2+}, the role of Zn^{2+} is to stimulate the activity in the presence of Mg^{2+}, and it does so by promoting multimeric forms of this enzyme.

VI. Protein Engineering and Design of Novel Zinc Proteins

The techniques of molecular biology have stimulated the fields of enzymology and structural chemistry in several ways, including the availability of large quantities of pure recombinant proteins. Site-directed and random mutagenesis are primarily used as analytical tools to probe enzyme mechanisms by disabling or modifying potent functional residues. However, a fascinating possibility that is becoming reality in several laboratories is the design of new enzymes not only with different specificities but also with novel reactivities.

New metallocatalysts can be obtained by different approaches: synthesis of (possibly biomimetic) small molecule compunds, *de novo* design of metal-binding sites in natural or synthetic proteins or in catalytic antibodies, or mutagenesis of existing metalloproteins. A detailed understanding of the architecture of metal sites in proteins appears necessary for a

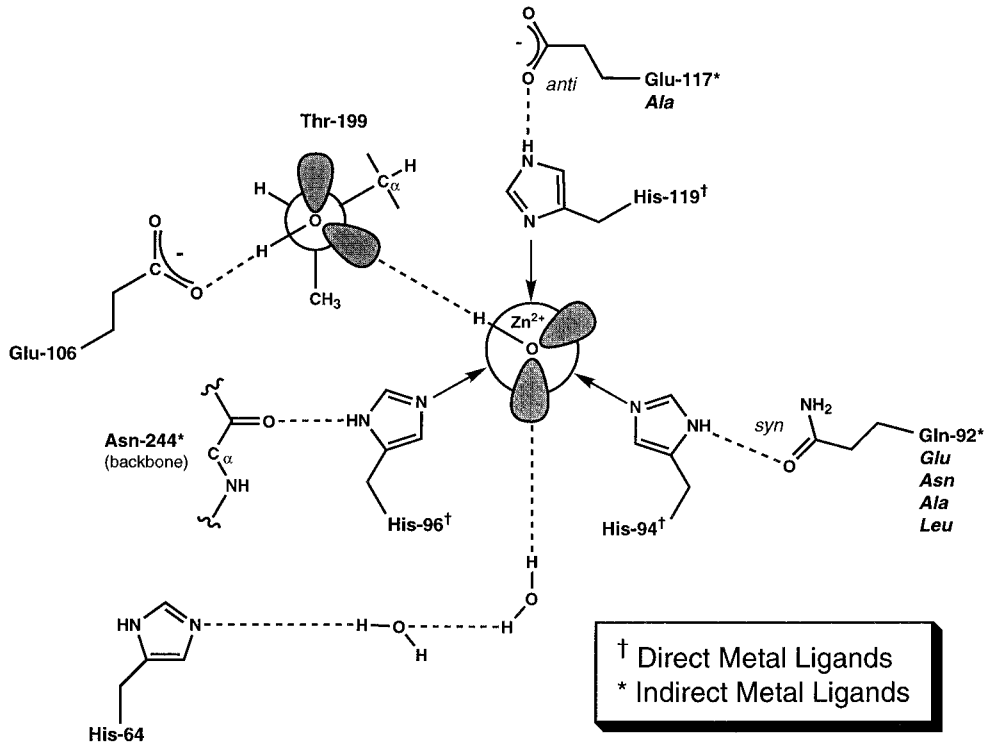

Figure 68. Hydrogen-bond networks in the active site of carbonic anhydrase II and the indirect metal ligands hydrogen bonded to the direct ligands. (Reprinted with permission from ref 345. Copyright 1995 American Chemical Society.)

successful design strategy. Fortunately, an ever increasing number of new metalloenzyme structures has led to comprehensive reviews and analyses on how protein ligands coordinate metal ions.[7,340−342] These include for example the *syn*, *anti*, direct, monodentate, or bidentate coordinating modes of carboxylate side chains, or the N_ϵ vs N_δ coordination of histidines. Also, the "second shell residues"[343] (indirect ligands), which are hydrogen bonded to the metal ligands are important for the stability, affinity, and catalytic properties of the metal binding site. Examples are the carboxylate−histidine−zinc triad, and carbonyl or carboxamide groups in interaction with a zinc-bound histidine.[340]

Carbonic Anhydrase. In carbonic anhydrase the zinc ion is coordinated by three histidines (94, 96, and 119) and by a water or hydroxide ion (Figure 68). All four zinc ligands are hydrogen bonded to indirect ligands. Site-directed mutagenesis of these indirect ligands showed that each hydrogen bond increases the zinc affinity by a factor of about 10.[344,345] The metal affinity is probably influenced by the entropic effect of preorientation of the metal ligands and by an increase of the basicity of the histidines by hydrogen bonding to a carboxylate ($\Delta pK_a \approx 2$) or a carbonyl ($\Delta pK_a \approx 1$) group. Since these effects are additive a maximum decrease of 10^4-fold of the binding affinity is possible for removal of all four hydrogen bonds.[344]

Metal ligand His-94 has been substituted with Cys and Asp; both new ligands were also coordinated to zinc.[346,347] The new $Zn(His)_2Cys$ carbonic anhydrase has a 3×10^3-fold decreased activity, presumably a result of the lower overall positive charge of the new metal center. Although Cys-94 is coordinated to zinc the zinc affinity of this mutant is decreased by almost 4 order of magnitudes ($K_d = 3 \times 10^{-8}$ M compared to 10^{-12} M for the wild-type enzyme). The weaker zinc binding might be due to unfavorable strain introduced into the protein scaffold by the mutation. In another mutant, H96C, the new Cys-96 does not coordinate to zinc, but a second water molecule is coordinated to the metal ion. Obviously here the protein scaffold was not flexible enough to accommodate the new side chain in a metal-coordinated conformation. Thr-199 has been mutated to Cys, Asp, Glu, and His.[348] In all mutants except for T199H the new side chain coordinates as a fourth ligand to zinc by replacing the catalytic water molecule. The T199E mutant showed a 200-fold increased zinc affinity ($K_d = 29$ fM).

Alkaline Phosphatase. The magnesium ion in the trinuclear Zn−Zn−Mg center of alkaline phosphatase does not directly participate in the catalytic steps. In some of the mammalian alkaline phosphatases, which are 10- to 20-fold more active than the *E. coli* enzyme, an excess of Mg^{2+} needs to be present for maximum activity. In these mammalian enzymes Asp-153 (of *E. coli*), which is not a direct ligand to Mg^{2+} but coordinated via a water molecule, is replaced by a histidine. This mutation, D153H, converts the octahedral magnesium site M3 of *E. coli* AP to a tetrahedral zinc site (Figure 69).[349] His-153 is now coordinated to the M3 metal ion and no longer forms a salt link to Lys-328. Instead, Lys-328 is hydrogen bonded to the phosphate group present in the active site. This interaction might cause the observed low activity of this mutant in the absence of magnesium. However, in the presence of magnesium this mutant enzyme is activated, as are the mammalian alkaline phosphatases. These experiments demonstrate the role of the magnesium M3 site in the stabilization of the active site in an active conformation, especially of Lys-328.

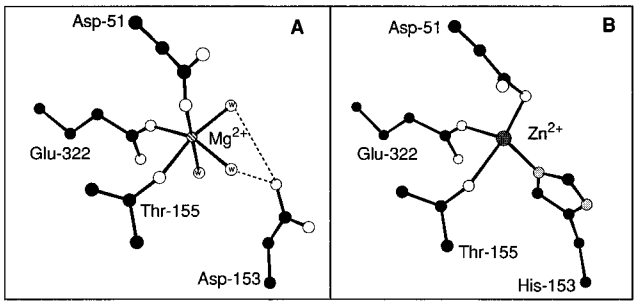

Figure 69. Coordination sphere of the site 3 metal ion binding site in wild-type alkaline phosphatase and in the D153H mutant.[349] The octahedral magnesium site is converted to a tetrahedral zinc site by this mutation. (Reprinted with permission from ref 349. Copyright 1993 by The American Society for Biochemistry and Molecular Biology, Inc.)

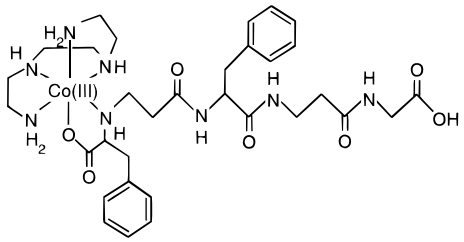

Figure 70. Structure of a hapten used to generate catalytic antibodies containing binding sites for a triethylentetramine metal complex and a peptide substrate.[350]

De Novo Designed Metal Sites. Catalytic antibodies, obtained by immunization against a stable transition-state analogue, can provide novel catalytic activities. However, the production of metalloantibodies is more difficult, since suitable metal−ligand complexes must be prepared for immunization. The complexes should induce a metal cofactor binding site (a binding site for a metal complex) together with the substrate binding site.[350,351] Using the kinetically inert Co(III) triethylenetetramine peptide hapten (Figure 70) metalloantibodies were prepared.[350] Peptidase activity was found in the presence of several divalent and trivalent metal ions, among which zinc was most active. In an alternative approach the metal-binding site is engineered into the antibody at a later step.[352] Zinc-binding sites were introduced into antibodies to form $Zn(His)_3$ sites and sites with His, Glu, and Asp as ligands.

An inhibitory metal-binding site was engineered into the serine protease trypsin by a Arg-96 to His mutation.[353] By binding to this His and to the catalytically essential His-57, divalent metal ions like Cu^{2+}, Ni^{2+}, and Zn^{2+} inhibit the esterase and amidase activities of trypsin.

De novo zinc-binding sites have also been introduced into existing and designed peptides and proteins.[354] A tetrahedral $Zn(His)_3Cys$ site was engineered into the B1 domain of streptococcal protein G.[355] The zinc dissociation constant was estimated as 10^{-9} M. A tetrahedral $Zn(His)_2(Cys)_2$ site of $K_d = 2.5 \times 10^{-8}$ M was introduced into a model four helix bundle protein consisting of four identical helices connected by three identical loops.[356] Mutations of each of these ligands to alanine probed the contribution of each residue to the metal affinity and also yielded four-coordinated zinc sites each with a zinc-bound water, as a first step toward a catalytic site.[357] In another study a $Zn(His)_3$ site was designed into two-helix and four-helix model proteins.[358] A zinc site was also introduced into a designed 61-residue all-β protein[359] and into a receptor molecule to increase hormone−receptor affinity.[360] Binding of metal ions to peptides containing metal-ligating residues also stabilized an α-helical relative to a random coil conformation of these peptides.[361] A zinc-induced conformational change was also used as the basis to design a selective fluorescent chemosensor for Zn^{2+}.[362,363] A 25 residue peptide inhibitor was synthetized which contains a zinc finger motif containing two cysteines and two histidines.[362] In addition, a fluorophore was covalently attached to the peptide. In the absence of zinc, the zinc finger peptide is disordered and the fluorophore is mainly in a polar environment. Upon zinc binding the peptide adopts a defined tertiary conformation, in which the fluorophore is in a nonpolar environment (Figure 71). As a result, the fluorescence emission changes significantly. With this chemosensor nanomolar zinc concentrations can be detected. Furthermore, a sufficient discrimination is provided against binding of Mg^{2+} or Co^{2+}.

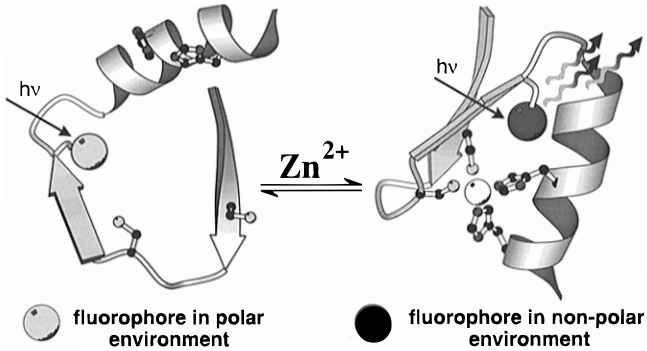

Figure 71. Schematic drawing of a chemosensor for Zn^{2+} based on a peptide containing a zinc-finger motif.[362] Metal binding induces peptide folding, shielding a fluorophore from solvent, and increasing emission intensity. (Reprinted with permission from ref 362. Copyright 1996 American Chemical Society.)

Future efforts in this area will be focused on the introduction of novel activities based on completely new designed metal sites, including nonnatural analogues of amino acid residues, or on existing metalloproteins. Besides the search for new catalysts these studies will also enhance our understanding of the efficiency and structure−function relationship of enzyme catalysis.

VII. Metal Analysis and Metal Localization

Besides the now classical chemical, tracer and spectroscopic methods to determine the metal content in proteins, there are some recent developments of interest.

An underdeveloped method is foreshadowed by the use of the strength of the anomalous scattering signal. In the structure determination of the catalytic subunit of protein serine/theonine phosphatase 1 an anomalous diffraction signal from the use of Cu K_α radiation established that there were two metal ions and ruled out the presence of Mg, Ni, Cu, or

Zn.[186] However, Mn, Fe, or Co remained as possible candidates. Here, the choice of Mn^{2+} was based on restoration of activity of the metal-free recombinant enzyme. Now that one can obtain X-rays of various wavelengths using synchrotron radiation, a more precise identification is possible.

Proton-induced X-ray emission (PIXE) spectroscopy was employed on a single crystal of the catalytic subunit of human protein phosphatase 1.[193] The results indicated the presence of one manganese and 0.5 iron, where Fe^{II} and Fe^{III} could not be distinguished, per molecule of the enzyme. In the electron density maps one metal-related peak (site 1) was twice as high as the other (site 2). This result allowed, in view of the similar atomic numbers of Mn and Fe, the tentative assignment of Mn^{2+} to site 1 and iron to site 2.

The unexpected discovery of an abnormally large peak in the electron density map led to the proposal that adenosine deaminase required one Zn^{2+} per molecule as a cofactor.[221] Subsequent metal analysis using atomic absorption spectroscopy confirmed this suggestion.

When there are two or more metal sites which differ in binding affinity, displacement of the more weakly bound metal by an ion of substantially different atomic number can establish the identity of this less strongly bound site. An example occurs in leucine aminopeptidase for which Mg^{2+} displaced Zn^{2+} in one of the two adjacent zinc sites, thus enabling the determination (in X-ray electron density maps) of which metal site was the low-affinity binding site.[364]

Because of its small atomic number Li^+ is particularly difficult to locate in electron density maps. The Li^+ ion is known to inhibit fructose-1,6-bisphosphatase and also the very closely related structure of inositol monophosphatase, the putative target of Li^+ therapy for manic depression. The Tl^+ ion binds to three sites in fructose-1,6-bisphosphatase, one of which is greatly reduced when Li^+ is added.[365] This site (one of the two divalent catalytic metal sites) is thus a candidate for the action of Li^+ in inhibiting these enzymes.

VIII. Computational Approaches

Molecular mechanics and molecular dynamics simulations are more and more often employed to aid in drug design or to study enzyme mechanisms. The interactions of zinc with small ligands have been studied by *ab initio* and semiempirical techniques.[366] These calculations can also be used to estimate the pK_a of a zinc-bound water for different zinc−ligand systems.[367] Molecular dynamics (MD) simulations have been used to study the binding of CO_2 to the active site of carbonic anhydrase.[262] Parameters for MD simulations of alcohol dehydrogenase containing four- and five-coordinated zinc have been developed.[368] The entrance ("fly") of L-leucine hydroxamic acid into the active site of thermolysin has been simulated and demonstrated the use of these calculations in computer-aided drug design.[369] Also, the proposed hinge-bending motion during catalysis by some thermolysins, as implicated by static crystal structures, was simulated by MD.[370] The free energy perturbation method can be used to estimate relative binding energies of inhibitors. The application of this method to the binding of sulfonamides to carbonic anhydrase showed that energetic trends could be predicted reasonably well.[371]

Docking of substrate and transition-state analogues in many different conformations into the active site of phospholipase C followed by calculation of the interaction energy was used to probe mechanistic aspects of catalysis by this enzyme.[372] These studies yielded a mechanism, which is different from that implied by crystallographic analysis of a complex of phospholipase C with an uncleavable substrate analogue (see section II.D) thus implying (among other possibilities) that the most stable mode for binding of the phosphate group is not necessarily the catalytically productive substrate-binding mode.

The D135H mutant of alkaline phosphatase has a higher phosphate affinity than does the wild-type enzyme. MD simulations indicated that this result might be due to an interaction of phosphate with Lys-328, which forms a salt bridge to Asp-135 in the wild-type enzyme.[349] This interaction was indeed later confirmed by an X-ray structure.[349]

HIV-1 protease is an aspartyl protease which is *in vitro* inhibited by zinc ions at neutral pH.[373] On the basis of the X-ray structure[374] and kinetic data,[373] metal binding to the two active-site aspartates was proposed as the inhibitory mechanism. Molecular and quantum chemical calculations support a coordination of the zinc ion by the two aspartates in a monodentate mode and by two or more water molecules.[375]

The catalytic mechanism of xylose isomerase has been investigated by molecular orbital calculations, especially with respect to the activation of the reaction by Mg^{2+} in contrast to an inhibition by Zn^{2+}.[376] The inhibitory effect of Zn^{2+} was explained by a larger charge transfer from the ligands to this metal ion, thus reducing the effective charge on the metal ion. Assuming that the main role of the metal ions in this reaction is the electrostatic stabilization of the substrate transition states, metals like Mg^{2+} which retain a higher effective charge are more efficient in catalysis. However, it remains to be shown if the relatively simple model can be extended to other reactions, especially those where zinc is most active; consequently, other factors than electrostatic stabilization must here be prevalent, possibly the charge transfer from the coordinated substrate to the metal ion.

Most of the MD simulations on zinc enzymes used an explicit bonded force field for the metal ion, which means that bond length and angles of the metal−ligand coordination sphere are restrained to parametrized values. This approach is especially useful for metals like Cu^{2+} which have a strong preference for certain coordination geometries. Zinc, however, due to its d^{10} electron configuration and lack of ligand field stabilization energy, tolerates more flexible coordination geometries (4-, 5-, and 6-fold). Zinc is therefore, like Ca^{2+} or Mg^{2+}, ideally suited for a nonbonded force-field representation, which includes only van der Waals and electrostatic terms. This approach is especially attractive since it allows the

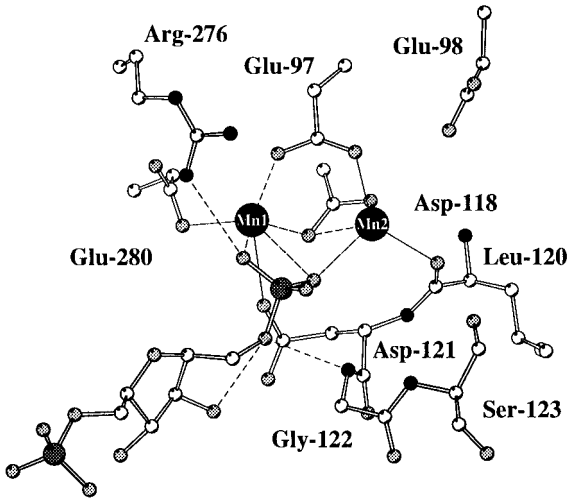

Figure 72. Binding of an substrate analogue inhibitor, in which the 2-OH group of fructose 1,6-bisphosphate is replaced by a hydrogen atom, to fructose-1,6-bisphosphatase. Generated from PDB file 1FBP.[380]

simulation of ligand exchange and a change in coordination geometry during catalysis. New force-field parameters for such a nonbonded representation of zinc have recently been developed, and it was shown that carboxypeptidase A and carbonic anhydrase can be modeled as accurately (in comparison to high-resolution crystal structures) as they can with the use of bonded force fields.[377]

IX. Enzymes with Mainly Low-Affinity Divalent Metal Binding Sites

A. Fructose-1,6-bisphosphatase and Other Li-Sensitive Metallophosphatases

The homotetrameric fructose-1,6-bisphosphatase (FBPase) removes the 1-phosphate from the α-anomer of fructose-1,6-bisphosphate. Allosteric regulation by AMP and active-site inhibition by fructose-2,6-bisphosphate control the flux of the gluconeogenic pathway. At low concentrations of Zn^{2+} the tetramer shows four binding sites for this ion (K_d < 0.1 μM for the strongest bound site). In the presence of substrate analogues and 8 μM Zn^{2+} four additional binding sites are present.[378] The enzyme is also activated by Mn^{2+} and by Mg^{2+}, although Zn^{2+} is probably preferred *in vivo*.[379]

In the structure of the R state of the enzyme bound to an analogue of the α-anomer of the substrate in which the 2′-OH group is replaced by a hydrogen atom, there are two metal ion sites each in a distorted tetrahedral geometry.[380] The high-affinity binding site, M1, is ligated by carboxylates of Glu-97, Asp-118, and Glu-280, and by the 1-phosphate of the analogue, whereas the metal ion in site M2 (3.7 Å from M1) is bound to carboxylates of Glu-97 and Asp-118, to the carbonyl group of Leu-120, and to the 1-phosphate (Figure 72). The carboxylate group of Asp-121 is at a somewhat longer distance of 3.0 Å from Mn1. In the proposed catalytic mechanism, the attack of a water molecule on the tetrahedral phosphorus occurs opposite the ester oxygen and is promoted by $M2^{2+}$ and by removal of a proton by Glu-98 (Figure 73). This proposed role of Glu-98 as a general base is supported by the finding that a mutation to glutamine diminishes k_{cat} 1600-fold.[381] The $M1^{2+}$ ion also aids the reaction by binding to an oxygen of the phosphate group. It is unclear whether a trigonal-bipyramidal phosphorane or a metaphosphate-like intermediate is formed. Resolution of the intermediate state requires protonation of the ester oxygen, probably by the 2′-OH of the substrate assisted by Asp-121. In the presence of a similar substrate analogue of the β-anomer Zn^{2+} or Mn^{2+} bind only to site M1, whereas the site M2 is unoccupied. Since biochemical and structural studies implicate a two-metal ion mechanism for FBPase, this finding supports the view that the α-anomer is the true substrate.

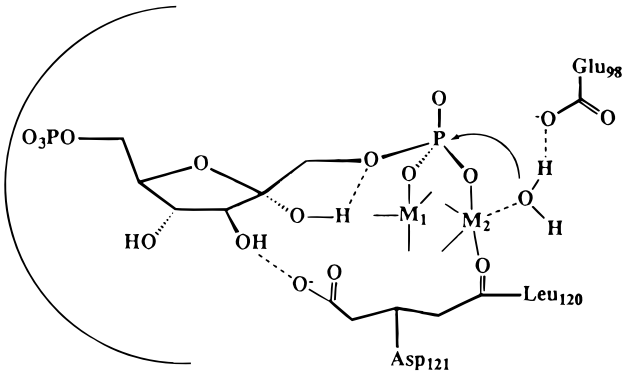

Figure 73. Substrate binding mode and attack of the nucleophile in the proposed mechanism for phosphoester hydrolysis by fructose-1,6-bisphosphatase.[380] Glu-98 may accept a proton from the water nucleophile. (Reprinted with permission from ref 380. Copyright 1993 American Chemical Society.)

When the analogue of the α-anomer is bound to the AMP-induced T state the M1 site is displaced by only 0.6 Å, whereas the M2 site is 1.4 Å away from its position in the more active R state.[382] This displacement of $M2^{2+}$ by a reorientation of the allosteric AMP domain by 2° relative to the active site domain greatly reduces the ability of the second metal ion to initiate the hydrolysis of the substrate.

The three-dimensional structures of FBPase[380] and inositol monophosphatase[383] are similar, including the protein fold and the active-site structure.[384] Together with inositol polyphosphate 1-phosphatase and other less well-characterized gene products, these enzymes form a family of lithium-inhibited metallophosphatases.[386]

Lithium ions inhibit FBPase by binding to site M1, possibly retarding turnover or product release.[387] This study provides a structural basis for a similar inhibition mechanism for inositol monophosphatase, the probable target of Li^+ in the treatment of manic depression. Finally, inhibition of FBPase may become an important therapy for the prevalent type II diabetes.[385]

B. *myo*-Inositol Monophosphatase, a Putative Target of Li^+ Therapy on Manic Depression

When phosphatidyl inositol 4,5-bisphosphate is hydrolyzed by phospholipase C the second messengers inositol 1,4,5-triphosphate and diacylglycerol are formed. This inositol triphosphate is metabolized into several pathways. As a last step in these pathways, inositol monophosphatase (IMPase, EC

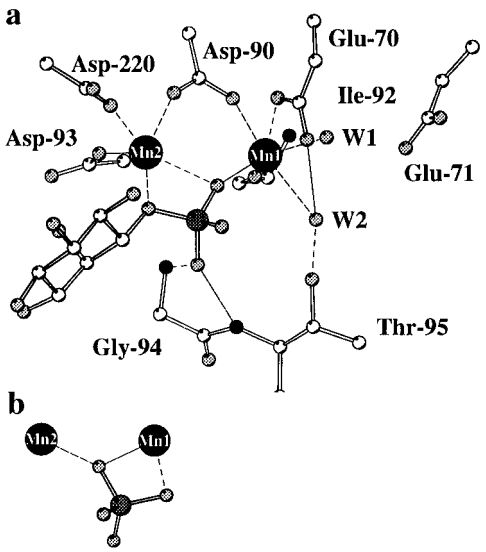

Figure 74. (a) Superposition of the binding mode of substrate D-inositol 1-phosphate to the inactive Li1-Gd2 inositol monophosphatase onto the structure of the active Mn1-Mn2 enzyme. (b) Binding mode of a product phosphate ion to Mn1-Mn2 IMPase. Generated from PDB files 1IMA, 1IMC, and 1IMD.[395]

3.1.3.25) hydrolyzes inositol 1-phosphate (I1-P), I3-P, and I4-P to regenerate D-*myo*-inositol, thus maintaining this signal cycle.[388] IMPase requires two Mg^{2+} for catalysis, although Mn^{2+}, Zn^{2+}, and Co^{2+} are active to some extent.[389,390] The inhibition of IMPase by Li^+ makes it a putative target for use of Li^+ in therapy of manic depression.[391,392]

The structural studies including complexes with substrates[393] provide evidence for two-metal catalysis.[394,395] The two metal ions are liganded by Glu-70, Asp-90, Asp-93, Asp-220, one water molecule (to site 1), the carbonyl group of Ile-92, and one Cl^- ion. A third Mn^{2+} ion near Glu-70 is displaced when phosphate binds. Upon binding of a phosphate anion to Mn1 and Mn2 the water from site 1 and the Cl^-, which is coordinated to all three metal sites, is displaced. The substrate D-*myo*-inositol 1-phosphate binds to the enzyme when it is inactivated by the presence of Gd^{3+} (in site 1) and Li^+ ions (site 2). Superimposed on the structure of the active Mn−Mn enzyme the substrate binding mode of the Gd−Li form provides a plausible model for the arrangement of the reactants prior to the transition state (Figure 74). In the proposed mechanism, an in-line attack of water molecule W2 bound to M1 occurs at phosphorus and inositol leaves (Figure 74). Metal ion 2 activates the leaving group and both metal ions may stabilize the transition state. In corroboration of this mechanism a product phosphate anion binds in an inverted way relative to the phosphate group of the substrate (Figure 74), as expected after an in-line displacement step.

Indirect evidence[389] suggests that the inhibitory Li^+ ion displaces the divalent metal at site 2. The observation[383] that IMPase and fructose-1,6-bisphosphatase (FBPase) have very similar three-dimensional structures, and that FBPase is also inhibited by Li^+, has led to a direct location[396] of Li^+ binding in FBPase to the M1 site which corresponds to the M2 site of IMPase.

C. Inositol Polyphosphate 1-Phosphatase

The monomeric bovine inositol polyphosphate 1-phosphatase, part of the phosphatidylinositol signaling pathway,[397] hydrolyzes the 1-phosphate from inositol 1,4-bisphosphate and inositol 1,3,4-triphosphate.[398] It is inhibited by Li^+ and Ca^{2+} ions, and activated by Mg^{2+} ions in an apparently cooperative way.[399]

The two Mg^{2+} sites are 3.9 Å apart, and the coordination around each site shows a distorted octahedral geometry. However, the metal to ligand distances are unusually long. For site 1 they are 3.8 Å for Glu-79, 3.13 Å and 3.24 Å for Asp-153, 3.28 Å for Asp-156, 3.14 Å for Asp-317, and 3.35 Å for H_2O; and for site 2, they are 3.47 Å and 3.54 Å for Asp-54, 2.63 Å for Glu-79, 2.48 Å for the carbonyl oxygen of Ile-155, and 3.91 Å for H_2O. Nevertheless, these binding sites are reasonably similar to those in FBPase[383] and IMPase.[400] Further study at increased (>3 mM) concentrations of $MgCl_2$ or using the more electron-rich Mn^{2+} or Zn^{2+} ions may exclude the possibility that the two metal sites are occupied by H_2O or H_3O^+.

The proposed mechanism includes an in-line attack of a metal-activated water ligand.[401] In FBPase, IMPase, and inositol polyphosphate 1-phosphatase, the Glu which is proposed to activate a metal-bound water in the mechanism of FBPase (98, 71 and 80, respectively), and the Asp which may assist in proton transfer to the oxygen of the leaving group (121, 93, and 156, respectively), are conserved. However, the proposed mechanisms of IMPase and FBPase differ in their substrate binding modes, on the basis of X-ray structures of inhibitor complexes.

D. RNA and DNA Polymerases: Two Metal Ions in the Transmission of Genetic Information

Including the Klenow fragment of *E. coli* DNA polymerase I (pol I)[402−407] there are five enzyme structures known containing a polymerase active site. The other four are the reverse transcriptase from the human immunodeficiency virus (HIV-RT),[408−413] rat DNA polymerase β,[414−416] bacteriophage T7 RNA polymerase,[417] and *Thermus aquaticus* DNA polymerase.[418] Comparison of these structures shows a similar topology of the three domains related to the polymerase site,[419] except for polymerase β, which has a different topology and is related to other nucleotidyl transferases.[420] Both the binding mode of a template primer and possibly the detailed mechanism for polymerase β are different from those aspects of the other polymerases,[415] a controversy[421,422] which is subject to experimental resolution. Nevertheless, all stereochemical studies have established an inversion of the configuration at phosphorus,[423−427] consistent with an in-line mechanism. Catalysis involves two adjacent metal ions, most probably Mg^{2+} or Mn^{2+}, or possibly Zn^{2+} in the strong binding sites.

E. 3′–5′ Exonuclease Site of DNA Polymerases I and T4

Many DNA and RNA polymerases contain nuclease activity at a different site from the polymerase active site. For example DNA polymerase I (pol I) of *E. coli*

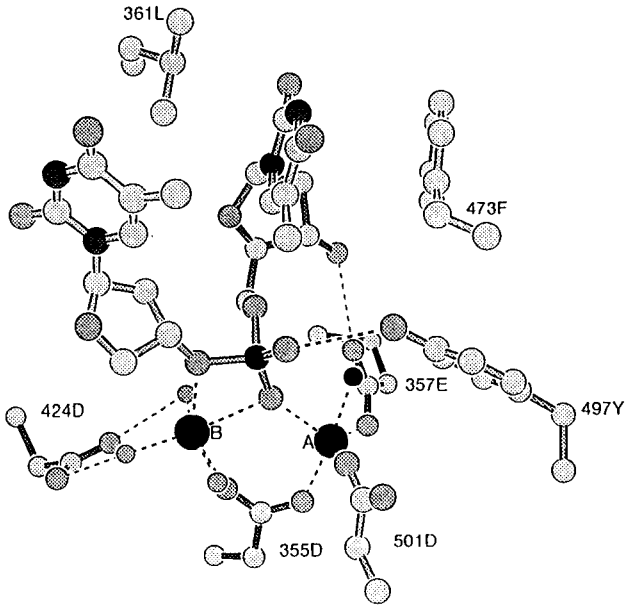

Figure 75. Structural model for the binding mode of a dinucleotide to the active site of the 3′−5′ exonuclease of *E. coli* DNA polymerase I.[405] The coordinates of the dinucleotide are from a tetranucleotide bound to an inactive D424A mutant enzyme (Mg in site A, no metal bound to site B). These coordinates are superimposed onto the structure of the protein with two bound metal ions taken from a complex of the wild-type enzyme with dTMP (dTMP not shown). Metal binding site A is supposed to be occupied by zinc *in vivo*. The water ligand (filled circle) coordinated to Me_A is the nucleophile in the proposed mechanism in Figure 76. Figure provided by authors.[405]

has three separate domains for the polymerase, 3′−5′ exonuclease and 5′−3′ exonuclease activities all within a polypeptide chain of 103 kDa. All of these activities require divalent metal ions (Mg^{2+}, Mn^{2+}, or Zn^{2+}), although it is not yet clear which metal ions occupy the catalytic sites *in vivo*. Moreover, the polymerase and 3′−5′ exonuclease sites and, possibly, the 5′−3′ exonuclease site use a two-metal ion mechanism. In the large proteolytic fragment (Klenow fragment) of pol I the DNA polymerase site and the 3′−5′ exonuclease site are about 33 Å apart.[402] Moreover, these two sites function independently[428] and have separate binding sites for DNA.

In the 3′−5′ exonuclease site of pol I the two metal ions A and B are 3.9 Å apart such that Zn^{2+} at site A is coordinated to Asp-355, Glu-357, and Asp-501 and to the 5′-phosphate of the product deoxynucleotide monophosphate (dNMP) in a structure to 2.6 Å resolution of a complex with the wild-type fragment; in addition a water molecule is coordinated to this Zn^{2+} distorting the tetrahedral bonding geometry. On the other hand, site B has six ligands in an octahedral arrangement. This site is unoccupied unless a nonprotein ligand, here dNMP, is bound. The ligands include Asp-355, two of the 5′-phosphate atoms of dNMP, and three water molecules which are bound to Asp-424 and to backbone amides (Figure 75).[405] In the presence of 20 mM $MgSO_4$ and 1 mM $ZnSO_4$, Zn^{2+} is present at site A, whereas Mg^{2+} is present at the octahedral site B.

In the Asp-424 to Ala mutant, metal site B is unoccupied, and a single strand tetranucleotide substrate could be complexed with the now-inactive

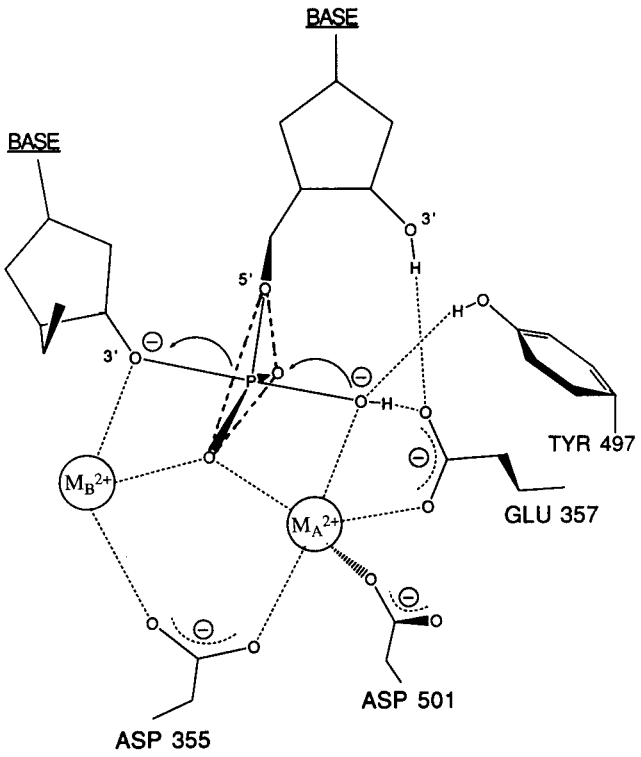

Figure 76. Proposed transition state for the 3′−5′ exonuclease reaction of DNA polymerase I.[405] Figure provided by authors.[405]

Klenow fragment.[403,405] This complex shows essentially no distortion in the enzyme as a result of the mutation or of the formation of the complex. The extension of this binding mode to a proposed transition state requires only small movements of atoms in the complex (Figure 76).[405] Metal cation A promotes the attack of a hydroxide ion to form a five-coordinated intermediate, which then loses the opposite in-line 3′ phosphoester oxygen as an anion stabilized by the metal cation at site B. This mechanism is in agreement with the observed inversion[429] of configuration at the 3′ terminal phosphorus.

The crystal structure of the NH_2-terminal 388-residue fragment of T4 DNA polymerase showed that the 3′−5′ exonuclease domain closely resembles the corresponding domain of Klenow fragment, despite minimal sequence homology.[430] Soaking crystals in various concentrations of Zn^{2+} and Mn^{2+} demonstrated zinc binding to site A and manganese binding to site B, similar to the situation in Klenow fragment.

F. Ribonuclease H and Other Homologous Nucleotidyl Transferases: One- or Two-Metal Ion Catalysis?

Ribonuclease H (RNase H) from *E. coli* hydrolyzes the RNA strand of specific DNA/RNA hybrids to yield 5′-phosphates. This RNAse H activity probably is involved in DNA replication. In the replication of retroviruses, an RNAse H domain carries out one of the three catalytic functions of reverse transcriptase.[431,432]

Only one metal ion (Mg^{2+}) is bound in the active center of RNAse H of *E. coli*.[433,434] This Mg^{2+} ion interacts with Asp-10, Gly-11 (carbonyl), and Glu-48 (Figure 77). Asn-44 is at a distance of 3.0 Å to

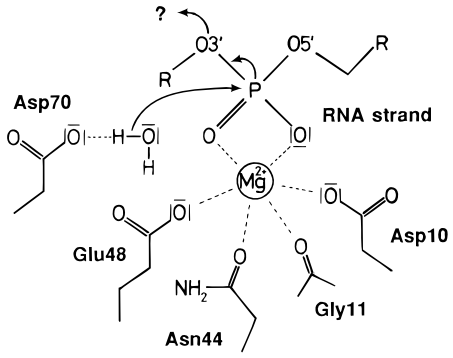

Figure 77. Proposed single-metal reaction mechanism of *E. coli* RNase HI.[433,434] (Reprinted with permission from ref 434. Copyright 1993 The American Society for Biochemistry and Molecular Biology, Inc.)

Mg^{2+}. This metal-binding site is sterically accessible to solvent, and presumably to nucleotides. In the proposed mechanism (Figure 77), Asp-70 promotes the attack of H_2O (or OH^-) at the phosphorus of the phosphate group of a DNA/RNA hybrid substrate. In further support of the single metal mechanism, addition of mononucleotides or of trinucleotides does not induce a second metal binding site at metal ion concentrations of 10 mM or less.[433,434]

In contrast, RNAse H of HIV-1 reverse transcriptase is reported to bind two Mn^{2+} ions, which are 4.0 Å apart, at very high concentrations of Mn^{2+} (45 mM).[435] One of these Mn^{2+} ions is near to the Mg^{2+} site of the *E. coli* enzyme. RNAse H from *E. coli*[433,434,436] and the RNAse H domain HIV-I reverse transcriptase have similar structures,[435] although there are some differences in other regions. Among 26 RNAse H sequences including some retrotransposons and other retroviruses types of genetic elements four residues are conserved: Asp-10, Glu-48, Asp-70, and Asp-134.[436] Mutations at each of the first three of these residues strikingly reduce activity in the *E. coli* enzyme.[437]

These similarities suggest that all these RNAse enzymes use metal ion cofactors (Mg^{2+} or, in some cases Mn^{2+}). Zn^{2+} does not activate RNAse H,[438] possibly due to a high coordination set of oxygen ligands to the activating divalent metal cation. Four other enzymes that have a similar folding topology[439] and active site geometry to ribonuclease H are RuvC resolvase of *E. coli* (an endonuclease that cleaves Holliday junctions),[440] two retroviral integrases (from HIV-1[339] and from avian sarcoma virus[441]), the DNA repair enzyme exonuclease III,[442] and the bacteriophage Mu transposase.[443]

The dimeric RuvC requires Mg^{2+} or Mn^{2+}, whereas Ca^{2+} or Zn^{2+} are relatively poorly efficient in catalysis.[444,445] A binding site for one Mn^{2+} was located near Asp-7 (2.5 Å) and Asp-141 (3.5 Å) in one of the four molecules of the asymmetric unit of a crystal which had been soaked in a solution containing 5 mM $MnCl_2$.

The multifunctional enzyme exonuclease III of *E. coli* binds Mg^{2+} or Mn^{2+} at a single site, and does not bind Zn^{2+} when the crystals are soaked in solutions containing 10 mM Zn^{2+}.[442] Also, only one Mn^{2+} site is observed in the ternary complex of the enzyme with Mn^{2+} and dCMP. In the proposed mechanism, the M^{2+} binds to a phosphate oxygen and helps nucleophilic attack by the OH^- which is created by the Asp-229 to His-259 relay (Figure 78).

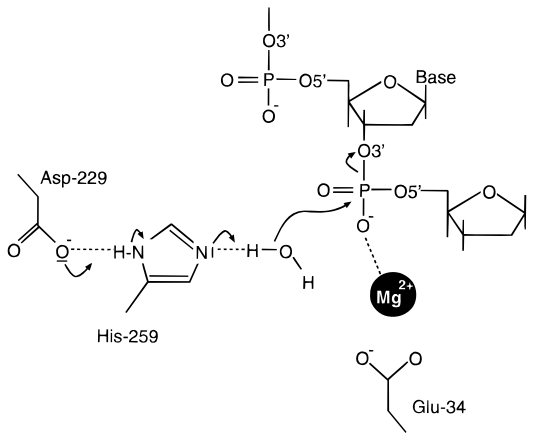

Figure 78. Proposed reaction mechanism for the endonuclease, 3′−5′ exonuclease, and RNase H activities of the exonuclease III of *E. coli*.[442] (Adapted from ref 442.)

In Mu transposase, the mechanism is expected to be similar to that in HIV integrase, and studies of binary complexes with M^{2+} ions and ternary complexes including also substrate analogues are anticipated.

In summary, it seems probable that most of these enzymes catalyze by a one-metal ion mechanism. These enzymes contain low-affinity metal binding sites, consisting mainly of carboxylate side chains and substrate atoms. However, even for evolutionarily related enzymes it has to be shown experimentally whether a certain enzyme uses one or two metal ions in catalysis. The change from a one-metal ion mechanism, in which for example one metal coordinates the phosphate group and a carboxylate side chain polarizes the water nucleophile (Figure 77), to a two-metal ion mechanism, in which the carboxylate group coordinates a second metal ion that in turn activates the nucleophile, may be a relatively small step in the evolution of an enzyme mechanism.

G. Restriction Endonucleases: One or Two Magnesium Ions in the Cleavage of DNA

Mg^{2+} is possibly the cofactor used by restriction endonucleases to cut the phosphodiester bond of DNA *in vivo*. For *Eco*RV and *Eco*RI less activity is also seen in the presence of Mn^{2+} and Co^{2+}, whereas Zn^{2+}, Ni^{2+}, and Cd^{2+} give only very low activity.[446] A two-metal ion mechanism is implicated for some of these enzymes. X-ray structures are available for *Eco*RI,[447] *Eco*RV,[448] *Pvu*II,[449] *Bam*HI,[450] and *Cfr*10I.[451]

H. Catalytic RNA: "Metalloribozymes"

Although all catalytic RNA's need divalent metal ions for activity, the role of these ions as structural or catalytic has not become clear until recently. In *Tetrahymena*, cleavage of exogenous RNA or DNA substrates requires Mg^{2+} or Mn^{2+}.[452] If in a DNA substrate the bridging 3′ oxygen at the scissile O−P bond is replaced by sulfur, the Mg^{2+}-promoted rate is reduced by a factor of about 1000. However, when Mn^{2+} or Zn^{2+} is added (in the presence of Mg^{2+}) the rate of cleavage of the 3′ S−P bond is comparable with the rate for the 3′ O−P bond. Thus the metal

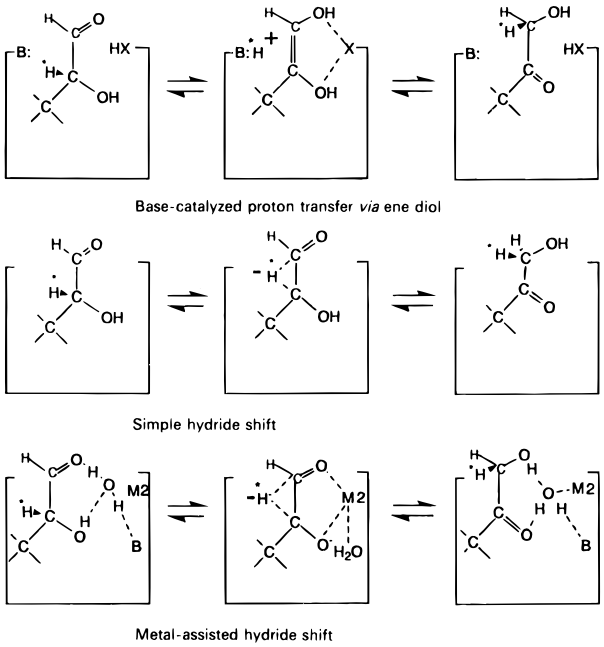

Figure 79. Three possible types of isomerization mechanisms for xylose isomerase. (Reprinted with permission from ref 465. Copyright 1994 International Union of Crystallography.)

ion contributes directly to catalysis, presumably by stabilizing the development of negative charge on the 3′ oxygen in the transition state. These results are consistent with the "hard, soft" matching of Mg^{2+} with oxygen on the hard side and of Zn^{2+} and sulfur on the intermediate region of polarizabilities.[452,453] A two-metal ion mechanism for catalytic RNA similar to the mechanism of 3′−5′ exonuclease (Figure 76) has been proposed.[454]

I. Xylose (Glucose) Isomerase

Xylose isomerase (EC 5.3.1.5) catalyzes the interconversion of various five- and six-carbon aldoses and ketoses, for example D-xylose to D-xylulose or D-glucose to D-fructose. The latter conversion is one of the most important biotransformations for the food industry in the manufacture of high fructose corn syrups (about 10 Mt/a).[455] In the reaction a hydrogen atom is moved between C1 and C2 of the substrate. Two metal ions, such as Mg^{2+}, Mn^{2+}, or Co^{2+} activate the enzyme, whereas Zn^{2+}, Cu^{2+}, Ca^{2+}, and Ba^{2+} are inhibitory.[456]

The hydrogen is transferred stereospecifically and does not exchange with solvent protons.[457,458] Proposals were made of a base-catalyzed proton transfer involving a *cis*-ene-diol intermediate,[459−461] or of hydride transfer between C1 and C2.[462]

Following solution of the $(\alpha\beta)_8$ barrel enzyme structure at 4 Å resolution[463] a large number of other X-ray diffraction studies have appeared.[464,465] Xylose isomerase seems to be evolutionarily related to other $(\alpha\beta)_8$ barrel enzymes but it employs a unique mechanism. The three types of proposed mechanisms include base-catalyzed proton transfer involving the ene-diol intermediate, a simple hydride shift, and a metal-assisted hydride shift (Figure 79).

The X-ray diffraction results favor the metal-assisted hydride shift mechanism.[464−467] In addition,

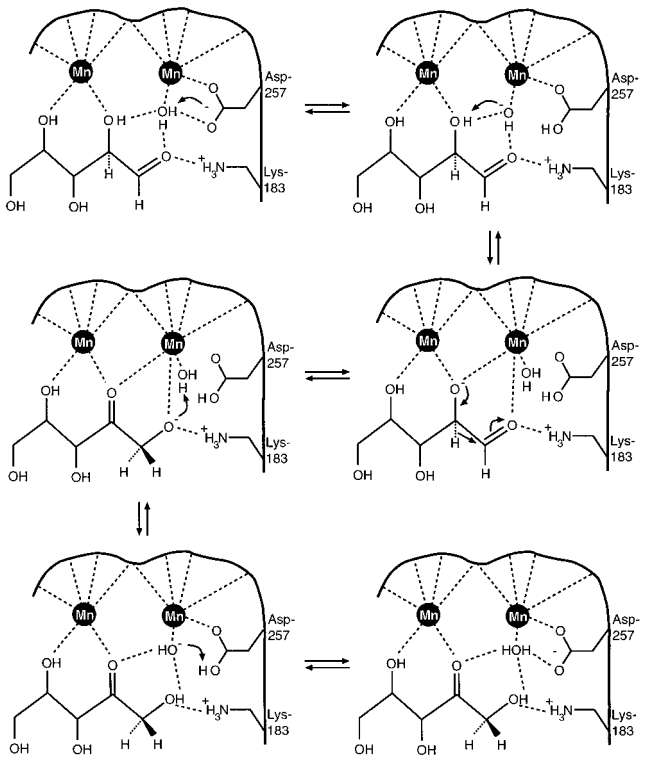

Figure 80. Proposed mechanism for a metal-mediated 1,2-hydride shift reaction in xylose isomerase.[467] (Adapted from ref 467.)

there is no suitable base available for a proton transfer between C1 and C2. Moreover, the high-resolution studies[467] at 1.6 Å of xylose isomerase from *Streptomyces rubiginosus* in the presence of Mn^{2+} and either xylitol or D-xylose are consistent with the steps shown in Figure 80. His-54 catalyzes the ring opening of the cyclic α-D-xylose, followed by binding of the extended form of D-xylose involving both Mn^{2+} ions. A metal ion-mediated 1,2-hydride shift occurs, followed by ring closure involving His-54 to yield α-D-xylulose. This mechanism is consistent with the observed lack of C1−C2 proton exchange with solvent, the requirement for two divalent metal ions, and the pH rate profile.

When substrates or analogues are present, various metal-binding modes occur. The M1 divalent metal ion may be part of a six-membered ring in various ways, by binding hydroxyl, carbonyl, carboxyl, or ring ether oxygens, e.g. when xylose, xylulose, xylitol, sorbitol, or threonate is bound.[465] Or, this metal ion may participate in a five-membered ring, binding hydroxyl or ring ether oxygen atoms, as seen when α-D-glucopyranose, ascorbic acid, or 1,5-dianhydrosorbitol is present.[465] In the Mn^{2+} complex of the enzyme from *S. rubiginosus*, there are two metal ions: Mn1 bound by Glu-181, Glu-217, Asp-245, and Asp-287; and Mn2 bound by Glu-217, His-220, Asp-257, and bidentately by Asp-255.[465] Other bonds to ligands or water molecules complete the octahedral coordination spheres. A displacement of 1 Å in site M2 has been found when a transition-state analogue is bound.[466]

Why does Zn^{2+} not activate xylose isomerase? Each of the three ions Co^{2+}, Mn^{2+}, and Zn^{2+} bind at pH 6 to both sites M1 and M2.[468−470] For both small chelating molecules and proteins the approximate

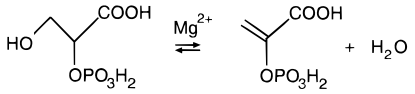

Figure 81. Dehydration of 2-phospho-D-glycerate to phosphoenolpyruvate catalyzed by enolase.

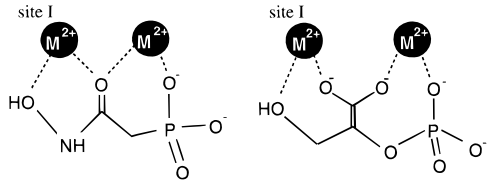

Figure 82. Binding of phosphonoacetohydroxamate to the two metals of enolase (left).[480] Model for the binding mode of the *aci*-carboxylate intermediate to enolase (right).[480]

binding constants are in the order $Ca^{2+} < Mg^{2+} < Mn^{2+} < Fe^{2+} < Co^{2+} < Zn^{2+} < Ni^{2+} < Cu^{2+}$,[458,460,461] approximately in order of ionic radius plus some degree of covalency. Molecular orbital calculations suggest that softer, polarizable ions such as Ni^{2+}, Cu^{2+}, and Zn^{2+} are not so effective in this reaction, which is dominated by electrostatic catalysis, because the charge transfer from the ligands to the metals reduces their effective charge (see also section VIII). Ions such as Ca^{2+} are too large to bind to or to be effective at site M2 in the transition state.

J. Enolase, a Metal-Catalyzed Dehydration Reaction

The dimeric enolase from yeast catalyzes the reversible dehydration of 2-phospho-D-glycerate to yield phosphoenolpyruvate (Figure 81). The two required divalent cations per monomer[471] are preferably Mg^{2+}, although Mn^{2+} and Zn^{2+} are also active,[472] whereas Co^{2+} is active when three cations are bound to the dimer, but is inactive when four are bound.[473] There is a high-affinity M^{2+} site, and a lower affinity site which binds as the substrate−enzyme complex is formed.[474]

In the Mg^{2+}-enzyme the single Mg^{2+} ion per monomer is octahedrally coordinated to Asp-246, Asp-320, Glu-295, and three water molecules.[475] The Zn^{2+}-enolase complex shows a trigonal-bipyramidal Zn^{2+} environment, in which Asp-246 and Asp-320 are axial ligands, and Glu-295 and two H_2O molecules are in the equatorial plane.[476] When the substrate is equilibrated with the Mg^{2+}-enzyme the structure at 2.2 Å shows five coordination, including Asp-246, Asp-320, Glu-295, one H_2O, and the 3′OH of phosphoglycerate.[477]

Inhibition at the 15 pM level is shown by phosphonoacetohydroxamate[474] (PhAH) which mimics the *aci*-carboxylate intermediate (Figure 82) formed upon release of H^+ from the 2-carbon of the substrate. X-ray diffraction studies of enolase−bis-Mg^{2+}−PhAH[478] and of enolase−bis-Mn^{2+}−PhAH[479] show differences in metal binding. In the bis-Mg^{2+} complex the metal−metal distance is 4.05 Å,[479] in accord with EPR measurements of 3.2−3.8 Å which indicate spin exchange in the bis-Mn^{2+} complex,[480] and in a product complex.[481] In the bis-Mn^{2+} complex the metal−metal distance is 8 Å,[478] in agreement with an EPR study of a phosphoglycolate complex with $2Mn^{2+}$ which showed no exchange.[482] Perhaps these results

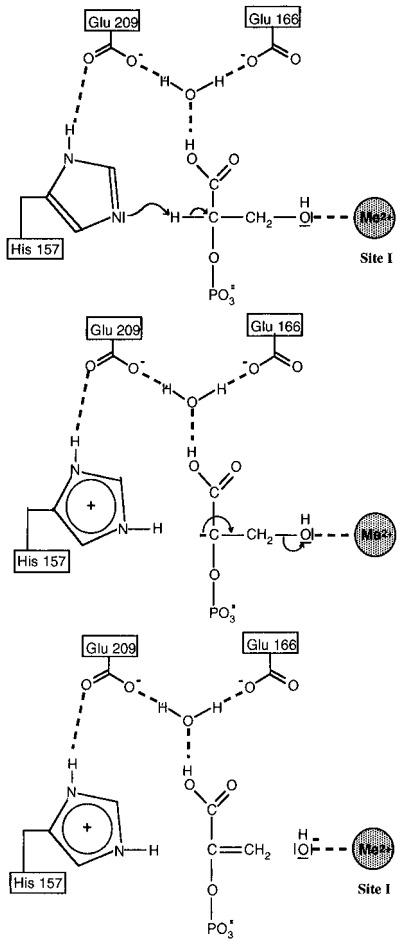

Figure 83. Proposal for the mechanism of enolase.[487] (Reprinted with permission from ref 487. Copyright 1995 American Chemical Society.)

on PhAH arise from the two different modes of binding,[474,478] from two stages in the latching of a gate which closes the active site,[479] or from use of a third metal site which is inhibitory.[483]

These studies, together with the EPR results, lead to structural models in which the *aci*-carboxylate form is stabilized by both metal ions following proton removal from the C2 atom of 2-phospho-D-glycerate (Figure 82).[479,480] In particular the strongly bound M^{2+} (site I) ligates to the primary OH group and the nearby oxygen of the carboxylate, as the less strongly bound M^{2+} binds to one oxygen of phosphate and to the other oxygen of the carboxylate (Figure 82). The metal ion stabilization[480] of this *aci*-carboxylate intermediate is consistent with studies which favor a mechanism via a carbanion formed by removal of a proton from C2 before OH^- departs,[484−486] a process which is possibly assisted by the strongly bound metal. The general base which accepts the C2 proton is still under consideration and may include Lys-345, a water molecule between Glu-211 and Glu-168,[477] or more likely,[487] the conserved His-157 in lobster enolase (His 159 in yeast enolase).[479] In the complex of lobster enolase with Mn^{2+} and the inhibitior phosphoglycolate ($^-O_2CCH_2OPO_3^{2-}$) the imidazole of His-157 is 4.5 Å from the carbon of the CH_2 group.

Also, in this complex with Mn^{2+} and phosphoglycolate only one Mn^{2+} ion, at site I, is seen, and it is coordinated in lobster enolase to Asp-244, Glu-294, Asp-319, and three water molecules. In the most

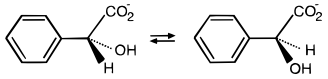

Figure 84. Isomerization of the *R* and *S* enantiomers of mandelate catalyzed by mandelate racemase.

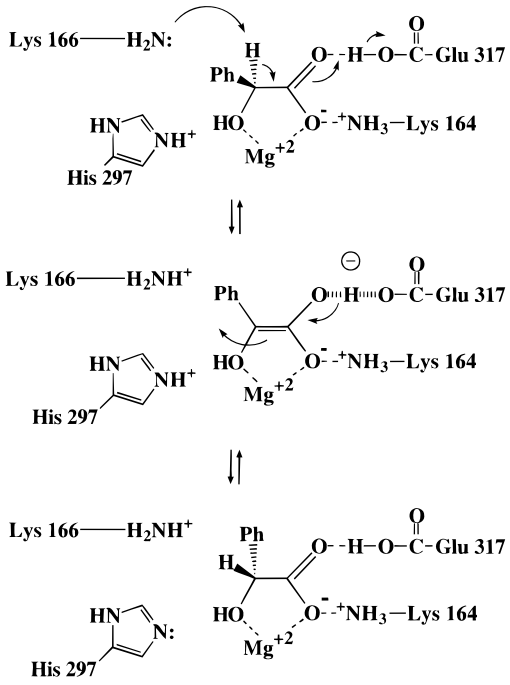

Figure 85. Proposed reaction mechanism for mandelate racemase.[492] Figure provided by authors.[492]

recent mechanistic proposal this site I metal ion aids in removal of the OH^- without necessarily forming the enolic intermediate (Figure 83). The H_2O bound to Glu-209, Glu-166 (Glu-211 and Glu-168 in yeast), and the carboxylate of substrate is proposed[487] to protonate the substrate's carboxylate group in order to reduce the pK_a of the leaving proton of the substrate's CH group. Alternatively, if the electron density that bridges the carboxylate of phosphoglycolate to Glu-166 and Glu-209 of lobster enolase is a low occupancy Mn^{2+} site, rather than H_2O as presently assigned, this second metal site could polarize a putative substrate's carboxylate group, possibly favoring enolization, stabilizing the *aci*-carboxylate intermediate and lowering the pK_a of the protons of the CH_2 group. On the other hand, if the second metal site is near the phosphate of the substrate,[478] an inductive stabilization of the CH_2^- part of the substrate would be reasonable, and if further this second metal ion also binds to one oxygen of the carboxylate, the *aci*-carboxylate may yet be a viable intermediate stage of the reaction.

K. Mandelate Racemase

Mandelate racemase (MR, EC 5.1.2.2) from *Pseudomonas putida* (ATCC 12633) catalyzes the racemization of either the *R* or the *S* enantiomer of mandelate to yield an equilibrium mixture (Figure 84). Proton−deuterium exchange experiments are consistent with two distinct general acid−general base catalysts from the protein.[488−490] In agreement with these results the three-dimensional structure

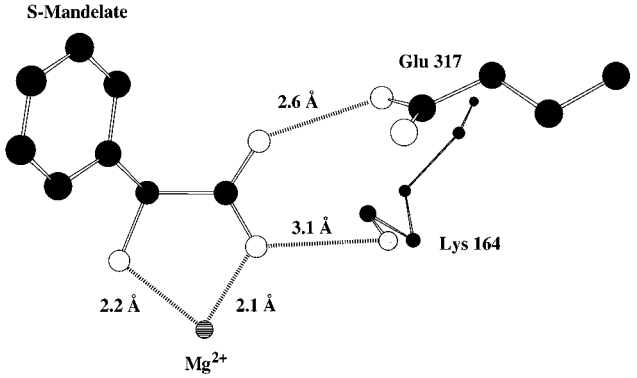

Figure 86. Binding mode of (*S*)-mandelate to the active site of the K166R mutant of *P. putida* mandelate racemase.[491] (Reprinted with permission from ref 491. Copyright 1995 American Chemical Society.)

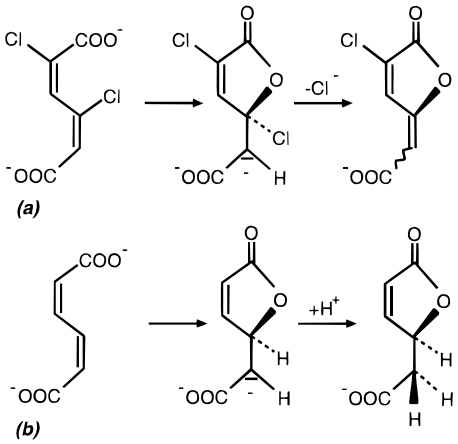

Figure 87. Cycloisomerization of (a) 2,4-dichloro-*cis*,*cis*-muconate and (b) *cis*,*cis*-muconate.[494] (Adapted from ref 494.)

suggests that the α-proton of (*S*)-mandelate is abstracted by Lys-166, whereas the α-proton of (*R*)-mandelate is abstracted by His-297 (Figure 85).[488−490] These two amino acid side chains also perform as proton donors in the reverse process.

The active-site metal ion, Mg^{2+} coordinated by Asp-195, Glu-221, and Glu-247, binds to the OH and one carboxylate oxygen of the substrate, as seen in complexes of (*S*)-mandelate bound to the K166R mutant (Figure 86),[491] or (*S*)-atrolactate (2-phenyllactate) bound to the wild-type enzyme.[492] The role of Glu-317 is important in stabilizing the enolic intermediate (Figure 85) and lowering the pK_a of the α-proton for its removal. Acting as a general acid catalyst Glu-317 forms a strong hydrogen bond with the enol tautomer. Mutation of Glu-317 to Gln reduces k_{cat}/K_m 3 × 10^4-fold for either the *R* or *S* substrate (mandelate).[492]

L. The Lactonizing Enzymes Muconate Cycloisomerase and Chloromuconate Cycloisomerase

The previously discussed enolase and mandelate racemase structures introduce part of a family of enzymes having a functional α/β barrel (sections IX.J−N).[251] These two closely related enzymes have 42% identity with the sequences of muconate cycloisomerase from *Pseudomonas putida* (MCI, EC 5.5.1.1,

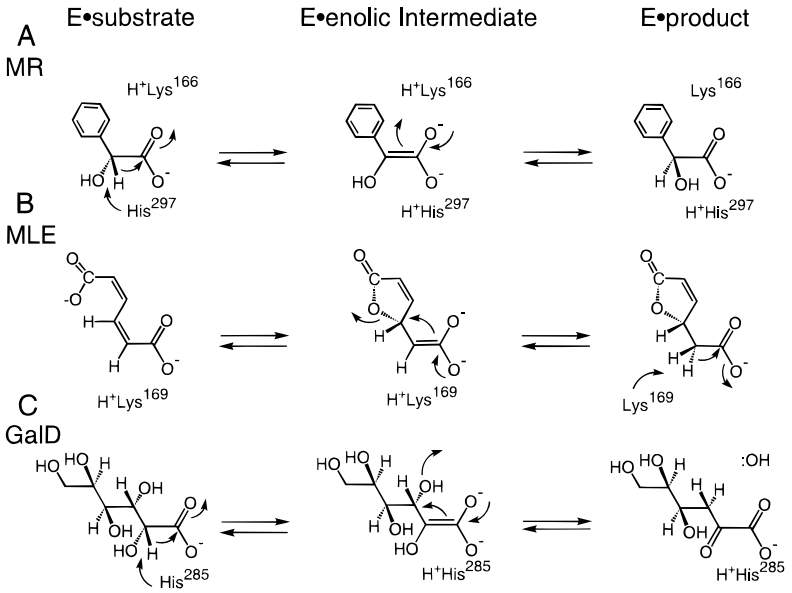

Figure 88. Mechanisms of the reactions catalyzed by mandelate racemase (A), muconate lactonizing enzyme (B), and galactonate dehydratase (C). (Reprinted with permission from ref 496. Copyright 1995 American Association for the Advancement of Science.)

also known as muconate lactonizing enzyme, MLE)[493] and chloromuconate cycloisomerase from *Alcaligenes eutrophus* (CMCI, EC 5.5.1.7, also known as chloromuconate lactonizing enzyme),[494] and the structures are similar.

The reactions with substrates are similar in that the cyclization produces a carbanion-like or an enolic intermediate (Figures 87 and 88). For MCI (MLE) *syn*-addition of the proton occurs from Lys-169 (Figure 87, lower part, Figure 88), whereas for CMCI enzyme-catalyzed loss of Cl^- gives rise to an additional double bond (Figure 87, upper part).

Both of these enzymes require a functional Mn^{2+}. In MCI Co^{2+} is about one third as active as Mn^{2+}, and Zn^{2+} was not tested in the early study.[495] The metal ion is near the binding site of an inhibitor, α-ketoglutarate.[493] The probable function of the metal is to bind and polarize the carboxylate adjacent to the C_α and to stabilize the enolic intermediate. In CMCI further structural studies with bound inhibitors may reveal whether or not the divalent metal is also involved in removal of Cl^- from the intermediate of the reaction. This appears likely since a chloride ion was found in the coordination sphere of Mn^{2+} in CMCI (distance Mn−Cl 3.0 Å).[393] This chloride ion is hydrogen bonded to three lysine residues (163, 165, 269) and to the side chain of Trp-55.

M. Galactonate Dehydratase

A three-dimensional structure is not established for galactonate dehydratase, which is homologous to mandelate racemase and muconate cycloisomerase.[496] The first step in the reaction is the removal of the proton at C_α by His-285 which is analogous to the *R*-specific base His-297 of MR. Stabilization of the enolic intermediate by a divalent metal is supported by the conservation of the metal binding residues of MR. Candidates for the divalent metal include Mg^{2+}, Mn^{2+}, and possibly others of the first transition row. Figure 88 compares the reactions catalyzed by the three homologous enzymes, MR, MCI, and galactonate dehydratase.

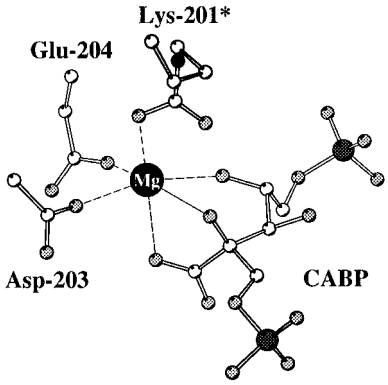

Figure 89. The distorted octahedral coordination sphere around Mg^{2+} and binding mode of the inhibitor 2-carboxy-D-arabinitol-1,5-bisphosphate (CABP, see Figure 90) to rubisco.[499] Generated from PDB file 8RUB.[499]

N. Ribulose-1,5-bisphosphate Carboxylase

In rubisco (ribulose-1,5-bisphosphate carboxylase) the preferred active site metal ion is one Mg^{2+}, although Ni^{2+} is about equally active, whereas Co^{2+}, Mn^{2+}, and Fe^{2+} are less active as cofactors.[497] Among other divalent cations Zn^{2+} and Cu^{2+} are not active.[498] A distorted octahedral coordination sphere surrounds Mg^{2+}, which is bound to an oxygen of the carbamylated Lys-201, Asp-203, Glu-204, and to three oxygens of the reaction intermediate analogue CABP (2-carboxy-D-arabinitol 1,5-bisphosphate) (Figure 89).[499] The probable function of the Mg^{2+} is to polarize the carbonyl group at C2 (Figure 89) in order to aid in deprotonation at C3 as the 2,3-enediol intermediate is formed (Figure 90, first step). If Mg^{2+} is replaced by the redox active cations Mn^{2+} or Co^{2+}, the oxygenation pathway is enhanced,[500−502] probably by a mechanism which favors a hydroperoxy intermediate.[503]

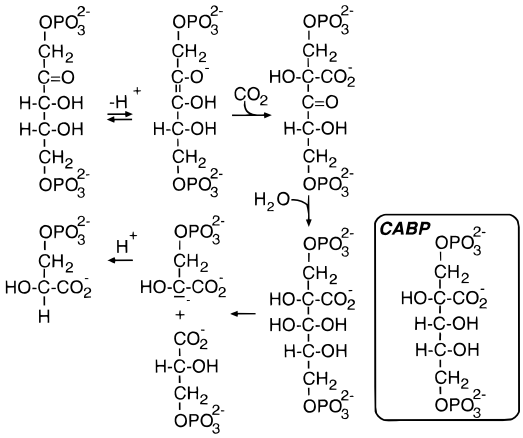

Figure 90. Five steps in the carboxylation of ribulose 1,5-bisphosphate catalyzed by rubisco: enolization, carboxylation, hydration, carbon−carbon cleavage, and protonation. Also shown is the reaction coordinate analogue 2-carboxy-D-arabinitol 1,5-bisphosphate (CABP).[499] (Adapted from ref 499.)

O. Pyruvate Kinase

Pyruvate kinase (PK, EC 2.7.1.40) connects ADP, phosphoenolpyruvate and H^+ to yield, in the first step, phosphoryl transfer from phosphoenolpyruvate to ADP to give the bound enolate of pyruvate and ATP. The second step is addition of H^+ to yield pyruvate, followed by release of product, which is the rate-determining step.[504] In thus producing ATP and pyruvate, divalent metal ions are required,[505] now established as two divalent metal ions.[506−508] In addition pyruvate kinase is stimulated by K^+.[504]

The divalent metal of choice is Mg^{2+}, followed by Co^{2+}, Mn^{2+}, Ni^{2+}, and Zn^{2+} in descending order of maximum velocity.[508] The synergism of various concentrations of Mn^{2+} or Co^{2+} at fixed Mg^{2+} levels indicates at least two kinds of metal sites.[508] EPR studies also indicate two sites, one bound to the enzyme forming a second sphere complex with ATP, and the other complexed only to ATP.[506,507]

The structure of the tetrameric enzyme indicates that the active site is in a cleft between the eight stranded β-barrel and the largest of the three other domains of the subunit.[509−511] In a recent study to 2.9 Å resolution rabbit muscle pyruvate kinase is complexed with Mn^{2+}, K^+, and pyruvate. The Mn^{2+} is ligated to Glu-271, Asp-295, most probably a carboxylate oxygen, the carbonyl oxygen of pyruvate, and possibly two water molecules not visible at 2.9 Å resolution.[512] The K^+ site is near this Mn^{2+} site, 5.7 Å away in agreement with NMR studies.[513,514] The second Mn^{2+} site is not present, because it requires the presence of the nucleotide substrate.[506] Thr-327 or Lys-269 might be the proton donor in the mechanism, either of which satisfies the stereochemistry[512] and the required high pK_a.[515]

P. Active-Site Stabilization by Zinc: Galactose-1-phosphate Uridylytransferase

This transferase from *E. coli* (EC 2.7.7.12) catalyzes the nucleotide exchange between UDP-hexoses and hexose 1-phosphates. A covalent intermediate with His-166 occurs in the two-step reaction:[516]

UDP-glucose + E-His-166 = glucose-1-P + E-His-166-UMP

and

galactose-1-P + E-His-166-UMP = UDP-galactose + E-His-166

The enzyme requires at least one, preferably two, divalent metal ions for activity, although the variety of such ions (Fe, Zn, Co, Cd, Mn) suggests structural roles.[517] As indicated by the three-dimensional structure,[518] zinc stabilizes the active-site conformation, whereas iron is bound at the subunit interface of the dimeric enzyme. In particular, the position of the catalytic His-166 is stabilized by a structural zinc ion, which is tetrahedrally bonded to Cys-52, Cys-55, His-115, and His-164 in the *E. coli* enzyme.

Q. tRNA Synthetases

tRNA synthetases (RSs) acylate their cognate tRNA's with a specific amino acid in a pathway which includes an aminoacyl adenylate. This process decodes genetic information in all organisms.

The roles of the zinc ions are still developing and are different among the various aminoacyl tRNA synthetases. One Zn is present in *E. coli* Glu-RS, Met-RS and Thr-RS, *Bacillus stearothermophilus* Met-RS, *Bacillus subtilis* Glu-RS, *Thermus thermophilus* Met-RS, and bovine Ile-RS and Met-RS.[519−524] One Zn per dimer binds to bovine Trp-RS.[525] Two Zn ions per monomer occur in *E. coli* Ile-RS.[521,526,527] Although two Zn ions bind per monomer in *T. thermophilis* Ile-RS and Val-RS, the monomer consists of two domains, each like Met-RS.[523] Several other aminoacyl tRNA synthetases contain no zinc.[528]

Methionyl-tRNA Synthetase of E. coli. The aminoacylation activity of Met-RS is reversibly inhibited upon removal of Zn^{2+} by 1,10-phenanthroline, although the activation of methionine by ATP remains.[529] Site-directed mutagenesis of each of the four Cys residues in the 138 to 163 region localized the zinc site.[530−532] An NMR structure of a 28-mer encompassing this region shows Zn^{2+} bound tetrahedrally to Cys-145, Cys-148, Cys-158, and Cys-161.[533] In the crystal structure of an active monomeric part of Met-RS[534] the Zn^{2+} was proposed to bind near residues 78−95. However, the refinement of the structure appears to have been incomplete, and the X-ray results are under reevaluation.

Isoleucyl-tRNA Synthetase of E. coli. Two tightly bound Zn^{2+} ions are present, one of which can be removed by 1,10-phenanthroline resulting in a decrease of k_{cat}/K_m only by a factor of 130.[527] An indirect role in catalysis is proposed for this removable Zn^{2+}, whereas a structural role is suggested for the other Zn^{2+}. Sequence comparisons[527,535] identify two putative Zn^{2+} finger domains His^{177}-X-His-X_8-Cys-X_2-Cys^{191} and Cys^{902}-X_2-Cys-X-His-X_{14}-Cys-X_2-Cys^{926}.

Alanyl-tRNA Synthetase. In this tetrameric aminoacyl-RS there is one zinc ion per subunit. The Zn^{2+} is bound at 0.97 μM free Zn^{2+} for half-maximal binding. Moreover, the binding shows a Hill coefficient of 1.9. Because zinc induces quenching of fluorescence of the protein, a conformational change is suggested upon zinc binding.[528] A sequence motif containing two cysteines and two histidines is reasonably suggested as a zinc-binding motif.[536]

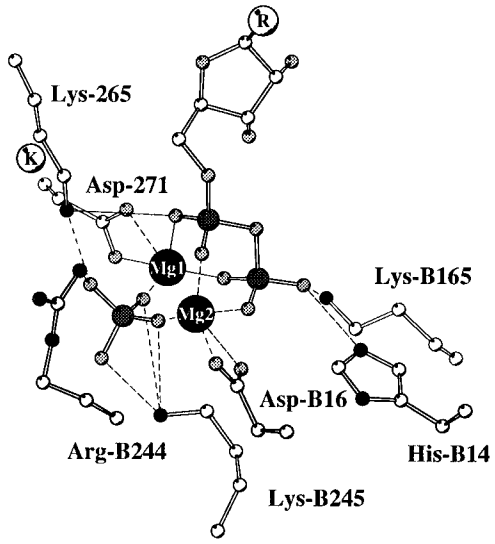

Figure 91. Structure of ADP and phosphate bound to the active site of *S*-adenosylmethionine synthetase.[539] Generated from PDB file 1MXB.[539]

R. *S*-Adenosylmethionine Synthetase: Attack of a Methionine Nucleophile at the 5′-Carbon of ATP and Hydrolysis of Triphosphate

The synthesis of *S*-adenosylmethionine (AdoMet) from L-methionine, ATP and H_2O is catalyzed by *S*-adenosylmethionine synthetase in the presence of divalent metal ions such as Mg^{2+}, Mn^{2+}, Co^{2+}, Zn^{2+}, or Ni^{2+} in an unusual two-step reaction.[537] In the first step the sulfur of methionine attacks the C5′ of ATP and the whole triphosphate group of ATP is replaced by methionine to yield AdoMet and PPP_i. In the second step the triphosphate anion is hydrolyzed to pyrophosphate and phosphate.[538] Monovalent cations, e.g. K^+, further activate the enzyme. The great variety of methylation reactions carried out by AdoMet as a cofactor for enzymes allows control of many cellular functions, e.g. DNA replication and its transcription, as well as RNA translation.

The X-ray structure at 3.0 Å resolution[539] shows a homotetramer of 222 symmetry. Each monomer has two metal ion sites separated by 5 Å. In the presence of ADP, phosphate, Mg^{2+}, and K^+, the two Mg^{2+} ions are bridged bidentately by all three phosphate groups (Figure 91). Asp-B16 coordinates to one Mg^{2+}, whereas Asp-A271 coordinates to the other (A and B refer to different subunits). Several positively charged side chains in the active site might participate in substrate binding or catalysis (Figure 91). Two divalent metal binding sites have also been found in cocrystal structures of the enzyme in the presence of phosphate or pyrophosphate and phosphate.[539] Thus, a two-metal ion mechanism is implicated for one or both steps catalyzed by *S*-adenosylmethionine synthetase.

The active site K^+ is close to Glu-42 and Ser-263, but not near the phosphate ions. This cation probably helps to organize the active site. In the Glu-42 to Glu mutant the activation by K^+ is abolished.[540]

S. Two-Metal Ion Catalysis in the Multistep Pathway of Glutamine Synthetase

Glutamine synthetase catalyzes the synthesis of glutamine from ammonia, glutamate, and ATP via

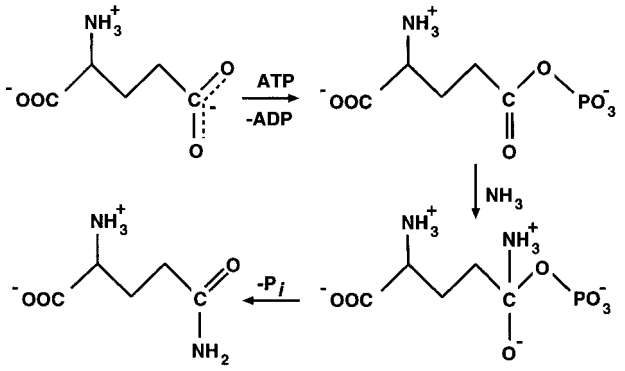

Figure 92. Synthesis of glutamine from glutamate catalyzed by glutamine synthetase.

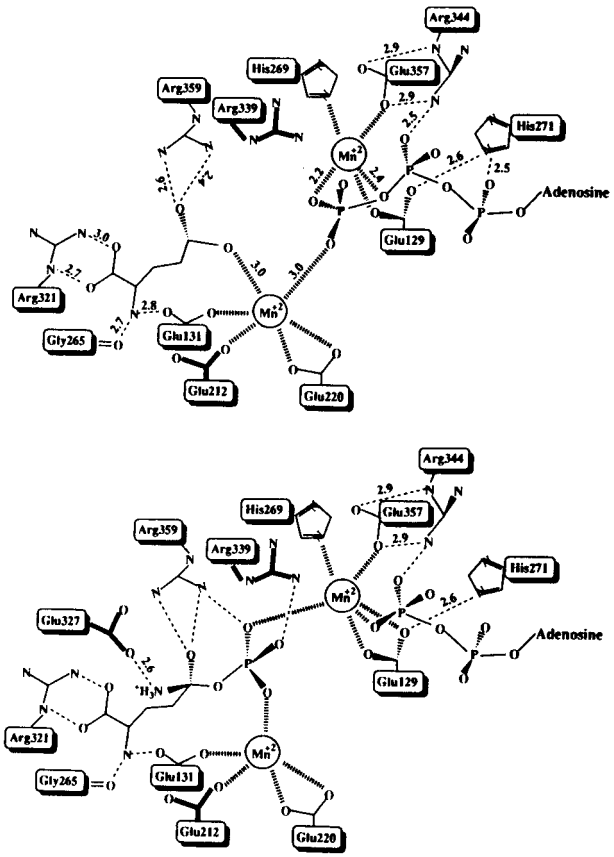

Figure 93. Structural models for the phosphoryl transfer step of the reaction pathway of glutamine synthetase.[544] (Reprinted with permission from ref 544. Copyright 1994 American Chemical Society.)

an enzyme-bound tetrahedral intermediate (Figure 92).[541] Divalent metal ions like Mg^{2+} or Mn^{2+} are necessary for activity.[542] X-ray structures of glutamine synthetase from *Salmonella typhimurium* and of complexes with substrate, product and intermediate analogue compounds, including L-methionyl-*S*-sulfoximine phosphorylated by the enzyme, have provided structural models for several stages of the reaction pathway (Figure 93).[543,544]

In the proposed mechanism Mn1, which is coordinated by three glutamates (131, 212, and 220), binds the nucleophilic carboxylate group of the substrate glutamate. The γ-phosphoryl group of ATP is polarized by both metal ions, but more strongly by Mn2, which has His-269, Glu-357, and Glu-129 as protein ligands. The two metal ions are 5.8 Å apart. Mn2

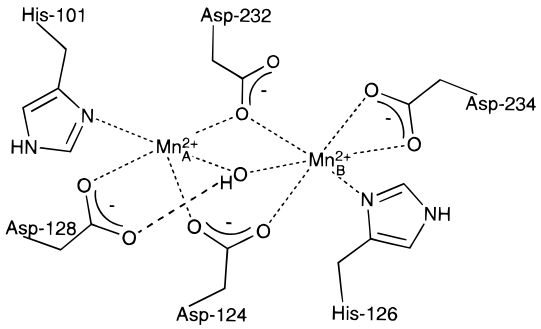

Figure 94. Structure of the dimetal center of arginase from rat liver. Figure provided by authors.[546]

also activates the AMP leaving group. After the phosphoryl group has been transferred to the substrate carboxylate group an ammonium ion attacks the carboxylate carbon and the tetrahedral intermediate is formed (Figure 93). In the last step the phosphate group leaves by cleavage of the carbon−oxygen bond. Arg-339 and Arg-359 may stabilize the transition state of the phosphoryl transfer reaction, in addition to one or both metal ions. Mutation of either of these two arginines severely diminishes the catalytic activity.[545] Interestingly, glutamine synthetase also catalyzes the arsenolysis of glutamine, probably by a mechanism in which phosphate is replaced by arsenate in the reversal of Gln synthesis.

T. The Mn_2^{2+} Arginase from Rat Liver

Arginase catalyzes the hydrolysis of arginine to yield urea and ornithine in the final step of the urea cycle. In the active site two spin-coupled Mn^{2+} ions are 3.3 Å apart. In the recently solved X-ray structure of the enzyme from rat liver,[546] MnA has a square-pyramidal coordination geometry, whereas MnB is octahedrally coordinated (Figure 94). A proposed mechanism assumes that the metal-bridging water ligand, which presumably is a hydroxide ion, acts as the nucleophile and the nearby Glu-277 binds the guanidinium group of the arginine substrate.[546] In contrast to many other metallohydrolases (phosphatases and amidases) the substrate cannot coordinate to the metal ions in this reaction (at least not in the forward reaction), and no polarization of the substrate by metal coordination takes place. Thus, the primary role of the metals is the generation of the nucleophile and the stabilization of the transition state. Yeast arginase contains a tightly bound zinc ion and a weakly bound manganese ion per subunit.[547]

U. The CheY Response Regulator Protein of Bacterial Chemotaxis

The CheY protein catalyzes phosphoryl transfer from the histidine of autophosphorylated histidine kinase to Asp-57 of itself (CheY), thereby regulating flagellar rotation in chemotaxis.[548] *In vivo* Mg^{2+} is the preferred divalent metal ion cofactor (K_d = 0.5 mM), although *in vitro* other divalent ions also catalyze phosphoryl transfer, e.g. Zn^{2+} (K_d = 0.1 mM).[548]

The crystal structure of CheY from *Salmonella typhimurium* shows an octahedrally coordinated

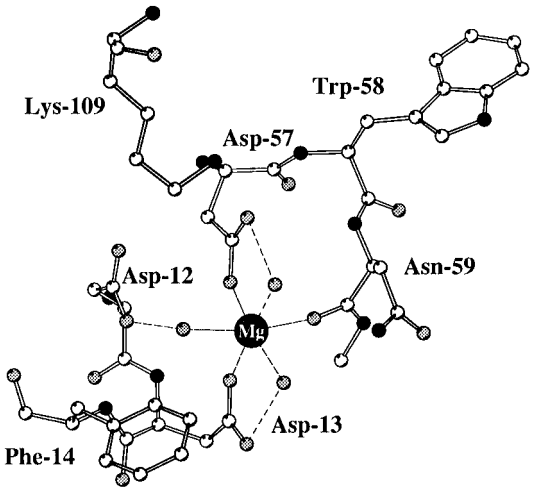

Figure 95. Magnesium-binding site in the CheY protein.[549] Three water molecules are bound to Mg^{2+}. Asp-57 is the phosphoryl acceptor in the reaction (Figure 91). Generated from PDB file 2CHE.[549]

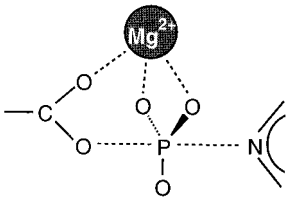

Figure 96. Transition-state stabilization in the proposed mechanism of the CheY protein.[549] (Adapted from ref 549.)

Mg^{2+} in the active site (Figure 95).[549] This metal ion is ligated by the carboxylates of Asp-13 and Asp-57, which is the phosphoryl acceptor, by the backbone carbonyl of Asn-59, and three water molecules. In the proposed mechanism the Mg^{2+} coordinates two oxygens of the five-coordinated intermediate and the carboxylate of the nucleophile Asp-57, in accord with a similar phosphoryl transfer in a model system (Figure 96).[550]

X. Concluding Remark

Many new interesting zinc enzymes have been identified and structurally characterized in the past few years, including adenosine and cytidine deaminases, 6-pyruvoyl tetrahydropterin synthase, and the Ada protein. Most of these, e.g. the Ada protein with its catalytic $Zn(Cys)_4$ center differ significantly from other well-known zinc enzymes. Also, many recently structurally characterized members in the group of monozinc peptidases which are functionally or evolutionary homologous to the prototypical zinc peptidases carboxypeptidase A and thermolysin contribute new aspects toward an understanding of the mechanistic features of these enzymes. In particular, a few functional residues seem to be most important for catalysis: the zinc ion, a zinc-coordinated water residue, and a carboxylate side chain. Sometimes further ionizable residues are positioned to participate in catalysis. Despite decades of intensive research in the area of monozinc peptidases some doubts concerning the most favored reaction mechanism and the protonation state of functional active site residues remain. It is important to clarify these fundamental points since they are at the basis of our understand-

ing of the action of these zinc enzymes, which fulfill a great variety of functions in all life forms.

Another emerging field of metalloenzyme catalysis are the polynuclear metal centers catalyzing acyl, phosphoryl, and other group-transfer reactions.[181,180] As for mononuclear metallopeptidases zinc is the preferably selected metal by nature for the dinuclear metallopeptidases. In many of these enzymes, especially those with metal−metal distances around 3−3.5 Å a metal-bridging water molecule or hydroxide ion is the most likely candidate for the water nucleophile. Interestingly, a nonmetal-coordinated carboxylate side chain or other suitable general base is present near this bridging water ligand in many cases. For mono- and dinuclear metallohydrolases, a role of the metal ion(s) in the polarization of the electrophilic group (carbonyl or phosphoryl) *and* in the activation of the nucleophile is an important factor in almost all proposed mechanisms.

Taken together, these studies provide a renewed and widened picture of the variety of catalyzed reactions and the diversity of the underlying structural elements amenable to zinc biochemistry. Future, yet unfulfilled goals include a detailed understanding why certain divalent metal ions show in some cases very different reactivities, how metal selectivity is achieved, and, most importantly, a more quantitative understanding of the various factors involved in enzyme catalysis, in order to differentiate between various possible mechanisms. Enzyme structure (by crystallography and NMR, and also from other spectroscopic techniques yielding more limited information) and function (activity, kinetic, or other properties under various conditions) are now determined at an unprecedented pace, thanks to advancements in computer technology, software, equipment, and molecular biology techniques. However, the bridge between these experimental results, often termed structure−function relationships, including a detailed kinetic and thermodynamic pathway of the reaction, namely the reaction mechanism, is not so easy to build. Presumed reaction coordinate analogue compounds, techniques for the study of intermediates, enzyme kinetics, mutant enzymes, novel designed enzymes, and small molecule metal complexes remain the primary experimental tools to probe certain aspects of (metallo)enzyme action. In addition, computational means, including *ab initio* and semiempirical quantum chemical calculations on active-site models, molecular mechanics force fields allowing the simulation of larger systems, continuum electrostatics,[551] and free-energy simulations,[552] all of which advance in theory or profit from increasing computer power, will provide significant contributions to build this bridge between structure and function. Metal ions, especially the transition metals, pose a special challenge for these techniques, due to their flexible nature in coordination chemistry and chemical bonding. However, a quantitative understanding of enzyme activity on the basis of enzyme structure remains the ultimative goal.

XI. Abbreviations

AAP	*Aeromonas proteolytica* aminopeptidase
ADA	adenosine deaminase
ADH	alcohol dehydrogenase
CA	carbonic anhydrase
CDA	cytidine deaminase
CMCI	chloromuconate cycloisomerase
DHAP	dihydroxyacetone phosphate
EPR	electron paramagnetic resonance
EXAFS	extended X-ray absorption fine structure
FBPase	fructose-1,6-bisphosphatase
GDH	glucose dehydrogenase
HIV	human immunodeficiency virus
IMPase	inositol monophosphatase
k_{cat}	maximum turnover number from Michaelis−Menten kinetics (s^{-1})
K_d	dissociation constant (mol/L)
K_i	inhibition constant (mol/L)
K_m	substrate binding constant from Michaelis−Menten kinetics (mol/L)
LAP	leucine aminopeptidase
MCI	muconate cycloisomerase
MD	molecular dynamics
MR	mandelate racemase
NMR	nuclear magnetic resonance
PhAH	phosphonoacetohydroxamate
pK_a	−log(acid dissociation constant)
RNase	ribonuclease
RS	tRNA synthetase
SGAP	*Streptomyces griseus* aminopeptidase
SOD	superoxide dismutase
TIMP	tissue inhibitor of matrix metalloproteinases

XII. Acknowledgments

We thank all colleagues who generously provided us with preprints, figures, and for their helpful discussions: C. W. Carter, D. W. Christianson, R. I. Christopherson, N. O. Concha, D. J. Creighton, O. Dideberg, D. Eisenberg, J. A. Gerlt, J. P. Glusker, H. M. Greenblatt, O. Herzberg, E. Hough, B. Imperiali, E. R. Kantrowitz, P. A. Karplus, A. Liljas, J. Kuriyan, S. F. Martin, B. W. Matthews, W. L. Mock, K. Morikawa, F. A. Quiocho, D. C. Rees, S. Rowsell, G. E. Schulz, G. Shoham, F. Solano, T. A. Steitz, W. Stöcker, F. W. Studier, D. Suck, B. J. Sutton, G. L. Verdine, D. E. Wilcox, J. F. Woessner, and R. Wolfenden. Research in the laboratory of W.N.L. was supported by grant NIH GM06920. N.S. thanks the Deutsche Forschungsgemeinschaft for financial support.

Note Added in Proof

Some important very recently published studies are included for reference.

Astacin (Section II.D.2). A structure of astacin with a bound phosphinic peptide shows that the tyrosine which is zinc bound in the uncomplexed enzyme is shifted to form a hydrogen bond to the phosphinyl group (Grams, F.; Dive, V.; Yiotakis, A.; Yiallouros, I.; Vassiliou, S.; Zwilling, R.; Bode, W.; Stöcker, W. *Nature Struct. Biol.* **1996**, *3*, 671). This structure thus demonstrates that the "tyrosine-switch" mechanism as proposed for the serralysins (section II.D.4) is most likely also present in the astacins. The two phosphinyl oxygens are at distances of 1.9 and 2.9 Å to the zinc ion.

Phosphotriesterase (Section III.F). The binding mode of the substrate analogue diethyl (4-methylbenzyl)phosphonate to Zn−Zn phosphotriesterase has been determined (Vanhooke, J.; Benning, M. M.; Raushel, F. M.; Holden, H. M. *Biochemistry* **1996**, *35*,

6020). An interesting feature is the almost complete lack of hydrogen-bonding interactions between the inhibitor and the protein. Also none of the inhibitor atoms is coordinated to the zinc cluster. A water ligand bridges the two zinc ions and is proposed to be the nucleophile. A thorough kinetic study of the action of various metal-exchanged enzyme forms (Co^{2+}, Ni^{2+}, Cd^{2+}, Zn^{2+}, Mn^{2+}) on substrates with different substituted phenol and thiophenol leaving groups indicated a direct coordination of the substrate phosphoryl sulfur or oxygen atoms to one or both metal ions (Hong, S.-B.; Raushel, F. M. *Biochemistry* **1996**, *35*, 10904). A possible mechanism supported by both studies suggests that the nonesterified phosphate oxygen is metal coordinated in the productive substrate binding mode and that the bridging water molecule (or hydroxide ion) becomes terminally coordinated to Zn1 prior to nucleophilic attack on the phosphorus.

Fructose-1,6-bisphosphatase (Section IX.A). X-ray structures of the Arg-243→Ala mutant enzyme have been determined in the T and R allosteric states (Stec, B.; Abraham, R.; Giroux, E.; Kantrowitz, E. R. *Protein Sci.* **1996**, *5*, 1541). This mutation reduces the affinity for the substrate fructose-1,6-bisphosphate 10-fold and for the inhibitor fructose-2,6-bisphosphate 1000-fold. Arg-243, which protrudes into the active site of the homotetrameric molecule from a neighboring subunit, binds to the 6-phosphate group of the substrate.

DNA Polymerases (Section IX.D). A structure of *Thermus aquaticus* DNA polymerase with duplex DNA bound to the polymerase active site confirms the binding mode of the primer-template as determined from the homologous DNA pol I (Eom, S. H.; Wang, J.; Steitz, T. A. *Nature* **1996**, *382*, 278).[402−407]

XIII. References

(1) ICBIC 7 Abstracts. *J. Inorg. Biochem.* **1995**, *59*, 90.
(2) Vahrenkamp, H. *Chem. Unserer Zeit* **1988**, *22*, 73.
(3) Vallee, B. L. *Adv. Protein Chem.* **1955**, *10*, 317.
(4) Fraústo da Silva, J. J. R.; Williams, R. J. P. *The Biological Chemistry of the Elements*; Clarendon Press: Oxford, 1991; p 299.
(5) Coleman, J. E. *Annu. Rev. Biochem.* **1992**, *61*, 897. Vallee, B. L.; Coleman, J. E.; Auld, D. S. *Proc. Natl. Acad. Sci. USA* **1991**, *88*, 999. Vallee, B. L.; Auld, D. S. *Biochemistry* **1990**, *29*, 5647.
(6) Vallee, B. L.; Auld, D. S. *Biochemistry* **1993**, *32*, 6493. Vallee, B. L.; Auld, D. S. *Proc. Natl. Acad. Sci. USA* **1993**, *90*, 2715. Vallee, B. L.; Auld, D. S. *Proc. Natl. Acad. Sci. USA* **1990**, *87*, 220. Vallee, B. L. *Adv. Protein Chem.* **1955**, *10*, 317.
(7) Christianson, D. W. *Adv. Protein Chem.* **1991**, *42*, 281.
(8) Auld, D. S. *Methods Enzymol.* **1995**, *248*, 228.
(9) Bock, C. W.; Katz, A. K.; Glusker, J. P. *J. Am. Chem. Soc.* **1995**, *117*, 3754.
(10) Bock, C. W.; Glusker, J. P. *Inorg. Chem.* **1993**, *32*, 1242.
(11) Pauling, L. *The Nature of the Chemical Bond*, 3rd ed.; Cornell University Press: Ithaca, NY, 1960; pp 514 and 518.
(12) Iwata, S.; Ostermeier, C.; Ludwig, B.; Michel, H. *Nature* **1995**, *376*, 660. Tsukihara, T.; Aoyama, H.; Yamashita, E.; Tomizaki, T.; Yamaguchi, H.; Shinzawa-Itoh, K.; Nakashima, R.; Yaono, R.; Yoshikawa, S. *Science* **1995**, *269*, 1069.
(13) Blundell, T.; Dodson, E.; Hodgkin, D.; Mercola, D. *Adv. Protein Chem.* **1972**, *26*, 166.
(14) Bentley, G.; Dodson, E. Dodson, G.; Hodgkin, D.; Mercola, D. *Nature* **1976**, *261*, 166.
(15) Harrison, P. M.; Ford, G. C.; Rice, D. W.; Smith, J. M. A.; Treffry, A.; White, J. L. *Rev. Port. Quim.* **1985**, *27*, 119.
(16) Formicka-Kozlowska, G.; Maret, W.; Zeppezauer, M. *Zinc Enzymes*; Bertini, I., Luchinat, C., Maret, W., Zeppezauer, M., Eds.; Birkhäuser: Boston, 1986; p 579.
(17) Berg, J. M.; Shi, Y. *Science* **1996**, *271*, 1081.
(18) Rawlings, N. D.; Barrett, A. J. *Methods Enzymol.* **1995**, *248*, 183.
(19) Rawlings, N. D.; Barrett, A. J. *Biochem. J.* **1993**, *290*, 205. Hooper, N. M. *FEBS Lett.* **1994**, *354*, 1.
(20) Stöcker, W.; Bode, W. *Curr. Opin. Struct. Biol.* **1995**, *5*, 383. Stöcker, W.; Grams, F.; Baumann, U.; Reinemer, P.; Gomis-Rüth, F.-X.; McKay, D. B.; Bode, W. *Protein Sci.* **1995**, *4*, 823. Bode, W. *Structure* **1995**, *3*, 527. Blundell, T. L. *Nature Struct. Biol.* **1994**, *1*, 73.
(21) Roques, B. P. *Biochem. Soc. Trans.* **1993**, *21*, 678.
(22) Artymiuk, P. J.; Grindley, H. M.; Park, J. E.; Rice, D. W.; Willett, P. *FEBS Lett.* **1992**, *303*, 48.
(23) Chevrier, B.; Schalk, C.; D'Orchymont, H.; Rondeau, J.-M.; Moras, D.; Tarnus, C. *Structure* **1994**, *2*, 283.
(24) Rowsell, S.; Pauptit, R. A.; Tucker, A. D.; Brick, P.; Lloyd, L. F.; Melton, R. G.; Blow, D. M. Abstract IUCr XVII 1996, personal communication. S. Rowsell, Ph.D. thesis, University of London, 1996. Tucker, A. D.; Rowsell, S.; Melton, R. G.; Pauptit, R. A. *Acta Crystallogr. Sect. D* **1996**, *52*, 890.
(25) Christianson, D. W.; Lipscomb, W. N. *Proc. Natl. Acad. Sci. USA* **1986**, *83*, 7568. Rees, D. C.; Lewis, M.; Lipscomb, W. N. *J. Mol. Biol.* **1983**, *168*, 367.
(26) Geoghegan, K. F.; Galdes, A.; Hanson, G.; Holmquist, B.; Auld, D. S.; Vallee, B. L. *Biochemistry* **1986**, *25*, 4669.
(27) Suh, J.; Cho, W.; Chung, S. *J. Am. Chem. Soc.* **1985**, *107*, 4530.
(28) Makinen, M. W.; Tamamura, K.; Kaiser, E. T. *Proc. Natl. Acad. Sci. USA* **1976**, *73*, 3882.
(29) Makinen, M. W.; Kuo, L. C.; Dymowski, J. J.; Jaffer, S. *J. Biol. Chem.* **1979**, *254*, 356.
(30) Kuo, L. C.; Fukuyama, J. M.; Makinen, M. W. *J. Mol. Biol.* **1983**, *163*, 63.
(31) Hoffman, S. J.; Chu, S. S.-T.; Lee, H.; Kaiser, E. T.; Carey, P. R. *J. Am. Chem. Soc.* **1983**, *105*, 6971.
(32) Osumi, A.; Rahmo, A.; King, S. W.; Przystas, T. J.; Fife, T. H. *Biochemistry* **1994,** *33*, 14750.
(33) Sander, M. E.; Witzel, H. *Biochem. Biophys. Res. Commun.* **1985**, *132*, 681.
(34) Christianson, D. W.; Lipscomb, W. N. *Acc. Chem. Res.* **1989**, *22*, 62.
(35) Rees, D. C.; Lipscomb, W. N. *J. Mol. Biol.* **1982**, *160*, 475.
(36) Gardell, S. J.; Craik, C. S.; Hilvert, D.; Urdea, M. S.; Rutter, W. J. *Nature* **1985**, *317*, 551.
(37) Gardell, S. Private communication. Gardell, S. J.; Craik, C. S.; Hilvert, D.; Urdea, M. S.; Rutter, W. J. *Abstracts*, Genetic Physico-Chemical Approaches for Analysis of Biological Catalysts, June 16−20, 1986, Florence, Italy (abstracts availaable from I. Bertini, conference chairman).
(38) Mock, W. L.; Zhang, J. Z. *J. Biol. Chem.* **1991**, *266*, 6393.
(39) Mock, W. L.; Xu, X. *Bioorg. Chem.* **1994**, *22*, 373. Mock, W. L.; Feeman, D. J.; Aksamawati, M. *Biochem. J.* **1993**, *289*, 185.
(40) Pétra, P. H. *Biochemistry* **1971**, *10*, 3163.
(41) Hass, G. M.; Neurath, H. *Biochemistry* **1971**, *10*, 3535.
(42) Hass, G. M.; Neurath, H. *Biochemistry* **1971**, *10*, 3541.
(43) Christianson, D. W.; Lipscomb, W. N. *J. Am. Chem. Soc.* **1985**, *107*, 828.
(44) Kaplan, A. P.; Bartlett, P. A. *Biochemistry* **1991**, *30*, 8165.
(45) Kim, H.; Lipscomb, W. N. *Biochemistry* **1991**, *30*, 8171. Kim, H.; Lipscomb, W. N. *Biochemistry*, **1990**, *29*, 5546.
(46) Feinberg, H.; Greenblatt, H. M.; Behar, V.; Gilon, C.; Cohen, S.; Bino, A.; Shoham, G. *Acta Crystallogr. Sect. D* **1995**, *51*, 428.
(47) Ondetti, M. A.; Rubin, B.; Cushman, D. W. *Science* **1977**, *196*, 441.
(48) Guasch, A.; Coll, M.; Avilés, F. X.; Huber, R. *J. Mol. Biol.* **1992**, *224*, 141.
(49) Coll, M.; Guasch, A.; Avilés, F. X.; Huber, R. *EMBO J.* **1991**, *10*, 1.
(50) Avilés, F. X.; Vendrell, J.; Guasch, A.; Coll, M. Huber, R. *Eur. J. Biochem.* **1993**, *211*, 381.
(51) Rees, D. C.; Lipscomb, W. N. *J. Mol. Biol.* **1982**, *160*, 475.
(52) Schmid, M. F.; Herriott, J. R. *J. Mol. Biol.* **1976**, *103*, 175.
(53) Teplyakov, A.; Polyakov, K.; Obmolova, G.; Strokopytov, B.; Kuranova, I.; Osterman, A.; Grishin, N.; Smulevitch, S.; Zagnitko, O.; Galperina, O.; Matz, M.; Stepanov, V. *Eur. J. Biochem.* **1992**, *208*, 281.
(54) Stepanov, V. M. *Methods Enzymol.* **1995**, *248*, 675.
(55) Carfi, A.; Pares, S.; Duée, E.; Galleni, M.; Duez, C. Frère, J. M.; Dideberg, O. *EMBO J.* **1995**, *14*, 4914.
(56) Sutton, B. J.; Artymiuk, P. J.; Cordero-Borboa, A. E.; Little, C.; Phillips, D. C.; Waley, S. G. *Biochem. J.* **1987**, *248*, 181.
(57) Dideberg, O.; Joris, B.; Frere, J. M.; Ghuysen, J. M.; Weber, G.; Robaye, R.; Delbrouck, J. M.; Roelandts, I. *FEBS Lett.* **1980**, *117*, 215.
(58) Dideberg, O.; Charlier, P.; Dive, G.; Joris, B.; Frere, J. M.; Ghuysen, J. M. *Nature* **1982**, *299*, 469. Charlier, P.; Dideberg, O.; Jamoulle, J.-C.; Frere, J.-M.; Ghuysen, J.-M.; Dive, G.; Lamotte-Brasseur, J. *Biochem. J.* **1984**, *219*, 763.
(59) Taylor, A. *Trends Biochem. Sci.* **1993**, *18*, 167. Taylor, A. *FASEB J.* **1993**, *7*, 290. Kenny, A. J.; Hopper, N. M. *Degradation of bioactive substances: Physiology and para physiology*; Hendricksson, J. H., Ed.; CRC Press: New York, 1991.
(60) Burley, S. K., David, P. R., Sweet, R. M., Taylor, A.; Lipscomb, W. N. *J. Mol. Biol.* **1990**, *224*, 113.
(61) Sträter, N.; Lipscomb, W. N. *Biochemistry* **1995,** *34*, 9200. Sträter, N.; Lipscomb, W. N. *Biochemistry* **1995**, *34*, 14792.

(62) Andersson, L.; Isley, T. C.; Wolfenden, R. *Biochemistry* **1982**, *21*, 4177.
(63) Andersson, L.; MacNeela, J.; Wolfenden, R. *Biochemistry* **1985**, *24*, 330.
(64) Vogt, V. M. *J. Biol. Chem.* **1970**, *245*, 4760. Stirling, C. J.; Colloms, S. D.; Collins, J. F.; Szatmari, G.; Sherratt, D. J. *EMBO J.* **1989**, *8*, 1623.
(65) McCulloch, R.; Burke, M. E., Sherratt, D. J. *Mol. Microbiol.* **1994**, *12*, 241.
(66) Chevrier, B.; D'Orchymont, H.; Schalk, C.; Tarnus, C.; Moras, D. *Eur. J. Biochem.* **1996**, *237*, 393.
(67) Maras, B.; Greenblatt, H. M.; Shoham, G.; Spungin-Bialik, A.; Blumberg, S.; Barra, D. *Eur. J. Biochem.* **1996**, *236*, 843.
(68) Greenblatt, H. M.; Almog, O.; Maras, B.; Spungin-Bialik, A.; Barra, D.; Blumberg, S.; Shoham, G. *J. Mol. Biol.* **1996**, in press.
(69) Roderick, S. L.; Matthews, B. W. *Biochemistry* **1993**, *32*, 3907.
(70) Chang, Y.-H.; Teichert, U.; Smith, J. A. *J. Biol. Chem.* **1992**, *267*, 8007.
(71) Becker, A. B.; Roth, R. A. *Proc. Natl. Acad. Sci. USA* **1992**, *89*, 3835.
(72) Becker, A. B.; Roth, R. A. *Biochem. J.* **1993**, *292*, 137.
(73) Matthews, B. W.; Jansonius, J. N.; Colman, P. M.; Schoenborn, B. P.; Dupourque, D. *Nature* **1972**, *238*, 37. Matthews, B. W.; Colman, P. M.; Jansonius, J. N.; Titani, K.; Walsh, K. A.; Neurath, H. *Nature* **1972**, *238*, 41. Colman, P. M.; Jansonius, J. N.; Matthews, B. W. *J. Mol. Biol.* **1972**, *70*, 701.
(74) Thayer, M. M.; Flaherty, K. M.; McKay, D. B. *J. Biol. Chem.* **1991**, *266*, 2864.
(75) Pauptit, R. A.; Karlsson, R.; Picot, D.; Jenkins, J. A.; Niklaus-Reimer, A.-S.; Jansonius, J. N. *J. Mol. Biol.* **1988**, *199*, 525. Stark, W.; Pauptit, R. A.; Wilson, K. S.; Jansonius, J. N. *Eur. J. Biochem.* **1992**, *207*, 781.
(76) Endo, S. *J. Ferment. Technol.* **1962**, *40*, 346.
(77) Feder, J.; Garrett, L. R.; Wildi, B. S. *Biochemistry* **1971**, *10*, 4552.
(78) Holland, D. R.; Hausrath, A. C.; Juers, D.; Matthews, B. W. *Protein Sci.* **1995**, *4*, 1955.
(79) Matthews, B. W. *Acc. Chem. Res.* **1988**, *21*, 333.
(80) Bartlett, P. A.; Marlowe, C. K. *Biochemistry* **1983**, *22*, 4618. Bartlett, P. A.; Marlowe, C. K. *Biochemistry* **1987**, *26*, 8553.
(81) Holden, H. M.; Tronrud, D. E.; Monzingo, A. F.; Weaver, L. H.; Matthews, B. W. *Biochemistry* **1987**, *26*, 8542.
(82) Bartlett, P. A.; Marlowe, C. K. *Science* **1987**, *235*, 569.
(83) Tronrud, D. E.; Holden, H. M.; Matthews, B. W. *Science* **1987**, *235*, 571.
(84) Shen, J.; Wendolowski, J *Protein Sci.* **1995**, *4*, 373.
(85) Kunugi, S.; Hirohara, H.; Ise, N. *Eur. J. Biochem.* **1982**, *124*, 157. Feder, J.; Schuck, J. M. *Biochemistry* **1970**, *9*, 2784. Pangburn, M. K.; Walsh, K. A. *Biochemistry* **1975**, *14*, 4050.
(86) Mock, W. L.; Stanford, D. J. *Biochemistry* **1996**, *35*, 7369. Mock, W. L.; Aksamawati, M. *Biochem. J.* **1994**, *302*, 57.
(87) Mock, W. L.; Chen, J.-T. *Arch. Biochem. Biophys.* **1980**, *203*, 542.
(88) Beaumont, A.; O'Donohue, M. J.; Paredes, N.; Rousselet, N.; Assicot, M.; Bohuon, C.; Fournie-Zaluski, M. C.; Roques, B. P. *J. Biol. Chem.* **1995**, *270*, 16803.
(89) Kimura, E. *Prog. Inorg. Chem.* **1994**, *41* 443.
(90) Shoham, G.; Rees, D. C.; W. N. Lipscomb *Proc. Natl. Acad. Sci. USA* **1984**, *81*, 7767.
(91) Makinen, M. W.; Kuo, L. C.; Dymowski, J. J.; Jaffer, S. *J. Biol. Chem.* **1979**, *254*, 356.
(92) Holmquist, B.; Vallee, B. L. *J. Biol. Chem.* **1974**, *249*, 4601.
(93) Kester, W. R.; Matthews, B. W. *J. Biol. Chem.* **1977**, *252*, 7704.
(94) Morihara, K. *Methods Enzymol.* **1995**, *248*, 242.
(95) Kawamoto, S.; Shibano, Y.; Fukushima, J.; Ishii, N.; Morihara, K.; Okuda, K. *Infect. Immun.* **1993**, *61*, 1400. McIver, K.; Kessler, E.; Ohman, D. E. *J. Bacteriol.* **1991**, *173*, 7781.
(96) Holland, D. R.; Tronrud, D. E.; Pley, H. W.; Flaherty, K. M.; Stark, W.; Jansonius, J. N.; McKay, D. B.; Matthews, B. W. *Biochemistry* **1992**, *21*, 11310.
(97) Sidler, W.; Niederer, E.; Suter, F.; Zuber, H. *Biol. Chem. Hoppe-Seyler* **1986**, *367*, 643.
(98) Sidler, W.; Kumpf, B.; Peterhans, B.; Zuber, H. *Appl. Microbiol. Biotechnol.* **1986**, *25*, 18.
(99) Toma, S.; Campagnoli, S.; De Gregoriis, E.; Gianna, R.; Margarit, I.; Zamai, M.; Grandi, G. *Protein Eng.* **1989**, *2*, 359. Litster, S. A.; Wetmore, D. R.; Roche, R. S.; Codding, P. W. *Acta Crystallogr. Sect. D* **1996**, *52*, 543.
(100) Bode, W.; Gomis-Rüth, F.-X.; Stöcker, W. *FEBS Lett.* **1993**, *331*, 134.
(101) Springman, E. B.; Angleton, E. L.; Birkedal-Hansen, H.; Van Wart, H. E. *Proc. Natl. Acad. Sci. USA* **1990**, *87*, 364.
(102) Becker, J. W.; Marcy, A. I.; Rokosz, L. L.; Axel, M. G.; Burbaum, J. J.; Fitzgerald, P. M. D.; Cameron, P. M.; Esser, C. K.; Hagmann, W. K.; Hermes, J. D.; Springer, J. P. *Protein Sci.* **1995**, *4*, 1966.
(103) Dumermuth, E.; Sterchi, E. E.; Jiang, W. P.; Wolz, R. L.; Bond, J. S.; Flannery, A. V.; Beynon, R. J. *J. Biol. Chem.* **1991**, *266*, 21381. Bond, J. S.; Beynon, R. J. *Protein Sci.* **1995**, *4*, 1247.
(104) Stöcker, W.; Zwilling, R. *Methods Enzymol.* **1995**, *248*, 305.
(105) Stöcker, W.; Wolz, R. L.; Zwilling, R.; Strydom, D. J.; Auld, D. S. *Biochemistry* **1988**, *27*, 5026.
(106) Butler, P. E.; McKay, M. J.; Bond, J. S. *Biochem. J.* **1987**, *241*, 229. Yasumasu, S.; Iuchi, I.; Yamagami, K. *J. Biochem.* **1989**, *105*, 204. Yasumasu, S.; Iuchi, I.; Yamagami, K. *J. Biochem.* **1989**, *105*, 212.
(107) Bode, W.; Gomis-Rüth, F. X.; Huber, R.; Zwilling, R.; Stöcker, W. *Nature* **1992**, *358*, 164.
(108) Stöcker, W.; Gomis-Rüth, F.-X.; Bode, W.; Zwilling, R. *Eur. J. Biochem.* **1993**, *214*, 215.
(109) Wolz, R. L.; Bond, J. S. *Methods Enzymol.* **1995**, *248*, 325.
(110) Gomis-Rüth, F. X.; Stöcker, W.; Huber, R.; Zwilling, R.; Bode, W. *J. Mol. Biol.* **1993**, *229*, 945.
(111) Gomis-Rüth, F.-X.; Grams, F.; Yiallouros, I.; Nar, H.; Küsthardt, U.; Zwilling, R.; Bode, W.; Stöcker, W. *J. Biol. Chem.* **1994**, *269*, 17111.
(112) Bjarnason, J. B.; Fox, J. W. *Methods Enzymol.* **1995**, *248*, 345.
(113) Bjarnason, J. B.; Tu, A. T. *Biochemistry* **1978**, *17*, 3395. Bjarnason, J. B.; Fox, J. W. *Pharmacol. Ther.* **1994**, *62*, 325.
(114) Gomis-Rüth, F.-X.; Kress, L. F.; Bode, W. *EMBO J.* **1993**, *12*, 4151. Gomis-Rüth, F.-X.; Kress, L. F.; Kellermann, J.; Mayr, I.; Lee, X.; Huber, R.; Bode, W. *J. Mol. Biol.* **1994**, *239*, 513.
(115) Zhang, D.; Botos, I.; Gomis-Rüth, F.-X.; Doll, R.; Blood, C.; Njoroge, F. G.; Fox, J. W.; Bode, W.; Meyer, E. F. *Proc. Natl. Acad. Sci. USA* **1994**, *91*, 8447.
(116) Kurecki, T.; Laskowski, M.; Kress, L. F. *J. Biol. Chem.* **1978**, *253*, 8340. Kress, L. F. *J. Cell. Biochem.* **1986**, *32*, 51. Kress, L. F.; Catanese, J. J. *Biochemistry* **1981**, *20*, 7432.
(117) Hite, L. A.; Shannon, J. D.; Bjarnason, J. B.; Fox, J. W. *Biochemistry* **1992**, *31*, 6203.
(118) Grams, F.; Huber, R.; Kress, L. F.; Moroder, L.; Bode, W. *FEBS Lett.* **1993**, *335*, 76.
(119) Fox, J. W.; Bjarnason, J. B. *Methods Enzymol.* **1995**, *248*, 368.
(120) Bjarnason, J. B.; Fox, J. W. *Biochemistry* **1983**, *33*, 3770.
(121) Kumasaka, T.; Yamamoto, M.; Moriyama, H.; Tanaka, N.; Sato, M.; Katsube, Y.; Yamakawa, Y.; Omori-Satoh, T.; Iwanaga, S.; Ueki, T. *J. Biochem.* **1996**, *119*, 49.
(122) Maeda, H.; Morihara, K. *Methods Enzymol.* **1995**, *248*, 395.
(123) Matsumoto, K.; Maeda, H.; Okamura, R. *J. Biochem.* **1984**, *96*, 1165. Miyata, K.; Tomoda, K.; Isono, H. *Agric. Biol. Chem.* **1971**, *35*, 460.
(124) Baumann, U.; Wu, S.; Flaherty, K. M.; McKay, D. B. *EMBO J.* **1993**, *12*, 3357.
(125) Hamada, K.; Hata, Y.; Katsuya, Y.; Hiramatsu, H.; Fujiwara, T.; Katsube, Y. *J. Biochem.* **1996**, *119*, 844. Miyatake, H.; Hata, Y.; Fujii, T.; Hamada, K.; Morihara, K.; Katsube, Y. *J. Biochem.* **1995**, *118*, 474.
(126) Baumann, U. *J. Mol. Biol.* **1994**, *242*, 244. Baumann, U.; Bauer, M.; Letoffe, S.; Delepelaire, P.; Wandersman, C. *J. Mol. Biol.* **1995,** *248*, 653.
(127) Dioszegi, M.; Cannon, P.; Van Wart, H. R. *Methods Enzymol.* **1995**, *148*, 413.
(128) Tschesche, H. *Methods Enzymol.* **1995**, *248*, 485.
(129) Murphy, G.; Crabbe, T. *Methods Enzymol.* **1995**, *248*, 470.
(130) Nagase, H. *Methods Enzymol.* **1995**, *248*, 449
(131) Woessner, J. F., Jr. *FASEB J.* **1991**, *5*, 2145.
(132) Faber, H. R.; Groom, C. R.; Baker, H. M.; Morgan, W. T.; Smith, A.; Baker, E. N. *Structure* **1995**, *3*, 551.
(133) Tschesche, H. *Methods Enzymol.* **1995**, *248*, 431.
(134) Bode, W.; Reinemer, P.; Huber, R.; Kleine, T.; Schnierer, S.; Tschesche, H. *EMBO J.* **1994**, *13*, 1263.
(135) Grams, F.; Reinemer, P.; Powers, J. C.; Kleine, T.; Pieper, M.; Tschesche, H.; Huber, R.; Bode, W. *Eur. J. Biochem.* **1995**, *228*, 830.
(136) Grams, F.; Crimmin, M.; Hinnes, L.; Huxley, P.; Pieper, M.; Tschesche, H.; Bode, W. *Biochemistry* **1995**, *34*, 14012.
(137) Reinemer, P.; Grams, F.; Huber, R.; Kleine, T.; Schnierer, S.; Piper, M.; Tschesche, H.; Bode, W. *FEBS Lett.* **1994**, *338*, 227.
(138) Stams, T.; Spurlino, J. C.; Smith, D. L.; Wahl, R. C.; Ho, T. F.; Qoronfleh, M. W.; Banks, T. M.; Rubin, B. *Nature Struct. Biol.* **1994**, *1*, 119.
(139) Lovejoy, B.; Cleasby, A.; Hassell, A. M.; Longley, K.; Luther, M. A.; Weigl, D.; McGeehan, G.; McElroy, A. B.; Drewry, D.; Lambert, M. H.; Jordan, S. R. *Science* **1994**, *263*, 375.
(140) Lovejoy, B.; Hassell, A. M.; Luther, M. A.; Weigl, D.; Jordan, S. R. *Biochemistry* **1994**, *33*, 8207.
(141) Borkakoti, N.; Winkler, F. K.; Williams, D. H.; D'Arcy, A.; Broadhurst, M. J.; Brown, P. A.; Johnson, W. H.; Murray, E. J. *Nature Struct. Biol.* **1994**, *1*, 106.
(142) Spurlino, J. C.; Smallwood, A. M.; Carlton, D. D.; Banks, T. M.; Vavra, K. J.; Johnson, J. S.; Cook, E. R.; Falvo, J.; Wahl, R. C.; Pulvino, T. A.; Wendoloski, J. J.; Smith, D. L. *Proteins* **1994**, *19*, 98.
(143) Li, J.; Brick, P.; O'Hare, M. C.; Skarzynski, T.; Lloyd, L. F.; Curry, V. A.; Clark, I. M.; Bigg, H. F.; Hazleman, B. L.; Cawston, T. E.; Blow, D. M. *Structure* **1995**, *3*, 541.
(144) Gooley, P. R.; O'Connell, J. F.; Marcy, A. I.; Cuca, G. C.; Salowe, S. P.; Bush, B. L.; Hermes, J. D.; Esser, C. K.; Hagmann, W. K.; Springer, J. P.; Johnson, B. A. *Nature Struct. Biol.* **1994**, *1*, 111.
(145) Browner, M. F.; Smith, W. W.; Castelhano, A. L. *Biochemistry* **1995**, *34*, 6602.
(146) Willenbrock, F.; Murphy, G.; Phillips, I. R.; Brocklehurst, K. *FEBS Lett.* **1995**, *358*, 189.

(147) Gohlke, U.; Gomis-Rüth, F.-X.; Crabbe, T.; Murphy, G.; Docherty, A. J. P.; Bode, W. *FEBS Lett.* **1996**, *378*, 126.
(148) Woessner, J. F., Jr. *Methods Enzymol.* **1995**, *248*, 485.
(149) Murphy, G.; Willenbrock, F. *Methods Enzymol.* **1995**, *248*, 496.
(150) Williamson, R. A.; Martorell, G.; Carr, M. D.; Murphy, G.; Docherty, A. J. P.; Freedman, R. B.; Feeney, J. *Biochemistry* **1994**, *33*, 11745.
(151) Schlagenhauf, E.; Etges, R.; Metcalf, P. *Proteins* **1995**, *22*, 58.
(152) Harada, S.; Kitadokoro, K.; Kinoshita, T.; Kai, Y.; Kasai, N. *J. Biochem.* **1991**, *110*, 46. Harada, S.; Kinoshita, T.; Kasai, N.; Tsunawasa, S.; Sakiyama, F. *Eur. J. Biochem.* **1995**, *233*, 683. Kuriso, G.; Kinoshita, T.; Sugimoto, A.; Nagara, A.; Kai, Y.; Kasai, N.; Harada, S. manuscript in preparation.
(153) Bumcrot, D. A.; McMahon, A. P. *Chem. Biol.* **1996**, *3*, 1. Lumsden, A.; Graham, A. *Curr. Biol.* **1995**, *5*, 1347.
(154) Tanaka Hall, T. M.; Porter, J. A.; Beachy, P. A.; Leahy, D. J. *Nature* **1995**, *378*, 212.
(155) Murzin, A. G. *Cur. Opin. Struct. Biol.* **1996**, *6*, 386.
(156) Inouye, M.; Arnheim, N.; Sternglanz, R. *J. Biol. Chem.* **1973**, *248*, 7247.
(157) Moffatt, B. A.; Studier, F. W. *Cell* **1987**, *49*, 221.
(158) Cheng, X.; Zhang, X.; Pflugrath, J. W.; Studier, F. W. *Proc. Natl. Acad. Sci. USA* **1994**, *91*, 4034.
(159) Meinnel, T.; Lazennec, C.; Blanquet, S. *J. Mol. Biol.* **1995**, *254*, 175.
(160) Lim, H. M.; Iyer, R. K.; Pene, J. J. *Biochem. J.* **1991**, *276*, 401.
(161) Clark, S. D. Ph.D. Thesis Texas Technical University, 1993.
(162) Sabath, L. D.; Abraham, E. P. *Biochem J.* **1966**, *98*, 11c.
(163) Davies, R. B.; Abraham, E. P. *Biochem. J.* **1974**, *143*, 129.
(164) Concha, N. O.; Rasmussen, B. A., Bush, K.; Herzberg, O. *Structure* **1996**, *4*, 823.
(165) Coleman, J. E.; Gettins, P. *Metal Forms in Biology*; Spiro, T. G., Ed.; John Wiley and Sons: New York, 1983; Vol. 5, Chapter 5, p 153.
(166) Coleman, J. E.; Gettins, P. *Adv. Enzymol. Relat. Areas Mol. Biol.* **1983**, *55*, 381.
(167) Coleman, J. E. *Annu. Rev. Biophys. Biomol. Struct.* **1992**, *21*, 441.
(168) Kim, E. E.; Wyckoff, H. W. *J. Mol. Biol.* **1991**, *218*, 449.
(169) Reid, T. W.; Wilson, I. B. *The Enzymes*, 3rd ed.; Boyer, P., Ed.; Academic Press: New York; 1971; Vol. IV, p 373.
(170) Fernley, H. N.; Walker, P. G. *Nature* **1966**, *212*, 1435.
(171) Albridge, W. N.; Barman, T. E.; Gutfreund, H. *Biochem. J.* **1964**, *92*, 236.
(172) Jones, S. R.; Kindman, L. A.; Knowles, J. P. *Nature* **1978**, *275*, 564.
(173) Schindelmeiser, J.; Münstermann, D.; Witzel, H. *Histochemistry* **1987**, *87*, 13. Schindelmeiser, J.; Schewe, P.; Zonka, T.; Münstermann, D. *Histochemistry* **1989**, *92*, 81. Zaidi, M.; Moonga, B.; Moss, D. W.; MacIntyre, I. *Biochem. Biophys. Res. Commun.* **1989**, *159*, 68. Lau, K. W.; Freeman, T. K.; Baylink, D. J. *J. Biol. Chem.* **1987**, *262*, 1389.
(174) Sträter, N.; Klabunde, T.; Tucker, P.; Witzel, H.; Krebs, B. *Science* **1995**, *268*, 1489. Klabunde, T.; Sträter, N.; Fröhlich, R.; Witzel, H.; Krebs, B. *J. Mol. Biol.* **1996**, *259*, 737.
(175) Klabunde, T.; Sträter, N.; Krebs, B.; Witzel, H. *FEBS Lett.* **1995**, *367*, 56.
(176) Holmes, M. A.; Trong, I. L.; Turley, L.; Sieker, L. C.; Stenkamp, R. E. *J. Mol. Biol.* **1991**, *218*, 583.
(177) Nordlund, P; Sjöberg, B.-M.; Eklund, H. *Nature* **1990**, *345*, 593.
(178) Rosenzweig, A. C.; Frederick, C. A.; Lippard, S. N.; Nordlund, P. *Nature* **1993**, *366*, 537.
(179) deMare, F.; Kurtz, D. M.; Nordlund, P. *Nature Struct. Biol.* **1996**, *3*, 539.
(180) Wilcox, D. E. *Chem. Rev.* **1996**, *96*, 2435 (this issue).
(181) Sträter, N.; Lipscomb, W. N.; Klabunde, T.; Krebs, B. *Angew. Chem.* **1996**, in press.
(182) Dietrich, M; Münstermann, D.; Suerbaum, H.; Witzel, H. *Eur. J. Biochem.* **1991**, *199*, 105.
(183) Mueller, E. G.; Crowder, M. W.; Averill, B. A.; Knowles, J. R. *J. Am. Chem. Soc.* **1993**, *115*, 2974.
(184) Aquino, M. A. S.; Lim, J.-S.; Sykes, A. G. *J. Chem. Soc., Dalton Trans.* **1994**, 429.
(185) Martin, B. L.; Graves, D. J. *J. Biol. Chem.* **1986**, *261*, 14545. Martin, B. L.; Graves, D. J. *Biochim. Biophys. Acta* **1994**, *1206*, 136.
(186) Goldberg, J.; Huang, H.-G.; Kwon, Y.-G.; Greengard, P.; Nairn, A. C.; Kuriyan, J. *Nature* **1995**, *376*, 745.
(187) Zhou, S.; Clemens, J. C.; Stone, R. L.; Dixon, J. E. *J. Biol. Chem.* **1994**, *269*, 26234.
(188) Koonin, E. V. *Protein Sci.* **1994**, 3, 356.
(189) King, M. M.; Huang, C. Y. *J. Biol. Chem.* **1984**, *259*, 8847.
(190) Chu, Y; Lee, E. Y. C.; Schlender, K. K. *J. Biol. Chem.* **1996**, *271*, 2574.
(191) Yu, L.; Haddy, A.; Rusnak, F. *J. Am. Chem. Soc.* **1995**, *117*, 10147. Qin, K. F.; Khangulov, S.; Liu, C.; Huang, C. Y. *FASEB J.* **1995**, *9*, A1347.
(192) Alessi, D. R.; Street, A. J.; Cohen, P.; Cohen, P. T. *Eur. J. Biochem.* **1993**, *220*, 225.
(193) Egloff, M.-P.; Cohen, P. T. W.; Renemer, P.; Barford, D. *J. Mol. Biol.* **1995**, *254*, 942.
(194) Lin, J.; Farmer, J. D., Jr.; Lane, W. S.; Friedman, J.; Weissman, I.; Schreiber, S. L. *Cell* **1991**, *66*, 807.
(195) O'Keefe, S. J.; Tamura, J.; Kincaid, R. L.; Tocci, M. J.; O'Neill, E. A. *Nature* **1992**, *357*, 692.
(196) Clipptone, N. K.; Crabtree, G. R. *Nature* **1992**, *357*, 695.
(197) Kissinger, C. R.; Parge, H. E.; Knighton, D. R.; Lewis, C. T.; Pelletier, L. A.; Tempczyk, A.; Kalish, V. J.; Tucker, K. D.; Showalter, R. E.; Moomaw, E. W.; Gastinel, L. N.; Habuka, N.; Chen, X.; Maldono, F.; Barker, J. E.; Bacquet, R.; Villafranca, J. E. *Nature* **1995**, *378*, 641.
(198) Griffith, J. P.; Kim, J. L.; Kim, E. E.; Sintchak, M. D.; Thomson, J. A.; Fitzgibbon, M. J.; Fleming, M. A.; Caron, P. R.; Hsiao, K.; Navia, M. A. *Cell* **1995**, *82*, 507.
(199) Bevidge, M. *Biochem. J.* **1984**, *220*, 345.
(200) Besterman, J. M.; Duronis, V.; Cuarrecasas, P. *Proc. Natl. Acad. Sci. USA* **1986**, *83*, 6785.
(201) Little, C.; Otnaess, A. *Biochim. Biophys. Acta* **1975**, *391*, 326.
(202) Little, C. *Acta Chem. Scand.* **1981**, *B35*, 39.
(203) Hough, E.; Hansen, L. K.; Birknes, B.; Jynge, K.; Hansen, S.; Hordvik, A.; Little, C.; Dodson, E.; Derewenda, Z. *Nature* **1989**, *338*, 357−360. Hansen, S.; Hansen, L. A.; Hough, E. *J. Mol. Biol.* **1992**, *225*, 543. Hansen, S.; Hansen, L. A.; Hough, E. *J. Mol. Biol.* **1993**, *231*, 870.
(204) Hansen, S.; Hough, E.; Svensson, L. A.; Wong, Y.; Martin, S. F. *J. Mol. Biol.* **1993**, *234*, 179.
(205) Martin, S. F.; Wong, Y.-L.; Wagman, A. S. *J. Org. Chem.* **1994**, *59*, 4821.
(206) Sundell, S.; Hansen, S.; Hough, E. *Protein Eng.* **1994**, *7*, 571.
(207) Shishido, K.; Ando, T. *Nucleases*; Linn, S. M., Roberts, R. J., Eds.; Cold Spring Harbor Laboratory Press: Cold Spring Harbor, NY, 1982; p 155.
(208) Fujimoto, M.; Kuninake, A.; Yoshino, H. *Agric. Biol. Chem.* **1974**, *38*, 785.
(209) Volbeda, A.; Lahm, A.; Sakiyama, F; Suck, D. *EMBO J.* **1991**, *10*, 1607. Suck, D. et al. Unpublished results.
(210) Potter, B. V.; Connolly, B. A.; Eckstein, F. *Biochemistry* **1983**, *22*, 1369
(211) Dumas, D. P.; Caldwell, S. R., Wild, J. R.; Raushel, F. M. *J. Biol. Chem.* **1989**, *264*, 19659.
(212) Scanlan, T. S.; Reid, R. C. *Chem. Biol.* **1995**, *2*, 71.
(213) Benning, M. M.; Kuo, J. M.; Raushel, F. M.; Holden, H. M. *Biochemistry* **1995**, *34*, 7973.
(214) Hong, S.; Kuo, J. M.; Mullins, L. S.; Raushel, F. M. *J. Am. Chem. Soc.* **1995**, *117*, 7580.
(215) Benning, M. M.; Kuo, J. M.; Raushel, F. M.; Holden, H. M. *Biochemistry* **1994**, *33*, 15001.
(216) Lai, K.; Dave, K. I.; Wild, J. R. *J. Biol. Chem.* **1994**, *269*, 16579.
(217) Lewis, V. E.; Donarski, W. J.; Wild, J. R.; Raushel, F. M. *Biochemistry* **1988**, *27*, 1591.
(218) Ronca, G.; Lucacchini, A.; Rossi, C. A. *Methods Enzymol.* **1977**, *46*, 327.
(219) Frick, L.; Mac Neela, J. P.,; Wolfenden, R. *Bioorg. Chem.* **1987**, *15*, 100. Kurz, L. C.; Weitkamp, E.; Friedem, C. *Biochemistry* **1987**, *26*, 3027.
(220) Kurz, L. C.; Frieden, C. *Biochemistry* **1987**, *26*, 8450. Jones, W.; Kurz, L. C.; Wolfenden, R. *Biochemistry* **1989**, *28*, 1242.
(221) Wilson, D. K.; Rudolph, F. B.; Quiocho, F. A. *Science* **1991**, *252*, 1278.
(222) Sharff, A. J.; Wilson, D. K.; Chang, Z.; Quiocho, F. A. *J. Mol. Biol.* **1992**, *226*, 917.
(223) Wilson, D. K.; Quiocho, F. A. *Nature Struct. Biol.* **1994**, *1*, 691.
(224) Kurz, L. C.; Moix, L.; Riley, M. C.; Frieden, C. *Biochemistry* **1992**, *31*, 39.
(225) Wilson, D. K.; Quiocho, F. A. *Biochemistry* **1993**, *32*, 1689.
(226) Bhaumik, D.; Medin, J.; Gathy, K.; Coleman, M. S. *J. Biol. Chem.* **1993**, *268*, 5464. Sideraki, V.; Mohamedali, K. A.; Wilson, D. K.; Chang, Z.; Kellems, R. E.; Quiocho, F. A.; Rudolph, F. B. *Biochemistry* **1996**, *35*, 7862.
(227) Kati, W. M.; Wolfenden, R. *Science* **1989**, *243*, 1591.
(228) Kati, W. M.; Acheson, S. A.; Wolfenden, R. *Biochemistry* **1992**, *31*, 7356.
(229) Kati, W. M.; Wolfenden, R. *Biochemistry* **1989**, *28*, 7919.
(230) Merckler, D. J.; Schramm, V. L. *Biochemistry* **1993**, *32*, 5792.
(231) Carter, C. W., Jr. *Biochimie* **1995**, *77*, 92.
(232) Frick, L.; Yang, C.; Marquez, V. E.; Wolfenden, R. *Biochemistry* **1989**, *28*, 9423.
(233) Ashley, G. W.; Bartlett, P. A. *J. Biol. Chem.* **1984**, *259*, 13621.
(234) Betts, L.; Xiang, S.; Short, S. A.; Wolfenden, R.; Carter, C. W., Jr. *J. Mol. Biol.* **1994**, *235*, 635.
(235) Xiang, S.; Short, S. A.; Wolfenden, R.; Carter, C. W. *Biochemistry* **1995**, *34*, 4516.
(236) Carlow, D. C.; Smith, A. A.; Yang, C. C.; Short, S. A.; Wolfenden, R. *Biochemistry* **1995**, *34*, 4220.
(237) Carlow, D. C.; Short, S. A.; Wolfenden, R. *Biochemistry* **1996**, *35*, 948.
(238) Xiang, S.; Short, S. A.; Wolfenden, R.; Carter, C. W. *Biochemistry* **1996**, *35*, 1335.
(239) Thorp, H. H. *Inorg. Chem.* **1992**, *31*, 1585. Liu, W.; Thorp, H. H. *Inorg. Chem.* **1993**, *32*, 4102. Brown, I. D. *Chem. Soc. Rev.* **1978**, *7*, 359.

(240) Reizer, J.; Buskirk, S.; Bairoch, A.; Reizer, A.; Saier, M. H., Jr. *Protein Sci.* **1994**, *3*, 853.
(241) Navaratnam, N.; Morrison, J. R.; Bhattacharya, S.; Patel, D.; Funahashi, T.; Giannoni, F.; Teng, B. B.; Davidson, N. O.; Scott, J. *J. Biol. Chem.* **1993**, *268*, 20709. Navaratnam, N.; Bhattacharya, S.; Fujino, T.; Patel, D.; Jarmuz, A. L.; Scott, J. *Cell* **1995**, *81*, 187. Yamanaka, S.; Poksay, K. S.; Balestra, M. E.; Zeng, G. Q.; Innerarity, T. L. *J. Biol. Chem.* **1994**, *269*, 21725.
(242) Sumner, J. B. *J. Biol. Chem.* **1926**, *69*, 435.
(243) Dixon, N. E.; Gazzola, C.; Blakeley, R. L.; Zerner, B. *J. Am. Chem. Soc.* **1975**, *97*, 4131.
(244) Park, I. S.; Hausinger, R. P. *Science* **1995**, *267*, 1156.
(245) Hartman, F. C.; Harpel, M. R. *Annu. Rev. Biochem.* **1993**, *63*, 197.
(246) Jabri, E.; Carr, M. B.; Hausinger, R. P.; Karplus, P. A. *Science* **1995**, *268*, 998.
(247) Park, I. S.; Carr, M. B.; Hausinger, R. P. *Proc. Natl. Acad. Sci. USA* **1994**, *91*, 3233.
(248) Lee, M. H.; Mulrooney, S. B.; Benner, M. J.; Marcowicz, Y.; Hausinger, R. P. *J. Bacteriol.* **1992**, *174*, 4324.
(249) Dixon, N. E.; Riddles, P. W.; Gazzola, C.; Blakeley, R. L.; Zerner, B. *Can. J. Biochem.* **1980**, *58*, 1335.
(250) Park, I.-S.; Hausinger, R. P. *Biochemistry* **1996**, *35*, 5345.
(251) Farber, G. K.; Petsko, G. A. *Trends. Biochem. Sci.* **1990**, *15*, 228.
(252) Farber, G. K. *Curr. Opin. Struct. Biol.* **1993**, *3*, 409.
(253) Duch, D. S.; Smith, G. K. *J. Nutr. Biochem.* **1991**, *2*, 411.
(254) Nar, H.; Huber, R.; Heizmann, C. W.; Thöny, B.; Bürgisser, D. M. *EMBO J.* **1994**, *13*, 1255.
(255) Bürgisser, D. M.; Thöny, B.; Redweik, U.; Hess, D.; Heizmann, C. W.; Huber, R.; Nar, H. *J. Mol. Biol.* **1995**, *253*, 358.
(256) Kubitz, F. *Biochem. Z.* **1938**, *299*, 32. Winkler, M.; Lerch, K.; Solomon, E. I. *J. Am. Chem. Soc.* **1981**, *103*, 7001. Oetting, W. S.; King, R. A. *Pigment Cell Res.* **1994**, *7*, 285. Wilcox, D. E.; Porras, A. G.; Hwang, Y. T.; Lerch, K.; Winkler, M. E.; Solomon, E. I. *J. Am. Chem. Soc.* **1985**, *107*, 4015.
(257) Jackson, I. J.; Chambers, D. M.; Tsukamoto, K.; Copeland, N. G.; Gilbert, D. J.; Jenkins, N. A.; Hearing, V. J. *EMBO J.* **1992**, *11*, 527.
(258) Solano, F.; Jiménez-Cevantes, C.; Martínez-Liarte, J. H.; García-Borrón, J. C.; Jara, J. R.; Lozano, J. A. *Biochem J.* **1996**, *313*, 447.
(259) Keilin, D.; Mann, T. *Biochem. J.* **1940**, *34*, 1163.
(260) Linskog, S.; Liljas, A. *Curr. Opin. Struct. Biol.* **1993**, *3*, 915.
(261) Lindahl, M.; Svensson, L. A.; Liljas, A. *Proteins* **1993**, *15*, 177.
(262) Liang, J.-Y.; Lipscomb, W. N. *Proc. Natl. Acad. Sci. USA* **1990**, *87*, 3675. Merz, K. M., Jr. *J. Am. Chem. Soc.* **1991**, *113*, 406.
(263) Xue, Y.; Vidgren, J.; Svensson, L. A.; Liljas, A.; Jonsson, B. H.; Lindskog, S. *Proteins* **1993**, *15*, 80.
(264) Håkansson, K.; Wehnert, A. *J. Mol. Biol.* **1992**, *228*, 1212.
(265) Paneth, P.; O'Leary, M. H. *Biochemistry* **1985**, *24*, 5143.
(266) Paneth, P.; O'Leary, M. H. *Biochemistry* **1987**, *26*, 1728.
(267) Mann, T.; Keilin, D. *Nature* **1940**, *146*, 164.
(268) Maren, T. H. *Drug Dev. Res.* **1987**, *10*, 255.
(269) Baldwin, J. J.; Ponticello, G. S.; Anderson, P. S.; Christy, M. E.; Murcko, M. A.; Randall, W. C.; Schwam, H.; Sugrue, M. F.; Springer, J. P.; Gautheron, P.; Grove, J.; Mallorga, P.; Viader, M. P.; McKeever, B. M.; Navia, M. A. *J. Med. Chem.* **1989**, *32*, 2510−2513.
(270) Smith, G M.; Alexander, R. S.; Christianson, D. W.; McKeever, B. M.; Ponticello, G. S.; Springer, J. P.; Randall, W. C.; Baldwin, J. J.; Habecker, C. N. *Protein Sci.* **1994**, *3*, 118−125.
(271) Tannen, R. L.; Ross, B. D. *J. Lab. Clin. Med.* **1983**, *102*, 536−542.
(272) Dodgson, S. J.; Forster, R. E. *Arch. Biochem. Biophys.* **1986**, *251*, 198−204.
(273) Erickson, E. A.; Jones, T. A.; Liljas, A. *Zinc Enzymes*; Bertini, I., Luchinat, C., Maret, W., Zeppezauer, M., Eds.; Birkhäuser: Boston, 1986; p 318.
(274) Liljas, A.; Håkansson, K; Jonsson, B. H.; Xue, Y. *Eur. J. Biochem.* **1994**, *219*, 1.
(275) Christianson, D. W.; Fierke, C. *Acc. Chem. Res.* **1996**, *29*, 331.
(276) Thompson, R. B.; Jones, E. R. *Anal. Chem.* **1993**, *65*, 730.
(277) Alber, B. E.; Ferry, J. G. Proc. *Natl. Acad. Sci. USA* **1994**, *91*, 6909.
(278) Kisker, C.; Schindelin, H.; Alber, B. E.; Ferry, J. G.; Rees, D. C. *EMBO J.* **1996**, *15*, 2323.
(279) Williams, N. K.; Manthey, M. K.; Hambley, T. W.; O'Donoghue, S. I.; Keegan, M.; Chapman, B. E.; Christopherson, R. I. *Biochemistry* **1995**, *34*, 11344.
(280) Christopherson, R. I.; Jones, M. E. *J. Biol. Chem.* **1980**, *255*, 3358. Taylor, W. H.; Taylor, M. L.; Balch, W. E.; Gilchrist, P. S. *J. Bacteriol.* **1976**, *127*, 863. Washabaugh, M. W.; Collins, K. D. *J. Biol. Chem.* **1984**, *259*, 3293. Kelly, R. E.; Mally, M. I.; Evans, D. R. *J. Biol. Chem.* **1986**, *261*, 6073.
(281) Christianson, D. W.; Alexander, R. S. *Nature* **1990**, *346*, 225.
(282) Walsh, C. *Enzymatic Reaction Mechanisms*; W. F. Freeman and Co.: San Francisco, 1979; p 154
(283) Myers, L. C; Verdine, G. L.; Wagner, G. *Biochemistry* **1993**, *32*, 14089.
(284) Myers, L. C.; Terranova, M. P.; Nash, H. M.; Markus, M. A.; Verdine, G. L. *Biochemistry* **1992**, *31*, 4541.
(285) Myers, L. C.; Terranova, M. P.; Ferentz, A. E.; Wagner, G.; Verdine, G. L. *Science* **1993**, *261*, 1164.
(286) Myers, L. C.; Jackow, F.; Verdine, G. L. *J. Biol. Chem.* **1995**, *270*, 6664.
(287) Ohkubo, T.; Sakashita, H.; Sakuma, T.; Kainosho, M.; Sekiguchi, M.; Morikawa, K. *J. Am. Chem. Soc.* **1994**, *116*, 6035. Myers, L. C.; Cushing, T. D.; Wagner, G.; Verdine, G. L. *Chem. Biol.* **1994**, *1*, 91.
(288) Lan, Y.; Lu, T.; Lovett, P. S.; Greighton, D. J. *J. Biol. Chem.* **1995**, *270*, 12957.
(289) Sellin, S.; Eriksson, L. E. G.; Mannervik, B. *Biochemistry* **1982**, *21*, 4850.
(290) Mannervik, B.; Sellin, S.; Eriksson, L. E. G. *Zinc Enzymes*; Bertini, L., Lucinat, C., Maret, W., Zeppezauer, M., Eds.; Birkhäuser: Boston, 1986; p 517.
(291) Garcia-Iniguez, L.; Powers, L.; Chance, B.; Sellin, S.; Mannervik, B.; Mildvan, A. S. *Biochemistry* **1984**, *23*, 685.
(292) Aronsson, A.-C.; Marmstål, W.; Mannervik, B. *Biochem. Biophys. Res. Commun.* **1978**, *81*, 1235.
(293) Cameron, A. D.; Olin, B.; Ridderström, M.; Mannervik, B.; Jones, *Acta Crystallogr. Sect. A*, in press (XVII Congress of the International Union of Crystallography, Seattle, 1996).
(294) Ghalambor, M. A.; Heath, E. C. *J. Biol. Chem.* **1962**, *237*, 2427.
(295) Dreyer, M. K.; Schulz, G. E. *J. Mol. Biol.* **1993**, *231*, 549.
(296) Dreyer, M. K.; Schulz, G. E. *J. Mol. Biol.* **1996**, *259*, 458.
(297) Tétreault, S.; Sygusch, J. Abstracts, American Crystallographic Association Meeting, Montréal, July 23−28, 1995; Abstract W120, p 177
(298) Eklund, H.; Brändén, C.-I. In *Zinc Enzymes*; Spiro, T. G., Ed.; John Wiley and Sons: New York, 1983; pp 125−152.
(299) Krassman, J.; Larsson, A.; Peterson, G. *Eur. J. Biochem.* **1981**, *114*, 55.
(300) Cedergren-Zeppezauer, E. S. *Zinc Enzymes*; Bertini, I., Luchinat, C., Maret, W., Zeppezauer, M., eds.; Birkhäuser: Boston, 1986; p 393.
(301) Eklund, H.; Jones, A.; Schneider, G. In *Zinc Enzymes*; Bertini, I., Luchinat, C., Maret, W., Zeppezauer, M., eds.; Birkhäuser: Boston, 1986; p 377.
(302) Huskey, W. P.; Schowen, R. L *J. Am. Chem. Soc.* **1983**, *105*, 5704.
(303) Klinman, J. P. *Trends Biochem. Sci.* **1989**, *14*, 368.
(304) Cha, Y.; Murray, C. J.; Klinman, J. P. *Science* **1989**, *243*, 1325.
(305) Ramaswamy, S.; Eklund, H.; Plapp, B. V. *Biochemistry* **1994**, *33*, 5230.
(306) Ehrig, T.; Hurley, T. D.; Edenberg, H. J.; Bosson, W. F. *Biochemistry* **1991**, *30*, 1062.
(307) John, J.; Crennell, S. J.; Hough, D. W.; Danson, M. J.; Taylor, G. L. *Structure* **1994**, *2*, 385.
(308) Thom, J. M.; Barton, J. D.; Dixon, N. E.; Ollis, D. L.; Edwards, K. J. *J. Mol. Biol.* **1995**, *249*, 785.
(309) Melord, J. M.; Fridovich, I. *J. Biol. Chem.* **1969**, *244*, 6049.
(310) Richardson, J. S.; Thomas, K. A.; Rubin, B. H.; Richardson, D. C. *Proc. Natl. Acad. Sci. USA* **1975**, *72*, 1349.
(311) Tainer, J. A.; Getzoff, E. D.; Beem, K. M.; Richardson, J. S.; Richardson, D. C. *J. Mol. Biol.* **1982**, *160*, 181.
(312) Carugo, K. D.; Battistoni, A.; Carri, M. T.; Polticelli, F.; Desideri, A.; Rotilio, G.; Coda, A.; Wilson, K. S.; Bolognesi, M. *Acta Crystallogr. Sect. D* **1996**, *52*, 176.
(313) Kitagawa, Y.; Tanaka, N.; Hata, Y.; Kusunoki, M.; Lee, G.; Katsube, Y.; Asada, K.; Aibara, S.; Morita, Y. *J. Biochem. (Tokyo)* **1991**, *109*, 447.
(314) Djinovic, K.; Gatti, G.; Coda, A.; Antolini, L.; Pelosi, G.; Desideri, A.; Falconi, M.; Marmocchi, F.; Rotilio, G.; Bolognesi, M. *J. Mol. Biol.* **1992**, *225*, 791.
(315) Parge, H. E.; Hallewell, R. A.; Tainer, J. A. *Proc. Natl. Acad. Sci. USA* **1992**, *89*, 6109.
(316) Carugo, K. D.; Battistoni, A.; Carri, M. T.; Polticelli, F.; Desideri, A.; Rotilio, G.; Coda, A.; Bolognesi, M. *FEBS Lett.* **1994**, *349*, 93.
(317) Bailey, D. B.; Ellis, P. D.; Fee, J. A. *Biochemistry* **1980**, *19*, 591.
(318) Bertini, I.; Banci, L.; Piccioli, M.; Luchinat, C. *Coord. Chem. Rev.* **1990**, *100*, 67.
(319) Blackburn, N. J.; Hasnain, S. S.; Binsted, N.; Diakun, G. P.; Garner, C. D.; Knowles, P. F. *Biochem. J.* **1984**, *219*, 985.
(320) Ogihara, N. L.; Parge, H. E.; Hart, P. J.; Weiss, M. S.; Goto, J. J.; Crane, B. R.; Tsang, J.; Slater, K.; Roe, J. A.; Selverstone Valentine, J.; Eisenberg, D.; Tainer, J. A. *Biochemistry* **1996**, *35*, 2316.
(321) Rypniewski, W. R.; Mangani, S.; Bruni, B.; Orioli, P. L.; Casati, M.; Wilson, K. S. *J. Mol. Biol.* **1995**, *251*, 282.
(322) Lippard, S. J.; Burger, A. R.; Ugurbil, K.; Pantoliano, M. W.; Valentine, J. S. *Biochemistry* **1977**, *16*, 1136.
(323) Polticelli, F.; Battistoni, A.; O'Neill, P.; Rotilio, G.; Desideri, A. *Protein Sci.* **1996**, *5*, 248.
(324) Shih, P.; Wolfenden, R. *Biochemistry* **1996**, *35*, 4697.
(325) Ding, J.; Choe, H.-W.; Granzin, J.; Saenger, W. *Acta Crystallogr. Sect. B* **1992**, *48*, 185.
(326) Itaya, M.; Inoue, Y. *Biochem. J.* **1982**, *207*, 357.
(327) Lipscomb, W. N. *Adv. Enzymol.* **1994**, *68*, 67.
(328) Miller, J.; McLachlan, A. D.; Klug, A. *EMBO J.* **1985**, *4*, 1609.
(329) Berg, J. M. *Science* **1986**, *237*, 486.

(330) Cohlberg, J. A.; Pigiet, V. P.; Schachman, H. K. *Biochemistry* **1972**, *11*, 3396. Nelbach, M. E.; Pigiet, V. P.; Gerhart, J. C.; Schachman, H. K. *Biochemistry* **1972**, *11*, 315.
(331) Fan, S.; Harrison, L. W.; Hammes, G. G. *Biochemistry* **1975**, *14*, 2219.
(332) Johnson, R. S.; Schachman, H. K. *Proc. Natl. Acad. Sci. USA* **1980**, *77*, 1995.
(333) Kuo, L. C.; Lipscomb, W. N.; Kantrowitz, E. R. *Proc. Natl. Acad. Sci. USA* **1982,** *79*, 2250.
(334) Villeret, V.; Tricot, C.; Stalon, V.; Dideberg, O. *Proc. Natl. Acad. Sci. USA* **1995,** *92*, 10762.
(335) Stebbins, J. W.; Xu, W.; Kantrowitz, E. R. *Biochemistry* **1989,** *28*, 2592.
(336) Stebbins, J. W.; Kantrowitz, E. R. *Biochemistry* **1992,** *31*, 2328.
(337) Lee, S. P.; Han, M. K. *Biochemistry* **1996**, *35*, 3837.
(338) Johnson, M. S.; McClure, M. A.; Ferg, D. F.; Gray, D. F.; Doolittle, R. F. *Proc. Natl. Acad. Sci. USA* **1986**, *83*, 7648.
(339) Dyda, F.; Hickman, A. B.; Jenkins, T. M.; Engelman, A.; Craigie, R.; Davies, D. R. *Science* **1994**, *266*, 1981.
(340) Christianson, D. W.; Alexander, R. S. *J. Am. Chem. Soc.* **1989**, *111*, 6412.
(341) Glusker, J. P. *Adv. Protein Chem.* **1991**, *42*, 1.
(342) Chakrabarti, P. *Protein Eng.* **1990**, *4*, 49. Chakrabarti, P. *Biochemistry* **1989**, *28*, 6081. Chakrabarti, P. *Biochemistry* **1990**, *29*, 651. Chakrabarti, P. *Protein Eng.* **1990**, *4*, 57.
(343) This expression is somewhat confusing since it is also used to denote residues which are at a longer (say 2.4−3.0 Å) coordinating distance to a metal ion. Perhaps "indirect ligands" is a better term
(344) Kiefer, L. L.; Paterno, S. A.; Fierke, C. A. *J. Am. Chem. Soc.* **1995**, *117*, 6831.
(345) Lesburg, C. A.; Christianson, D. W. *J. Am. Chem. Soc.* **1995**, *117*, 6838.
(346) Alexander, R. S.; Kiefer, L. L.; Fierke, C. A.; Christianson, D. W. *Biochemistry* **1993**, *32*, 1510. Kiefer, L. L.; Ippolito, J. A.; Fierke, C. A.; Christianson, D. W. *J. Am. Chem. Soc.* **1993**, *115*, 12581.
(347) Ippolito, J. A.; Christianson, D. W. *Biochemistry* **1994**, *33*, 15241.
(348) Kiefer, L. L.; Krebs, J. F.; Paterno, S. A.; Fierke, C. A. *Biochemistry* **1993**, *32*, 9896. Ippolito, J. A.; Christianson, D. W. *Biochemistry* **1993**, *32*, 9901. Ippolito, J. A.; Baird, T. T., Jr.; McGee, S. A.; Christianson, D. W. *Proc. Natl. Acad. Sci. USA* **1995**, *92*, 5017.
(349) Murphy, J. E.; Xu, X.; Kantrowitz, E. R. *J. Biol. Chem.* **1993**, *268*, 21497. Janeway, C. M. L.; Xu, X.; Murphy, J. E.; Chaidaroglou, A.; Kantrowitz, E. R. *Biochemistry* **1993**, *32*, 1601. Murphy, J. E.; Tibbitts, T. T.; Kantrowitz, E. R. *J. Mol. Biol.* **1995**, *253*, 604. Murphy, J. E.; Kantrowitz, E. R. *Mol. Microbiol.* **1994**, *123*, 351.
(350) Iverson, B. L.; Lerner, R. A. *Science* **1989**, *243*, 1184.
(351) Chochran, A. G.; Schultz, P. G. *J. Am. Chem. Soc.* **1990**, *112*, 9414.
(352) Iverson, B. L.; Iverson, S. A.; Roberts, V. A.; Getzoff, E. D.; Tainer, J. A.; Benkovic, S. J.; Lerner, R. A. *Science* **1990**, *249*, 659. Wade, W. S.; Koh, J. S.; Han, N.; Hoekstra, D. M.; Lerner, R. A. *J. Am. Chem. Soc.* **1993**, *115*, 4449. Roberts, V. A.; Iverson, B. L.; Iverson, S. A.; Benkovic, S. J.; Lerner, R. A.; Getzoff, E. D.; Tainer, J. A. *Proc. Natl. Acad. Sci. USA* **1990**, *87*, 6654.
(353) Higaki, J. N.; Haymore, B. L.; Chen, S.; Fletterick, R. J.; Craik, C. S. *Biochemistry* **1990**, *29*, 8582. McGrath, M. E.; Haymore, B. L.; Summers, N. L.; Craik, C. S.; Fletterick, R. J. *Biochemistry* **1993**, *32*, 1914.
(354) Regan, L. *Trends Biochem. Sci.* **1995**, *20*, 280. Regan, L. *Annu. Rev. Biophys. Biomol. Struct.* **1993**, *22*, 257. Higaki, J. N.; Fletterick, R. J.; Craik, C. S. *Trends Biochem. Sci.* **1992**, *17*, 100. Kraatz, H.-B. *Angew. Chem., Int. Ed. Engl.* **1994**, *33*, 2055.
(355) Klemba, M.; Gardner, K. H.; Marino, S.; Clarke, N. D.; Regan, L. *Nature Struct. Biol.* **1995**, *2*, 368.
(356) Regan, L.; Clarke, N. D. *Biochemistry* **1990**, *29*, 10878.
(357) Klemba, M.; Regan, L. *Biochemistry* **1995**, *34*, 10094.
(358) Handel, T.; DeGrado, W. F. *J. Am. Chem. Soc.* **1990**, *112*, 6710.
(359) Pessi, A.; Bianchi, E.; Crameri, A.; Venturini, S.; Tramontano, A.; Sollazzo, M. *Nature* **1993**, *362*, 367.
(360) Matthews, D. J.; Wells, J. A. *Chem. Biol.* **1994**, *1*, 25.
(361) Ruan, F.; Chen, Y.; Hopkins, P. B. *J. Am. Chem. Soc.* **1990**, *112*, 9403. Ghadiri, M. R.; Choi, C. *J. Am. Chem. Soc.* **1990**, *112*, 1630.
(362) Walkup, G. K.; Imperiali, B. *J. Am. Chem. Soc.* **1996**, *118*, 3053.
(363) Godwin, H. A.; Berg, J. M. *J. Am. Chem. Soc.* **1996**, *118*, 6514.
(364) Kim, H.; Lipscomb, W. N. *Proc. Natl. Acad. Sci. USA* **1993**, *90*, 5006.
(365) Villeret, V.; Huang, S.; Fromm, H. J.; Lipscomb, W. N. *Proc. Natl. Acad. Sci. USA* **1995**, *92*, 8916.
(366) Gresh, N. *J. Comput. Chem.* **1995**, *16*, 856. Gresh, N.; Stevens, W. J.; Krauss, M. *J. Comput. Chem.* **1995**, *16*, 843. Liang, J.-Y.; Lipscomb, W. N. *Biochemistry* **1987**, *26*, 5293. Demoulin, D.; Pullman, A. *Theoret. Chim. Acta* **1978**, *49*, 161. Nakagawa, S.; Umeyama, H. *J. Theor. Biol.* **1982**, *96*, 473.
(367) Bertini, I.; Luchinat, C.; Rosi, M.; Sgamellotti, A.; Tarantelli, F. *Inorg. Chem.* **1990**, *29*, 1460.
(368) Ryde, U. *Proteins* **1995**, *21*, 40.
(369) Wasserman, Z. R.; Hodge, C. N. *Proteins* **1996**, *24*, 227.
(370) van Aalten, D. M. F.; Amadei, A.; Linssen, A. B. M.; Eijsink, V. G. H.; Vriend, G.; Berendsen, H. J. C. *Proteins* **1995**, *22*, 45.
(371) Rossi, K. A.; Merz, K. M., Jr.; Smith, G. M.; Baldwin, J. J. *J. Med. Chem.* **1995**, *38*, 2061.
(372) Sundell, S.; Hansen, S.; Hough, E. *Protein Eng.* **1994**, *7*, 571.
(373) Zhang, Z.; Reardon, I.; Hui, J.; O'Connell, K.; Poorman, R.; Tomasselli, A.; Heinrikson, R. *Biochemistry* **1991**, *36*, 8717.
(374) Wlodawer, A.; Miller, M.; Jaskólski, M.; Sathyanarayana, B. K.; Baldwin, E.; Weber, I. T.; Selk, L. M.; Clawson, L.; Schneider, J.; Kent, S. B. H. *Science* **1989**, *245*, 616.
(375) York, D. M.; Bartolotti, L. J.; Darden, T. A., Pedersen, L. G.; Anderson, M. W. *J. Comput. Chem.* **1994**, *15*, 61.
(376) Fuxreiter, M.; Farkas, Ö.; Náray-Szabó, G. *Protein Eng.* **1995**, *8*, 925.
(377) Stote, R. H.; Karplus, M. *Proteins* **1995**, *23*, 12.
(378) Liang, J.-Y.; Zhang, Y.; Huang, S.; Ke, H.; Lipscomb, W. N. *Proc. Robert A. Welch Found. Conf. Chem. Res.* **1992**, *36*, 57.
(379) Bencovic, P. A.; Coperelli, C. A.; De Maine, M.; Bencovic, S. J. *Proc. Natl. Acad. Sci. USA* **1978**, *75*, 2185.
(380) Zhang, Y., Liang, J.-Y., Huang, S., Ke, H.; Lipscomb, W. N. *Biochemistry* **1993**, *32*, 1844.
(381) Kelley, N.; Giroux, E. L.; Lu, G.; Kantrowitz, E. R. *Biochem. Biophys. Res. Commun.* **1996**, *219*, 848.
(382) Villeret, V.; Huang, S.; Zhang, Y.; Lipscomb, W. N. *Biochemistry* **1995**, *34*, 4307−4314.
(383) Zhang, Y.; Liang, J.-Y.; Lipscomb, W. N. *Biochem. Biophys. Res. Commun.* **1993**, *190*, 1080.
(384) Bone, R.; Springer, J. P.; Atack, J. R. *Proc. Natl. Acad. Sci. USA* **1992**, *89*, 10031.
(385) Vincent, M. F.; Marangos, P. J.; Gruber, H. E.; Van der Berghe, G. *Diabetes* **1991**, *40*, 1259.
(386) York, J. D.; Ponder, J. W.; Majerus, P. W. *Proc. Natl. Acad. Sci. USA* **1995**, *92*, 5149.
(387) Villeret, V., Huang, S., Fromm, H. J.; Lipscomb, W. N. *Proc. Natl. Acad. Sci. USA* **1995**, *92*, 8916−8920.
(388) Atack, J. R.; Broughton, H. B.; Pollack, S. J. *FEBS Lett.* **1995**, *361*, 1.
(389) Pollack, S. J.; Atack, J. R.; Knowles, M. R.; McAllister, G.; Ragan, C. I; Baker, R.; Fletcher, S. R.; Iversen, L. L.; Broughton, H. B. *Proc. Natl. Acad. Sci. USA* **1994**, *91*, 5766.
(390) Strasser, F.; Pebton, P. D.; Ganzhorn, A. J. *Biochem. J.* **1995**, *307*, 585.
(391) Cade, J. F. *Med. J. Aust.* **1949**, *36*, 349.
(392) Baraban, J. M. *Proc. Natl. Acad. Sci. USA* **1994**, *91*, 5738.
(393) Bone, R.; Frank, L.; Spinger, J. P.; Pollack, S. J. Osborne, S.; Atack, J. R.; Knowles, M. R.; Melellister, G.; Ragan, C. I.; Broughton, H. B.; Baker, R.; Fletcher, S. R. *Biochemisty* **1994**, *33*, 9468.
(394) Bone, R.; Spinger, J. P.; Atack, J. R. *Proc. Natl. Acad. Sci. USA* **1992**, *89*, 10031.
(395) Bone, R.; Frank, L.; Springer, J. P.; Atack, J. R. *Biochemistry* **1994**, *33*, 9468.
(396) Villeret, V.; Huang, S.; Fromm, H. J.; Lipscomb, W. N. *Proc. Natl. Acad. Sci. USA* **1995**, *92*, 8916.
(397) Potter, B. V.; Lampe, D. *Angew. Chem., Int. Ed. Engl.* **1995**, *34*, 1933. Majerus, P. W.; Ross, T. S.; Cunningham, T. W.; Caldwell, K. K.; Jefferson, A. B. Bansal, V. S. *Cell* **1990**, *63*, 489. York, J. D.; Saffitz, J. E.; Majerus, P. W. *J. Biol. Chem.* **1994**, *269*, 19992.
(398) Inhorn, R. C.; Bansal, V. S.; Majerus, P. W. *Proc. Natl. Acad. Sci. USA* **1987**, *84*, 2170.
(399) Inhorn, R. C.; Majerus, P. W. *J. Biol. Chem.* **1988**, *263*, 14559.
(400) Pollack, S. J.; Atack, J. R.; Knowles, M. R.; McAllister, G.; Ragan, C. I.; Baker, R.; Fletcher, S. R.; Iversen, L. L.; Broughton, H. B. *Proc. Natl. Acad. Sci. USA* **1994**, *91*, 5766−5770.
(401) York, J. D.; Ponder, J. W.; Chen, Z.-W.; Matthews, F. S.; Majerus, P. W. *Biochemistry* **1994**, *33*, 13164.
(402) Ollis, D. L.; Brick, P.; Hamlin, R.; Xuong, N. G.; Steitz, T. A. *Nature* **1985**, *313*, 762.
(403) Freemont, P. S.; Friedman, J. M.; Beese, L. S.; Sanderson, M. R.; Steitz, T. A. *Proc. Natl. Acad. Sci. USA* **1988**, *85*, 8924.
(404) Derbyshire, V.; Freemont, P. S.; Sanderson, M. R.; Beese, L. S.; Friedman, J. M.; Joyce, C. M.; Steitz, T. A. *Science* **1988**, *240*, 199.
(405) Beese, L. S.; Steitz, T. A. *EMBO J.* **1991**, *10*, 25.
(406) Beese, L. S.; Derbyshire, V.; Steitz, T. A. *Science* **1993**, *260*, 352.
(407) Beese, L. S.; Friedman, J. M.; Steitz, T. A. *Biochemistry* **1993**, *32*, 14095.
(408) Kohlstaedt, L. A.; Wang, J.; Friedman, J. M.; Rice, P. A.; Steitz, T. A. *Science* **1992**, *256*, 1783.
(409) Jacobo-Molina, A.; Ding, J.; Nanni, R. G.; Clark, A. D.; Lu, X.; Tantillo, C.; Williams, R. L.; Kramer, G.; Ferris, A. L.; Clark, P.; Hizi, A.; Hughes, S. E.; Arnold, E. *Proc. Natl. Acad. Sci. USA* **1993**, *90*, 6320.
(410) Smerdon, S. J.; Jäger, J.; Wang, J.; Kohlstaedt, L. A.; Chirino, A. J.; Friedman, J. M.; Rice, P. A.; Steitz, T. A. *Proc. Natl. Acad. Sci. USA* **1994**, *91*, 3911.
(411) Wang, J.; Smerdon, S. J.; Jäger, J.; Kohlstaedt, L. A.; Rice, P. A.; Friedman, J. M.; Steitz, T. A. *Proc. Natl. Acad. Sci. USA* **1994**, *91*, 7242.

(412) Patel, P. H.; Jacobo-Molina, A.; Ding, J.; Tantillo, C.; Clark, A. D., Jr.; Raag, R.; Nanni, R. G.; Hughes, S. H.; Arnold, E. *Biochemistry* **1995**, 34, 5351.
(413) Rodgers, D. W.; Gamblin, S. J.; Harris, B. A.; Ray, S.; Culp, J. S.; Hellmig, B.; Woolf, D. J.; Debouck. C.; Harrison, S. C. *Proc. Natl. Acad. Sci. USA* **1995**, *92*, 1222.
(414) Davies, J. F., II; Almasy, R. J.; Hostomska, Z.; Ferre, R.; Hostomsky, Z. *Cell* **1994**, *76*, 1123.
(415) Pelletier, H.; Sawaya, M. R.; Kumar, A.; Wilson, S. H.; Kraut, J. *Science* **1994**, *264*, 1891.
(416) Sawaya, M. R.; Pelletier, H.; Kumar, A.; Wilson, S. H.; Kraut, J. *Science* **1994**, *264*, 1930.
(417) Sousa, R.; Chung, Y.; Rose, J. P.; Wang, B. *Nature* **1993**, *364*, 593.
(418) Kim, Y.; Eom, S. H.; Wang, J.; Lee, D.; Suh, S. W.; Steitz, T. A. *Nature* **1995**, *376*, 612.
(419) Joyce, C. M.; Steitz, T. A. *Annu. Rev. Biochem.* **1994**, *63*, 777.
(420) Holm, L.; Sander, C. *Trends Biochem. Sci.* **1995**, *20*, 345.
(421) Steitz, T. A.; Smerdon, S. J.; Jäger, J.; Joyce, C. M. *Science* **1994**, *266*, 2022.
(422) Pelletier, H. *Science* **1994**, *266*, 2025.
(423) Brody, R. S.; Adler, S.; Modrich, P.; Stec, W. J.; Leznikowski, Z. J.; Frey, P. A. *Biochemistry* **1982**, *21*, 2570.
(424) Burgers, P. M.; Eckstein, F. *J. Biol. Chem.* **1979**, *254*, 6889.
(425) Romaniuk, P. J.; Eckstein, F. *J. Biol. Chem.* **1982**, *257*, 7684.
(426) Brody, R. S.; Frey, P. A. *Biochemistry* **1981**, *20*, 1245.
(427) Bartlett, P. A.; Eckstein, F. *J. Biol. Chem.* **1982**, *257*, 8879.
(428) Catalaro, C. E.; Bencovic, S. *Biochemistry* **1989**, *28*, 4374.
(429) Gupta, A. P.; Bencovic, S. J. *Biochemistry* **1984**, *23*, 5874.
(430) Wang, J.; Yu, P.; Lin, T. C.; Konigsberg, W. H.; Steitz, T. A. *Biochemistry* **1996**, *35*, 8110.
(431) Crouch, R. J. *New Biol.* **1990**, *2*, 771.
(432) Varmus, H. *Science* **1988**, *240*, 1427.
(433) Katayanagi, K.; Okumura, M.; Morikawa, K. *Proteins* **1993**, *17*, 337. Huang, H.-W.; Cowan, J. A. *Eur. J. Biochem.* **1994**, *219*, 253.
(434) Katanayagi, K.; Ishikawa, M.; Okumura, M.; Ariyoshi, M.; Kanaya, S.; Kawano, Y.; Suzuki, M.; Tanaka, I.; Morikawa, K. *J. Biol. Chem.* **1993**, *268*, 22092.
(435) Davies, J. F.; Hostomska, Z.; Hostomsky, Z.; Jordan, S. R.; Matthews, D. A. *Science* **1991**, *252*, 88.
(436) Yang, W.; Hendrickson, W. A.; Crouch, R. J.; Satow, Y. *Science* **1990**, *249*, 1398.
(437) Kanaya, S.; Kohara, A.; Miura, Y.; Sekiguchi, A.; Iwai, S.; Inoue, H.; Ohtsuka, E.; Ikehara, M. *J. Biol. Chem.* **1990**, *265*, 4615.
(438) Modak, M. J.; Srivastava, A. *J. Biol. Chem.* **1979**, *254*, 4756.
(439) Yang, W.; Steitz, T. A. *Structure* **1995**, *3*, 131.
(440) Ariyoshi, M.; Vassylyev, D. G.; Iwasaki, H.; Nakamura, H.; Shinagawa, H.; Morikawa, K. *Cell* **1994**, *78*, 1063.
(441) Bujacz, G.; Jaskolski, M.; Alexandratos, J.; Wlodawer, A.; Merkel, G.; Katz, R. A.; Skalka, A. M. *Structure* **1996**, *4*, 89.
(442) Mol, C. D.; Kuo, C.-F.; Thayer, M. M.; Cunningham, R. P. Tainer; J. A. *Nature* **1995**, *374*, 381.
(443) Rice, P.; Mizuuchi, K. *Cell* **1995**, *82*, 209.
(444) Bennett, R. J.; Dunderdale, H. J.; West, S. C. *Cell* **1993**, *74*, 1021.
(445) Takahagi, M.; Iwasaki, H.; Shinagawa, H. *J. Biol. Chem.* **1994**, *269*, 15132.
(446) Vipond, I. B.; Baldwin, G. S.; Halford, S. E. *Biochemistry* **1995**, *34*, 697.
(447) Kim, Y.; Grable, J. C.; Choi, P. J.; Greene, P.; Rosenberg, J. M. *Science* **1990** *249*, 1307.
(448) Kostrewa, D.; Winkler, F. K. *Biochemistry* **1995**, *34*, 683.
(449) Cheng, X.; Balendiran, K.; Schildkraut, I.; Anderson, J. E. *EMBO J.* **1994**, *13*, 3927.
(450) Newman, M.; Strzelecka, T.; Dorner, L. F.; Schildkraut, I.; Aggarwal, A. K. *Science* **1995**, *269*, 656.
(451) Bozic, D.; Grazulis, S.; Siksnys, V.; Huber, R. *J. Mol. Biol.* **1996**, *255*, 176.
(452) Grosshans, C. A.; Cech, T. R. *Biochemistry* **1989**, *28*, 6888. Piccirilli, J. A.; Vyle, J. S.; Caruthers, M. H.; Cech, T. R. *Nature* **1993**, *361*, 85.
(453) Pyle, A. M. *Science* **1993**, *261*, 709.
(454) Steitz, T. A.; Steitz, J. A. *Proc. Natl. Acad. Sci. USA* **1993**, *90*, 6498.
(455) Cheetham, P. S. J. *Chem. Ind.* **1995**, 265.
(456) Callenz, M.; Tomme, P.; Kerstens-Hildenson, H.; Cornelis, W.; Vangrysperre, W.; De Bruyne, C. K. *Biochem. J.* **1988**, *250*, 285.
(457) Feather, M. S.; Deshpande, V.; Lybyer, M. J. *Biochem. Biophys. Res. Commun.* **1970**, *38*, 859.
(458) Schray, K. J.; Rose, I. A. *Biochemistry* **1972**, *10*, 1058.
(459) Rose, I. A.; O'Connell, E. L.; Mortlock, R. P. *Biochim. Biophys. Acta* **1969**, *178*, 376.
(460) Makkee, M.; Kieboom, A. P. G.; van Bekkum, H. *Rec. Trav. Chim. Pay. Bas.* **1984**, *103*, 361.
(461) Bock, K. B.; Meldal, M.; Meyer, B.; Wiebe, L. *Acta Chem. Scand.* **1983**, 1337, 101.
(462) Ramchander, S.; Feather, M. S. *Arch. Biochem. Biophys.* **1977**, *178*, 576.
(463) Carrell, H. L.; Rubin, B. H.; Hurley, T. J.; Glusker, J. P. *J. Biol. Chem.* **1984**, *259*, 3230.
(464) Farber, G. K.; Glasfield, A.; Tiraby, G.; Ringe, D.; Petsko, G. A. *Biochemistry* **1989**, *28*, 7289.
(465) Carrell, H. L.; Hoier, H.; Glusker, J. P. *Acta Crystallogr. Sect. D* **1994**, *50*, 113.
(466) Collyer, C. A.; Henrick, K.; Blow, D. M. *J. Mol. Biol.* **1990**, *212*, 211.
(467) Whitlow, M.; Howard, A. J.; Finzel, B. L.; Poulos, T. L.; Winbourne, E., Gilliland, G. I. *Proteins: Struct. Funct. Genet.* **1991**, *9*, 153.
(468) Vallee, B. L.; Williams, R. J. P. *Proc. Natl. Acad. Sci. USA* **1968**, *59*, 498.
(469) Williams, R. J. P. *Q. Rev. Chem. Soc.* **1970**, *24*, 331.
(470) Kidani, Y.; Hirose, J. *Zinc Enzymes*; Bertini, I., Lucinat, C., Maret, W., Zeppezauer, M., Eds.; Birkäuser: Boston, 1986; Chapter 5, p 59.
(471) Faller, L. D.; Baroudy, B. M.; Johnson, A. M.; Ewall, R. X. *Biochemistry* **1977**, *16*, 3864.
(472) Wold, F.; Ballou, C. E. *J. Biol. Chem.* **1957**, *227*, 313.
(473) Rose, S. L.; Dickinson, L. C.; Westhead, E. W. *J. Biol. Chem.* **1984**, *259*, 4405.
(474) Anderson, V. E.; Weiss, P. M.; Cleland, W. W. *Biochemistry* **1984**, *23*, 2779.
(475) Wedekind, J. E.; Reed, G. H.; Rayment, I. *Biochemistry* **1995**, *34*, 4325.
(476) Lebioda, L.; Stec, B. *J. Am. Chem. Soc.* **1989**, *111*, 8511.
(477) Lebioda, L.; Stec, B. *Biochemistry* **1991**, *30*, 2817.
(478) Zhang, E.; Hatada, M.; Brewer, J. M.; Lebioda, L. *Biochemistry* **1994**, *33*, 6295.
(479) Wedekind, J. E.; Poyner, R. R.; Reed, G. H.; Rayment, I. *Biochemistry* **1994**, *33*, 9333.
(480) Poyner, R. R.; Reed, G. H. *Biochemistry* **1992**, *31*, 7166.
(481) Chien, J. V. C.; Westhead, E. W. *Biochemistry* **1971**, *10*, 3198.
(482) Lee, M. E.; Nowak, T. *Biochemistry* **1992**, *31*, 2172.
(483) Elliott, J. I.; Brewer, J. M. *J. Inorg. Biochem.* **1980**, *12*, 323.
(484) Dinovo, E. C.; Boyer, P. D. *J. Biol. Chem.* **1971**, *246*, 4586.
(485) Stubbe, J.; Abeles, R. H. *Biochemistry* **1980**, *19*, 5505.
(486) Anderson, S. R.; Anderson, V. E.; Knowles, J. R. *Biochemistry* **1994**, *33*, 10545.
(487) Duquerroy, S.; Camus, C.; Janin, J. *Biochemistry* **1995**, *34*, 12513.
(488) Kenyon, G. L.; Hegeman, G. D. *Adv. Enzymol. Relat. Areas Mol. Biol.* **1979,** *50*, 325.
(489) Powers, V. M.; Koo, C. W.; Kenyon, G. L.; Gerlt, J. A.; Kozarich, J. W. *Biochemistry* **1991**, *30*, 9255.
(490) Gerlt, J. A.; Kenyon, G. L.; Neidhart, D. J.; Petsko, G. A.; Powers, V. M. *Curr. Opin. Struct. Biol.* **1992**, *2*, 736.
(491) Kallarakal, A. T.; Mitra, B.; Kozarich, J. W., Gerlt, J. A.; Clifton, J. G.; Petsko, G. A.; Kenyon, G. L. *Biochemistry* **1995**, *34*, 2788.
(492) Mitra, B.; Kallarakal, A. T.; Kozarich, J. W.; Gerlt, J. A.; Clifton, J. G.; Petsko, G. A.; Kenyon, G. L. *Biochemistry* **1995**, *34*, 2777.
(493) Goldman, A.; Ollis, D. L.; Steitz, T. A. *J. Mol. Biol.* **1987**, *194*, 143.
(494) Hoier, H.; Schlömann, M.; Hammer, A.; Glusker, J. P.; Carrell, H. L.; Goldman, A.; Stezowski, J. J.; Heinemann, U. *Acta Crystallogr. Sect. D* **1994**, *50*, 75. Kleywegt, G. J.; Hoier, H.; Jones, T. A. *Acta Crystallogr. Sect. D* **1996**, *52*, 858.
(495) Sistrom, W. R.; Stainier, R. Y. *J. Biol. Chem.* **1954**, *210*, 821.
(496) Babbitt, P. C.; Mrachko, G. T.; Hasson, M. S. Huisman, G. W.; Kolter, R.; Ringe, D.; Petsko, G. A.; Kenyon, G. L.; Gerlt, J. A. *Science* **1995**, *267*, 1159.
(497) Weissbach, A.; Horeker, B. L.; Hurwitz, J. *J. Biol. Chem.* **1956**, *218*, 795.
(498) Christeller, J. T. *Biochem. J.* **1981**, *193*, 839.
(499) Knight, S.; Andersson, I.; Brändén, C.-I. *J. Mol. Biol.* **1990**, *215*, 113. Schreuder, H. A.; Knight, S.; Curmi, P. M. G.; Andersson, I.; Cascio, D.; Sweet, R. M.; Brändén, C. I.; Eisenberg, D. *Protein Sci.* **1993**, *2*, 1136.
(500) Robinson, P. D.; Martin, M. N.; Tabita, F. R. *Biochemistry* **1979**, *18*, 4453.
(501) Christeller, J. T.; Laing, W. A. *Biochem. J.* **1979**, *183*, 747.
(502) Jordan, D. B.; Ogden, W. L. *Arch. Biochem. Biophys.* **1983**, *227*, 425.
(503) Lorimer, G. H.; Andrews, T. J.; Tolbert, N. E. *Biochemistry* **1973**, *12*, 18.
(504) Robinson, J. L.; Rose, I. A. *J. Biol. Chem.* **1972**, *247*, 1096.
(505) Boyer, P. D.; Lardy, H. A.; Phillips, P. H. *J. Biol. Chem.* **1942**, *146*, 673.
(506) Gupta, R. K.; Oesterling, R. M.; Mildvan, A. S. *Biochemistry* **1976**, *15*, 2881.
(507) Gupta, R. K.; Mildvan, A. S. *J. Biol. Chem.* **1977**, *52*, 5967.
(508) Baek, Y. H.; Nowak, T. *Arch. Biochem. Biophys.* **1982**, *217*, 491.
(509) Stammers, D. K.; Muirhead, H. *J. Mol. Biol.* **1975**, *95*, 213.
(510) Stuart, D. I.; Levine, M.; Muirhead, H.; Stammers, D. K. *J. Mol. Biol.* **1979**, *134*, 109.
(511) Muirhead, H.; Clayden, D. A.; Barford, D.; Lorimer, C. G.; Fothergill-Gilmore, L. A.; Schlitz, E.; Schmitt, W. *EMBO J.* **1986**, *5*, 475.
(512) Larsen, T. M.; Laughlin, L. T.; Holden, H. M.; Rayment, I.; Reed, G. H. *Biochemistry* **1994**, *33*, 6301.

(513) Reuben, J.; Kayne, F. J. *J. Biol. Chem.* **1971**, *246*, 6227.
(514) Raushel, F. M.; Villafranca, J. J. *Biochemistry* **1980**, *19*, 5481.
(515) Rose, I. A.; Kuo, D. J.; Warms, J. V. B. *Biochemistry* **1991**, *30*, 722.
(516) Yang, S.-L. L.; Frey, P. A. *Biochemistry* **1979**, *18*, 2980.
(517) Ruzicka, F. J.; Wedekind, J. E.; Kim, J.; Rayment, I.; Frey, P. A. *Biochemistry* **1995**, *34*, 5610.
(518) Wedekind, J. E.; Frey, P. A.; Rayment, I. *Biochemistry* **1995**, *34*, 11049.
(519) Liu, J.; Lin, S.-X.; Blochet, J.-E.; Pezolet, M.; Lapointe, J. *Biochemistry* **1993**, *32*, 11390.
(520) Posorske, L. H.; Cohn, M.; Yanagisawa, N.; Auld, D. S. *Biochim. Biophys. Acta* **1979**, *576*, 128.
(521) Nureki, O.; Kohno, T.; Sakamoto, K.; Miyazawa, T.; Yokoyama, S. *J. Biol. Chem.* **1993**, *268*, 15368.
(522) Mayaux, J.-F.; Blanquet, S. *Biochemistry* **1981**, *20*, 4647.
(523) Kohda, D.; Yokoyama, S.; Miyazawa, T. *FEBS Lett.* **1984**, *174*, 20.
(524) Lazard, M.; Mirande, M.; Waller, J.-P. *Biochemistry*, **1985**, *24*, 5099.
(525) Kisselev, L. L.; Favorova, O. O.; Nurbekov, M. K.; Dmitriyenko, S. G.; Engelhardt, W. A. *Eur. J. Biochem.* **1981**, *120*, 511.
(526) Schimmel, P.; Landro, J. A.; Schmidt, E. *J. Biomol. Struct. Dyn.* **1993**, *11*, 571.
(527) Xu, B.; Trawick, B.; Krudy, G. A.; Phillips, R. M.; Zhou, L.; Rosevear, P. R. *Biochemistry* **1994**, *33*, 398.
(528) Wu, M.-X.; Filley, S. J.; Hill, K. A. W. *Biochem. Biophys. Res. Commun.* **1994**, *201*, 1079.
(529) Mayaux, J. F.; Kalogerakos, T.; Brito, K. K.; Blanquet, S. *Eur. J. Biochem.* **1982**, *128*, 41.
(530) Fourmy, D.; Meinnel, T.; Mechulam, Y.; Blanquet, S. *J. Mol. Biol.* **1993**, *231*, 1068.
(531) Landro, J. A.; Schimmel, P. *Proc. Natl. Acad. Sci. USA* **1993**, *90*, 2261.
(532) Xu, B.; Krudy, G. A.; Rosevear, P. R. *J. Biol. Chem.* **1993**, *268*, 16259.
(533) Fourmy, D.; Dardel, F.; Blanquet, S. *J. Mol. Biol.* **1993**, *231*, 1078. Zelwer, C.; Risler, J. L.; Brunie, S. *J. Mol. Biol.* **1982**, *155*, 63. Brunie, S.; Mellot, P.; Zelwer, C.; Risler, J. L.; Blanquet, S.; Fayat, G. *J. Mol. Graph.* **1987**, *5*, 18.
(534) Brunie, S.; Zelwer, C.; Risler, J. L. *J. Mol. Biol.* **1990,** *216*, 411.
(535) Webster, T.; Tsai, H.; Kula, M.; Mackie, G. A.; Schimmel, P. *Science* **1984**, *226*, 1315.
(536) Miller, W. T.; Hill, K. A. W.; Schimmel, P. *Biochemistry* **1991**, *30*, 6970.
(537) Markham, G. D.; Hafner, E. W.; Tabor, C. W.; Tabor, H. *Methods Enzymol.* **1983**, *94*, 219.
(538) Mudd, S. H.; Cantoni, B. L. *J. Biol. Chem.* **1958**, *231*, 481.
(539) Takusagawa, F.; Kamitori, S.; Misaki, S.; Markham, G. D. *J. Biol. Chem.* **1996**, *271*, 136. Takusagawa, F.; Kamitori, S.; Markham, G. D. *Biochemistry* **1996**, *35*, 2586.
(540) McQueney, M. S.; Markham, B. D. *J. Biol. Chem.* **1955**, *270*, 18277.
(541) Meek, T. D.; Villafranca, J. J. *Biochemistry* **1980**, *19*, 5513; Weisbrod, R. E.; Meister, A. *J. Biol. Chem.* **1973**, *248*, 3997.
(542) Abell, L. M.; Villafranca, J. J. *Biochemistry* **1991**, *30*, 1413.
(543) Yamashita, M. M.; Almassy, R. J.; Janson, C. A.; Cascio, D.; Eisenberg, D. *J. Biol. Chem.* **1989**, *264*, 17681. Liaw, S.; Pan, C.; Eisenberg, D. *Proc. Natl. Acad. Sci. USA* **1993**, *90*, 4996. Almassy, R. J.; Janson, C. A.; Hamlin, R.; Xuong, N. H.; Eisenberg, D. *Nature* **1986**, *323*, 304. Liaw, S.; Jun, G.; Eisenberg, D. *Biochemistry* **1994**, *33*, 11184.
(544) Liaw, S.; Eisenberg, D. *Biochemistry* **1994**, *33*, 675.
(545) Dhalla, A. M.; Li, B.; Alibhai, M. F.; Yost, K. J.; Hemmingsen, J. M.; Atkins, W. M.; Schineller, J.; Villafranca, J. J. *Protein Sci.* **1994**, *3*, 476.
(546) Kanyo, Z. F.; Scolnick, L. R.; Ash, D. E.; Christianson, D. W. Unpublished results.
(547) Green, S. M.; Ginsburg, A.; Lewis, M. S.; Hensley, P. *J. Biol. Chem.* **1991**, *266*, 21474.
(548) Lukat, G. S.; Stock, A. M.; Stock, J. B. *Biochemistry* **1990**, *29*, 5436.
(549) Stock, A. M.; Mottonen, J. M.; Stock, J. B.; Schutt, C. E. *Nature* **1990**, *337*, 745. Volz, K.; Matsummara, P. *J. Biol. Chem.* **1991**, *266*, 15511. Stock, A. M.; Martinez-Hackert, E.; Rasmussen, B. F.; West, A. H.; Stock, J. B.; Ringe, D.; Petsko, G. A. *Biochemistry* **1993**, *32*, 13375.
(550) Herschlag, D.; Jencks, W. P. *J. Am. Chem. Soc.* **1990**, *112*, 1442.
(551) Honig, B.; Nicholls, A. *Science* **1995**, *268*, 1144.
(552) Beveridge, D. L.; DiCapua F. M. *Annu. Rev. Biophys. Chem.* **1989**, *18*, 431.

CR950042J